CZTS BASED THIN FILM SOLAR CELLS: DESIGN & PERFORMANCE ANALYSIS

by

Md. Mamunur Rahaman

Id-13321051

Arbab Chowdhury

Id-13121140

Syed Irshan Waky

Id-12221093

A Thesis Submitted In Partial Fulfillment of the

Requirements for the Degree

Of

Bachelor of Science in Electrical and Electronic Engineering

Department of Electrical and Electronic Engineering

BRAC University

Dhaka-1212, Bangladesh

April 2017

Dedication

This work is dedicated to our beloved Prophet Hazrat Muhammad (Sm), to our professor Dr. Md. Mosaddequr Rahman for his invaluable teaching in our life and our parents who always supported us and motivated us.

Declaration of Originality

This is to certify that this thesis titled "CZTS Based Solar Cells: Design & Performance Analysis" submitted to the department of EEE, BRAC University is our original work and no part of this work has been submitted to any university or elsewhere for the award of any academic degree.

(Author)
Md. Mamunur Rahaman
Id 13321051
BSC. Engg. (EEE)
Department of Electrical and Electronic Engineering
BRAC University
Bangladesh

(Author)
Arbab Chowdhury
Id 13121140
BSC. Engg. (EEE)
Department of Electrical and Electronic Engineering
BRAC University
Bangladesh

(Author)
Syed Irshan Waky
Id 12221093
BSC. Engg. (EEE)
Department of Electrical and Electronic Engineering
BRAC University
Bangladesh

Acknowledgement

All the appreciation to Allah (Swt), the merciful and beneficial who has enabled us to submit this work leading to the BSC. Engineering Degree.

We would like to express our sincere gratitude to our supervisor, Dr. Md. Mosaddequr Rahman, Professor, Department of Electrical & Electronic Engineering, BRAC University, Dhaka, for his constant support, patience and motivation. His guidance and support helped us throughout the period of this research work.

Abstract

In recent year's climate change and renewable energy resources were put into the limelight to a greater extend. The main limitations of fossil fuels are that they are a finite resource and release CO2, a greenhouse gas implicated in an-made climate change. Thus renewable energy sources have gained greater importance and of those, solar energy is one of the more encouraging areas for development. However, electricity from solar cells is more expensive than energy from conventional sources like coal, gas. One approach to solve this problem is the thin film solar cell. Thin film solar cells have a thickness of only few micrometers which means less material is used which saves energy and money.

Copper zinc tin sulphide or CZTS is a compound semiconductor made of copper, zinc, tin and sulphur which are sufficiently abundant elements and none of them are harmful to the environment. CZTS is a material with promising electrical and optical characteristics with the advantage that it is made of nontoxic and less expensive materials compared to many other thin film materials, making it a compound of interest in the search for suitable materials for thin film solar cells.

The goal of this work is to select a CZTS-based solar cell design and evaluate its performance under different parameters and conditions, namely doping density, thin film thickness and temperature to find the optimal values of doping density and thickness and at different operating temperatures.

TABLE OF CONTENTS

	Page Number
Abstract	v
List of Tables	viii
List of figures	ix
List of Equations	xii
Chapter 1: Introduction	1
1.1 Introduction	2
1.2 Background	2
1.3 Solar Technology	4
1.4 Types of Solar Cells	6
1.4.1 Crystalline Silicon	6
1.4.2 Thin Films	6
1.4.3 Possible thin film materials	6
1.4.4 CZTS	9
1.5 Scope of Work	11
1.6 Thesis Organization	11
Chapter 2: Theory of solar cells	12
2.1 Introduction	13
2.2 Intrinsic and extrinsic semiconductor	13
2.3 Fermi level, conduction band and valance band	14
2.4 Depletion region formation, drift and diffusion currents	14
2.5 J-V Characteristics of junction	16

Chapter 3: Dark current, Photo-current, I-V calculation for CZTS 19
3.1 Introduction 20
3.2 Solar cell structure 20
3.3 Energy band diagrams 21
3.4 Dark current 22
3.4.1 Trap-assisted Tunneling recombination 23
3.4.2 CdS/CZTS Interface Recombination 28
3.4.3 Diffusion 29
3.4.4 Thermionic Emission 31
3.4.5 Radiative Recombination 32
3.5 Photocurrent 33
3.5.1 N-side photocurrent 35
3.5.2 P-side Photocurrent 37
3.5.3 Depletion Region Photocurrent 38

Chapter 4: Calculations and Results 40
4.1 Introduction 41
4.2 Efficiency and Fill Factor 41
4.3 Model Parameters 42
4.4 Doping Density and Thickness Optimization 44
4.5 Effect of Temperature on Efficiency and Fill Factor 59
4.6 Limitations and Future Work 65

List of tables

Table No	and Name	Page No
1	n-CdS thin film solar cell parameters	42
2	p-CZTS thin film solar cell parameters	42
3	Temperature coefficients of solar cell performance parameter	64

List of Figures Page No

Fig 1.1: Breakdown of US energy consumption as of March 2016 2
Fig 1.2: Increase in prices of common fossil fuels and uranium 3
Fig 1.3: Photoelectric effect. 5
Fig 1.4: Various combinations of possible semiconductors 7
Fig 1.5: Market share of different types of solar cells in 2007 and 2010. 8
Fig 1.6: Normalized abundance of materials used in thin film solar cells. 8
Fig 1.7: Kesterite structure of CZTS 9
Fig 1.8: Minimum cost of raw materials for different solar cells 10
Fig: 2.1 a) intrinsic, b) n-type and c) p-type Si 13
Fig 2.2 Energy band diagrams for n-type and p-type semiconductors 14
Fig 2.3 p-n junction before and after equilibrium 15
Fig 2.4 Diagram of p-n junction and its charge densities, electric field and potential difference 15
Fig 2.5 Band bending and drift current 16
Fig 2.6 I-V characteristics of semiconductor diode 17
Fig 2.7 Equivalent circuit of a real solar cell 17
Fig 3.1 A typical schematics representation of CZTS, CdS solar cell 20
Fig 3.2 Energy band diagram before junction formation 21
Fig 3.3 Energy band diagram at thermal equilibrium 21
Fig 3.4 Energy band diagram at illumination 22
Fig 3.5 Trap-assisted tunneling mechanism 24
Fig 3.6 Interface recombination 28
Fig 3.7 Diffusion 29
Fig 3.8 Thermionic emission 31
Fig 3.9 Radiative recombination 32
Fig 3.10 Solar cell dimensions under consideration, assumed

abrupt doping profiles ND >> NA and generation rate as a function of distance for long and short wavelengths. 34

Fig 3.11 Depletion region and shifting axis 37

Fig 4.1 Absorption coefficient of CdS, absorption coefficient of CZTS, Standard terrestrial solar spectral irradiance at AM 1.5 vs. Wavelength 43

Fig 4.2 Photocurrent Density vs. Acceptor Concentration. 44

Fig 4.3 Dark Current Density vs. Acceptor Concentration 45

Fig 4.4 Current Density vs. Output Voltage for Donor Concentration 10^{17} cm^{-3} and varying acceptor concentration 45

Fig 4.5 Current Density vs. Output Voltage for Donor Concentration 10^{18} $cm^{-3}$and varying acceptor concentration 46

Fig 4.6 Open Circuit Voltage vs. Acceptor Concentration 46

Fig 4.7 Short Circuit Current vs. Acceptor Concentration 47

Fig 4.8 Fill Factor vs. Acceptor Concentration 47

Fig 4.9 Efficiency vs. Acceptor Concentration 48

Fig 4.10 Photocurrent Density vs. CdS thickness 49

Fig 4.11 Dark Current Density vs. CdS thickness 49

Fig 4.12 Current Density vs. Output Voltage for constant CZTS thickness 5 μm and varying CdS thickness 50

Fig 4.13 Open Circuit Voltage vs. CdS thickness 51

Fig 4.14 Short Circuit Current vs. CdS thickness 51

Fig 4.15 Fill Factor vs. CdS thickness 52

Fig 4.16 Efficiency vs. CdS thickness 53

Fig 4.17 Photocurrent density vs. CZTS thickness 54

Fig 4.18 Dark Current Density vs. CZTS thickness 54

Fig 4.19 Current Density vs. Output Voltage for constant CdS thickness 50 nm and CZTS thickness varying from1 to 5 μm 55

Fig 4.20 Current Density vs. Output Voltage for constant CdS Thickness 50 nm and CZTS thickness varying from 6 to 10 μm 55
Fig 4.21 Open Circuit Voltage vs. CZTS thickness 56
Fig 4.22 Short Circuit Current vs. CZTS thickness 56
Fig 4.23 Fill Factor vs. CZTS Thickness 57
Fig 4.24 Efficiency vs. CZTS Thickness 57
Fig 4.25 Quantum Efficiency (QE) at optimized doping density and Thickness parameters. 58
Fig 4.26 Photocurrent Density vs. Temperature 59
Fig 4.27 Dark Current and its components vs. Temperature 60
Fig 4.28 Current Density vs. Output Voltage for temperatures 5-25 C 61
Fig 4.29 Current Density vs. Output Voltage for temperatures 30-50 C 61
Fig 4.30 Current Density vs. Output Voltage for temperatures 55-75 C 62
Fig 4.31 Open Circuit Voltage vs. Temperature 62
Fig 4.32 Short Circuit Current vs. Temperature 63
Fig 4.33 Fill Factor vs. Temperature 63
Fig 4.34 Efficiency vs Temperature 64

List of equations

Page Number

Equation 1 J-V relationship 22
Equation 2 trap assisted tunneling recombination 24
Equation 3 intrinsic carrier concentration for CdS 24
Equation 4 intrinsic carrier concentration for CZTS 24
Equation 5 Effective density of state of conduction band for CZTS 25
Equation 6 Effective density of state of valence band for CZTS 25
Equation 7 Depletion width of CdS 25
Equation 8 Depletion width of CZTS 28
Equation 9 Built in voltage 26
Equation 10 Built in voltage (CdS) 26
Equation 11 Built in voltage (CZTS) 26
Equation 12 Difference between conduction band edge and Fermi level of CdS 26
Equation 13 Difference between VALENCE band edge and Fermi level of CZTS 26
Equation 14 Minority carrier lifetime 26
Equation 15 Bulk lifetime 27
Equation 16 Surface Lifetime 27
Equation 17 Effect of tunneling for CdS 27
Equation 18 Effect of tunneling for CZTS 27
Equation 19 Built in electric field for CdS 27
Equation 20 Built in electric field for CZTS 27
Equation 21 Interface Recombination 28
Equation 22 Density of state enhancement factor 28
Equation 23 Electron diffusion current 29
Equation 24 Diffusion coefficient of electrons (CZTS) 30
Equation 25 Minority electron diffusion length (CZTS) 30
Equation 26 Minority electron concentration (CZTS) 30

Equation 27 Hole diffusion current (CdS) 30
Equation 28 Diffusion coefficient of holes (CdS) 30
Equation 29 Minority hole diffusion length (CdS) 30
Equation 30 Minority hole concentration (CdS) 30
Equation 31 Total diffusion current 30
Equation 32 Thermionic emission current 31
Equation 33 Barrier height 31
Equation 34 Effective Richardson constant 31
Equation 35 Radiative recombination 32
Equation 36 Radiative recombination coefficient (CdS) 32
Equation 37 Radiative recombination coefficient (CZTS) 33
Equation 38 Generation rate of electron hole pair 33
Equation 39 Steady State continuity equation for holes 35
Equation 40 Steady State continuity equation for electrons 35
Equation 41 Current density equation for n layer 35
Equation 42 Current density equation for p layer 35
Equation 43 Equation for the N side of the junction 35
Equation 44 General solution for equation 43 35
Equation 45 General solution after putting the boundary conditions in n-side 36
Equation 46 Hole photo current density at depletion edge 36
Equation 47 Equation for P-side of junction 37
Equation 48 General solution of equation 47 37
Equation 49 General solution after putting the boundary condition in p-side 38
Equation 50 Photocurrent due to electron in p-side 38
Equation 51 Total deletion region photocurrent 39
Equation 52 Total photocurrent 39
Equation 53 Efficiency 41
Equation 54 Maximum output power density 41
Equation 55 Fill factor 41

CHAPTER-1

INTRODUCTION

1.1 Introduction

In this chapter an overview of solar cell technology and thin films are provided. Copper zinc tin sulphide (CZTS) and the characteristics of this material which are of interest in photovoltaic are discussed.

1.2 Background

The development methods of transmitting power through the use of alternating current made central power generation economically feasible as the power was transferred at high voltage but low current, and thus low loss. Central power stations have been in use since the late 1880s. Hydropower-used to directly move the turbines and fossil fuels-mostly used to provide energy to turn water to steam to move turbines and produce electricity through electromagnetic induction. However both these methods have disadvantages.

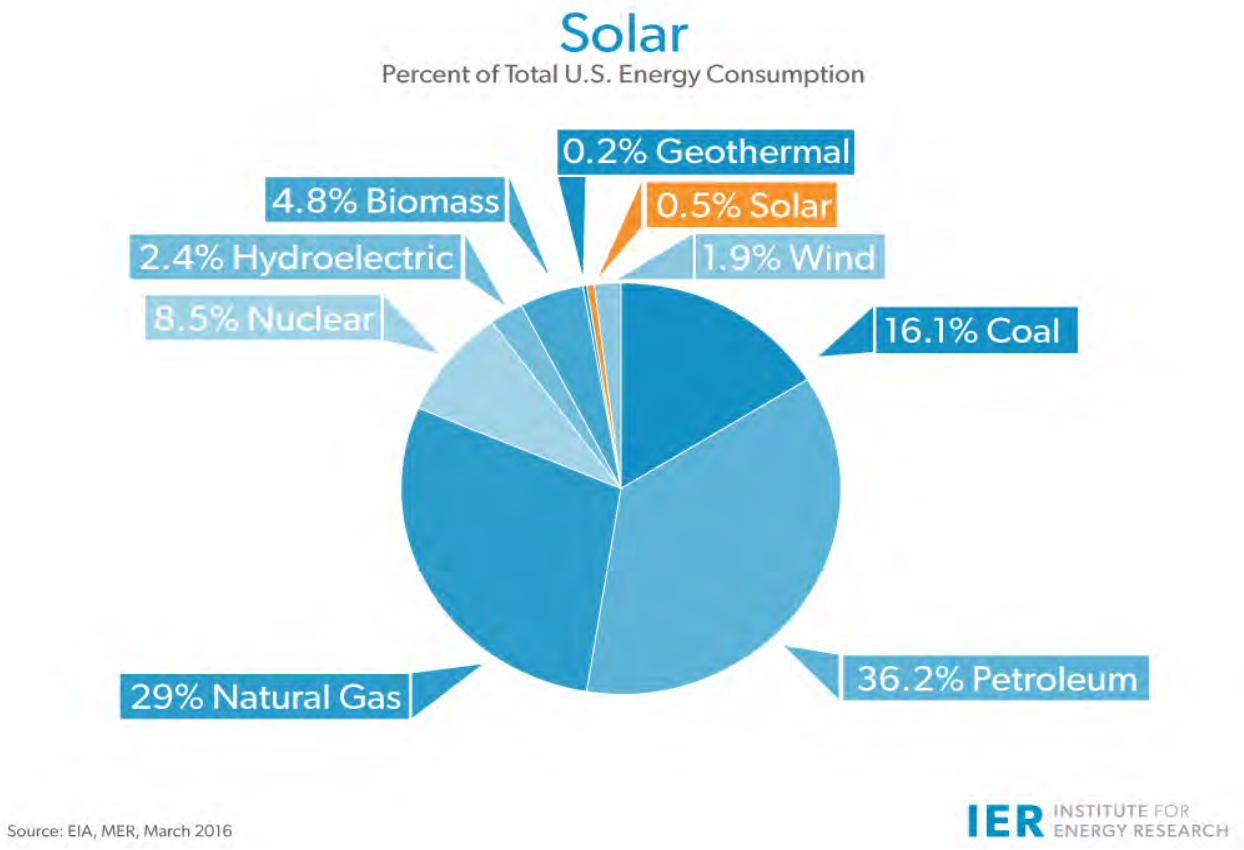

Fig 1.1: Breakdown of US energy consumption as of March 2016

Hydroelectric dams flood large areas, which results in people living in those areas to losing their homes and being relocated, as well as the loss of fertile arable land and the natural habitats of plants and animals. Siltation and changes in the water flow of the river lead to loss of efficiency of electricity generation. In addition damage to the dam can lead to catastrophic flooding, killing many and leaving others homeless.TheBanqaio Dam in China was damaged in a hurricane, leading directly to 26,000 deaths as well as an additional 145,000 due to disease.

The combustion of fossil fuels negatively affects the environment in various ways. Carbon dioxide (CO_2), a greenhouse gas, is one of the main products of the combustion reaction. It builds up in the atmosphere and traps heat from the Sun, contributing to climate change. Other pollutants released during the combustion process include nitrous oxides (NO_X) and sulfur dioxide (SO_2)which react with water in the atmosphere to form acidic compounds such as nitric and sulfurous and sulfuric acid which fall to the ground as acid rain. [1] Toxic metals such as cadmium, nickel and mercury and particulate matter which causes respiratory and cardiovascular diseases are another hazard. In addition, fossil fuels are a non-renewable resource. Fossil fuels are generated, as their name suggests by the transformation of the remains of living organisms into hydrocarbons by geological forces. This occurs much slower than the rate at which they are extracted and used by modern industrialized economies. As supplies of fossil fuels decreases, their prices will increase according to the laws of supply and demand. It is predicted by the International Energy Agency (IEA) thatglobal power demand will increase by 60% by the year 2030, so if fossil fuels continue to be used as a primary means of power generation, these problems will only become more pronounced.

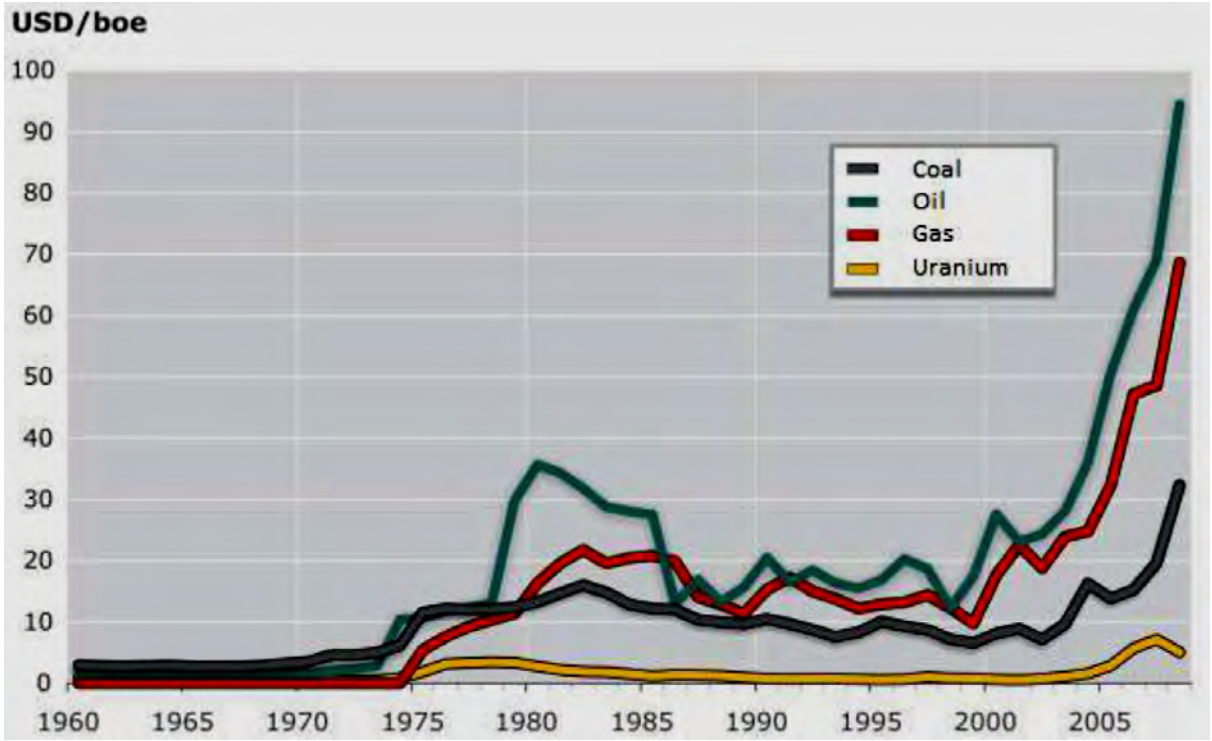

Fig 1.2: Increase in prices of common fossil fuels and uranium

Nuclear reactors are another source of electric power. Nuclear fission causes a nuclear chain reaction which provides energy to turn water into steam to move turbines and produce electricity. The starting material for the fission reaction is usually enriched uranium. The disadvantages of nuclear power plants include the risk of accidents and the problem of disposal of nuclear waste. Several accidents at nuclear power plants have taken place, such as at Three Mile Island, Chernobyl and Fukushima negatively affecting people's health, damaging the environment and leading to evacuations of the surrounding area. Radioactive waste materials release radioactive particles so they must be placed in secure containment until they are no longer hazardous to human health and the environment but they have a long half-life so long term waste management solutions (time frame: 10,000 to 1 million years, though current studies do not go beyond 100 years) need to be put into effect, adding to the cost of nuclear power. In addition, uranium, like fossil fuels is a non-renewable resource.

1.3Solar Technology:

One alternative to conventional energy sources is solar energy (energy from sunlight). Sunlight is termed a renewable energy source, alongside wind, water (from the aforementioned hydroelectric dams as well as energy from tides and waves), geothermal energy and biomass. Each of these methods has drawbacks. Power output from wind power installations is dependent on weather conditions such as wind speed. Geothermal energy releases pollutant gases such as CO_2, hydrogen sulfide (H_2S), methane (CH_4) and ammonia (NH_3) responsible for global warming and acid rain, as well as toxic metals such as mercury, arsenic, antimony and boron. Tidal power installations require specific environmental characters for their operation, limiting the number of suitable sites, and have a high cost. Their performance can be negatively affected by corrosion due to seawater and fouling due to marine organisms. In addition they pose a threat and coastal wildlife and ecosystems. Wave power plants can deny lucrative fishing grounds to fishermen and can be a navigational hazard.

Utilization of solar energy depends on devices called solar cells. Solar cells are electronic devices that convert energy from electromagnetic waves (light) to electric energy via the photovoltaic effect, discovered by French physicistEdmond Becquerel in 1839, where photons of sufficiently high energy excite electrons, moving them to higher energy levels from the valence band to the conduction band, causing the formation of electron-holes pairs (EHPs).[2]Solar cells are composed of semiconductor materials with a bandgap that allows them to absorb the energy of photons to generate these EHPs. Solar cell contains a p-n junction and thus a depletion region is formed. The voltage of the depletion generation causes EHP to separate, the electron moving to positive end and hole to negative end. The movement of these electrons and holes, which are charge carriers, enables a current to be generated by the solar cell. When a load is connected to the solar cell, the current will flow through the load.

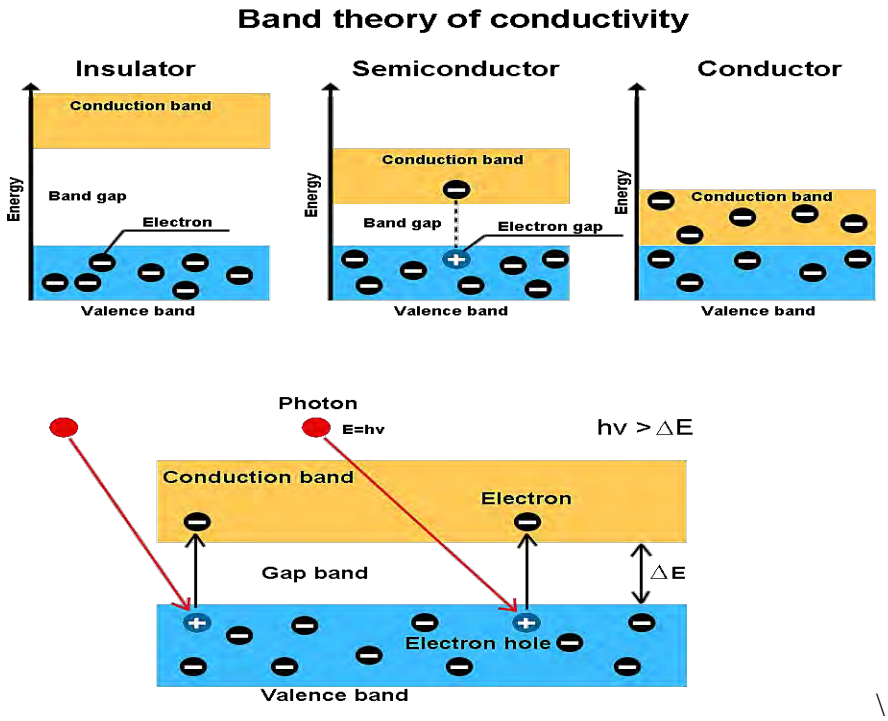

Fig 1.3: Photoelectric effect. The energy of a photon is the product of its frequency with the Boltzmann constant h and if this energy is higher than the bandgap of the material, EHPs are formed.

The realization that coal was a non-renewable resource was responsible for initial interest in solar energy. In1873 Willoughby Smith, an electrical engineer from England, discovered that selenium's photoconductivity i.e. it conducts electricity after absorbing light. In 1876 William Grylls Adams and Richard Evans Day discovered that producing electricity from selenium through photoconductivity had the advantage of producing less heat and not requiring moving parts that were at risk of being damaged. In 1883 Charles Fritts developed the first rooftop solar array composed of selenium cells along with a gold layer (efficiency: 1-2%) in New York. In 1953, physicists working at Bell Laboratories found that silicon had a greater efficiency than selenium (around 6%), a discovery which made the development of solar cells that produced enough power to run electrical equipment possible. Western Electric was the first company to sell commercial licenses for silicon based photovoltaic technology. Solar technologywas used in a satellite, Vanguard 1, as early as 1958.

1.4 Types of Solar Cells

1.4.1 Crystalline Silicon:

Crystalline Silicon (C-Si) solar cells are the most common. There are two types: Mono-crystalline silicon cells which are made from one large crystal and have high efficiency but are expensive and poly-crystalline silicon cells which are composed of many small crystals which are cheaper but have a lower efficiency. Both these types are contrasted by thin film solar cells.

1.4.2 Thin Films:

For all its advantages, electricity derived from solar energy is more expensive than electricity derived from fossil fuels. One method of reducing cost is to use less material which leads us to thin-film solar cells. For thin-film solar cells, around 1 cm^3 of material is needed for 1 m^2 solar cell while crystalline silicon requires around 200 cm^3material.[3] Thus thin film solar cells are less expensive,and sometimes more flexible which broadens the range of their potential applications. Another advantage of solar cells is that connection of many cells into modules is accomplished during the fabrication process, which the saves the time and cost associated with a separate stage of the production process which would be needed for this. Thin film solar cells are manufactured by depositing suitable materials in layers on a substrate such as glass or metal.

1.4.3 Possible thin film materials:

To be usable, materials in thin films must fulfill some important conditions. Light should be absorbed only in a few micrometers of material so large absorption coefficient is required. Moreover, band gap should be around 1-1.6 eV. Possible combinations of different elements from different groups can be made to form compounds which can fulfill these conditions. III–V– (like GaAs) and II–VI–semiconductors (like CdTe) can be made based on silicon. Various more substitution can be done like substituting in the latter one half of the group-II element with a group-III element and one half witha group-III. An example can be CIS ($CuInS_2$) which is a combination of I–III–VI compound semiconductors. Another example might be replacing half of the group-II element with a group-III element and half with a group-IV element. For CIGS we can substitute In/Ga with Zn and Sn, which takes us to CZTS(Cu_2ZnSnS_4). [4] Also, the availability the compounds, its price and environmental friendly thus toxicity should also be kept into account for usable conditions. Compounds such as cadmium telluride (CdTe), copper indium (gallium) sulfide or selenide(CIGS), amorphoussilicon (a-Si) and CZTS are found to be suitable.

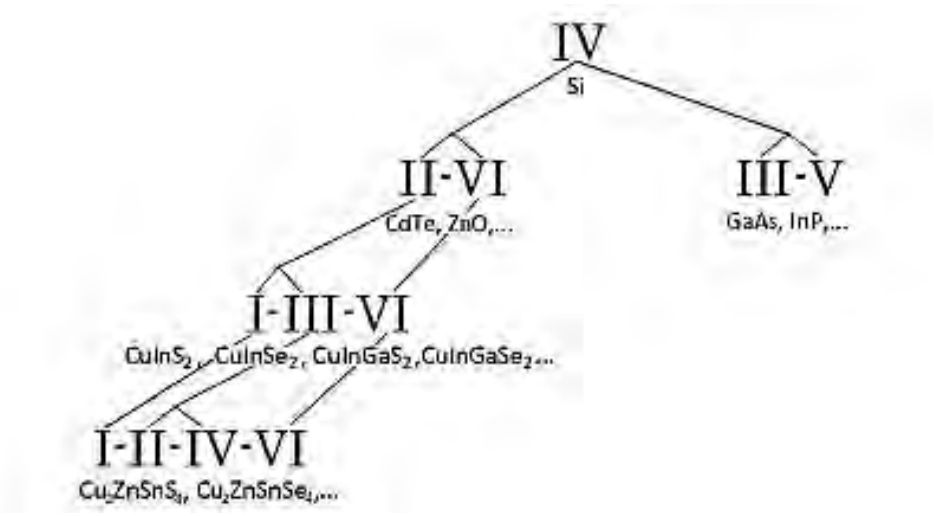

Fig 1.4: Various combinations of possible semiconductors

These thin film materials possess their own advantages and disadvantages. Amorphous silicon (a-Si) is less toxic and made of comparatively less rare and expensive materials. It is also capable ofoperation at low light levels as its bandgap of 1.7 eV allows photons from a large portion of the electromagnetic spectrum to be absorbed, so it suitable for low energy applications such as calculators and torch lights. However on prolonged exposure to sunlight it undergoes the Staebler-Wronski effect, large (10-30%) drop in efficiency. Cadmium Telluride (CdTe) is a prominent thin film material boasting a large fraction of total thin film production. It has comparatively high efficiency and low cost, but its main drawbacks are that Cd is a very toxic material and the limited availability of Te.Gallium Arsenide (GaAs) has a wide direct bandgap which makes it more resistant to radiation damage, which is why it has been used in space, most prominently in the Mars Rovers Spirit and Opportunity as well as in solar cars. It also has comparatively high efficiency but high cost.Copper Indium Gallium Selenide (CIGS) has the highest efficiency among all commercially available thin film materials (around 20%) but it requires Indium which is rare and costly ($300-$375 per kg). The British Geological Survey gave In a relative supply risk of 8.1 (on a scale of 1 to 10 where 1- very low risk and 10-very high risk) in its 2015 risk list.

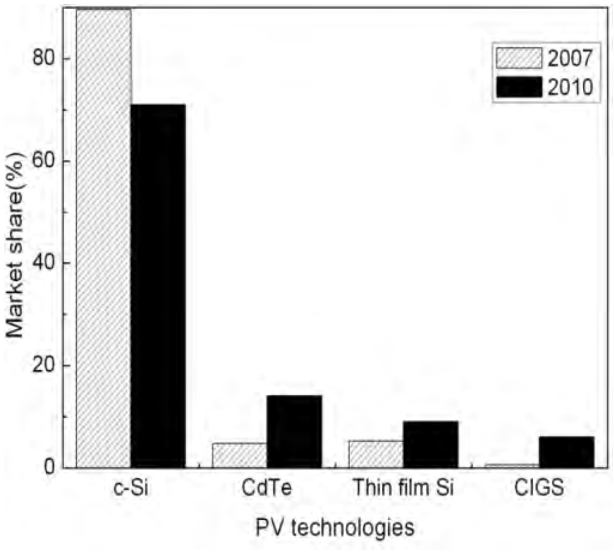

Fig 1.5market share of different types of solar cells in 2007 and 2010. Note that the relative market share of C-Si decreased while that of thin films increased over the period

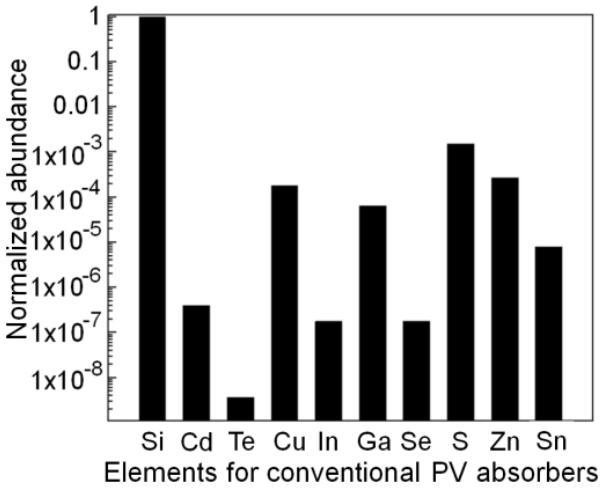

Fig 1.6: Normalized abundance of materials used in thin film solar cells. Those with a higher value are more readily available

However, since fossil fuels were relatively economical and easily available, research into solar technology declined until fuel shortages (the 1973 oil embargo and the 1979 oil crisis) provided the impetus for governments to provide incentives for solar technology research and the formation of institutes such as the National Renewable Energy Laboratory (NREL) in the US, the New Energy and Industrial Technology Development Organization (NEDO) in Japan and Fraunhofer ISE in Germany.Photovoltaic systems usage rose from 1970 to 1983, but falling oil prices slowed growth from 1984 to 1996. In 1982 the first solar power plant, called a solar park, was built by Arco Solar in Hesperia, California. It had a maximum capacity of 1 megawatt-hour.

From themid-1990s solar technology again saw increasing usage due to fossil fuel supply problems and rising awareness of global warming. In 1995, Thomas Faludypatented a design for using solar cells to provide power for recreational vehicles (RVs), consisting solar cells integrated onto a retractable awning. NREL developed solar cells form new materials, gallium indium phosphide and gallium arsenide which had an efficiency of over 30%. By 1999 the efficiency of these devices exceeded 32%. Feed in tariffs-a policy of providing long-term contracts to manufacturers of renewable energy technology-made solar technology a more profitable investment option and so helped foster the growth of this technology since the early 2000s.DIY solar panels became available from 2005 onwards. Thin films began to see use from the 1970s. The main advantage of thin-films over conventional crystalline silicon (c-Si) is that is cheaper though possessing lower efficiency. Flexible and relatively inexpensive paper thin solar cells with a power conversion efficiency of 20% and a power output of 50 W/m^2were produced using an industrial printer in 2015.

1.4.4 CZTS:

Copper zinc tin sulfide (CZTS) was first synthesized in 1966 but it wasn't until 1988 that this material was observed to exhibit the photovoltaic effect. Since then it has been proposed as an alternative to cadmium indium gallium selenide (CIGS) since CZTS is composed of less expensive materials and so is cheaper to produce. Most importantly CZTS, unlike CIGS, does not require indium (In).Copper zinc tin sulphide (CZTS) is a p-type semiconductor material. It has an energy bandgap of around 1.5 eV and abruption coefficients of 10^4 cm^{-1} and above allowing it to absorb a significant number of photons and consequently generate many electron-hole pairs.[5]CZTS can be considered a p-type material due to the presence of defects, most prominently Cu-on-Zn antisites and Cu vacancies which provide a deep acceptor layer which can cause hole formation.These properties make it suitable for use as a thin film material. It possesses a tetragonal crystal structure called kesterite.

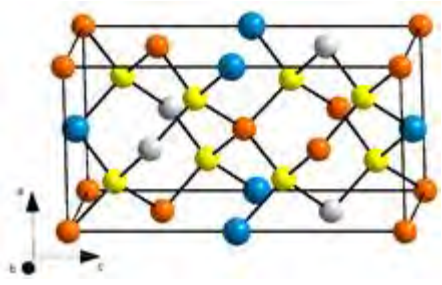

Fig 1.7: Kesterite structure of CZTS. Orange: Cu, blue: Sn, grey: Zn/Fe, yellow: S

It has lattice constants a=0.54, c=1.08, Z=2 and a density of 4.6 gcm^{-3}. It has relatively low carrier lifetimes and diffusion lengths, possibly due to high defect density. Sputtering, chemical bath deposition and thermal evaporation have been used to fabricate CZTS layers. Sputtering involves bombardment of a target substance (in the case of CZTS precursor substances such as

Cu, ZnS and SnS) with high-energy particles (e.g. gaseous ions) to remove atoms from the target which hit the substrate layer (e.g. Mo coated glass) and thus are deposited on this substrate. Annealing (example conditions being temperature of 500-525 ℃ and atmospheric pressure in H_2S/N_2 atmosphere for 3-4 hours). In thermal evaporation, bombardment is replaced by heating, sometimes by high current (e.g.100-260 A), of the source material (e.g. CZTS powder prepared by hydrothermal method from CuS, ZnS and SnS precursor). The material evaporates in a vacuum which prevents other matter from preventing it from reaching the substrate where it cools and is deposited. Annealing follows e.g.300 C for 40 minutes in N_2 atmosphere. Chemical bath deposition involves deposition of thin film layer on a substrate immersed in a chemical solution (e.g. copper sulfate, zinc sulfate heptahydrate, tin sulfate dihydrate, and sodium thiosulfate solution with glass substrate at 60°C.One method used by Katagiri et al. involved electron beam deposition of precursors followed by sulphurization. A complication is the formation of secondary phases which can affect the J-V characteristics of the material. Secondary phases include copper sulphide (Cu_2S), tin sulphide (SnS_2) and zinc sulphide (ZnS).

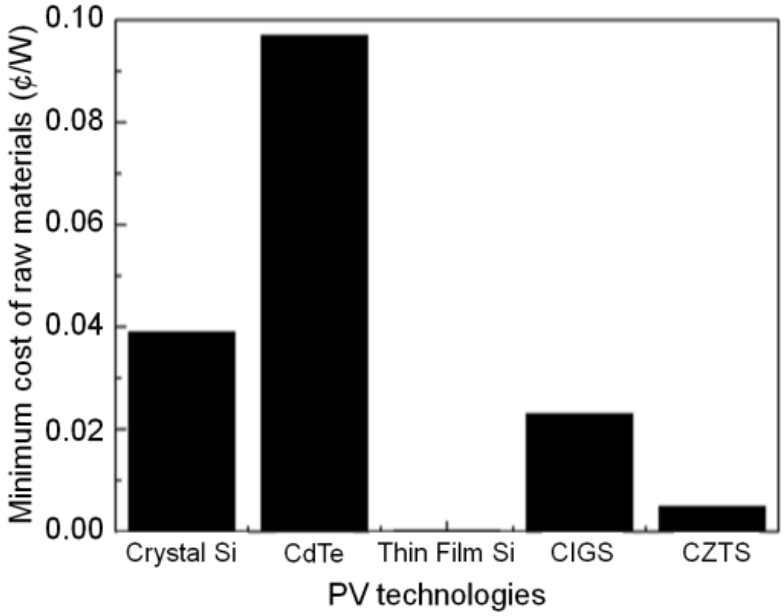

Fig 1.8: Minimum cost of raw materials for different solar cells

By 1997, CZTS thin films were observed to possess 2.3% efficiency. The deposition process was optimized to the point where efficiency rose to 5.7% in 2005. In 2010 a solar conversion efficiency of 10%was realized using CZTS. In 2012 IBM developed a device with 11.1% efficiency. Solar Frontier, IBM and Tokyo Ohka Kogyo (TOK) developed a CZTSSe solar cell with an efficiency of 12.6%. [6]

1.5Scope of Work

Solar energy could be a potential solution to rising global energy demand and the drawbacks of fossil fuels. CZTS thin films are relatively inexpensive and so could help improve the cost-effectiveness of solar technology. The aim of this work is to create a mathematical model of the current density-voltage relationship and investigate the effect of various parameters (doping densities, thickness of the material, temperature) on the output current density to determine the optimal values of these parameters to provide acceptable output current density and efficiency values. The contributions of the n-side and the p-side bulk as well the depletion region towards the photocurrent were considered when calculating photocurrent. The following sources of loss were taken into account: diffusion, radiative recombination, thermionic emission, non-radiative recombination, CdS/CZTS interface recombination and trap-assisted tunneling recombination. Matlab R2010a software was used to calculate the results of the equations used for electrical analysis provided later in this work.

1.6 Thesis Organization

In chapter 1 the background of solar technology, the different types of solar cells and thin films and an overview of CZTS were discussed. In Chapter 2, the theory behind solar cell operation will be explored in greater detail. Chapter 3 will focus on the equations used in analyzing a CZTS solar cell's electrical properties. Chapter 4 will provide the results of these calculations and the conclusions regarding operation of the solar cell under different conditions that can be drawn from them.

CHAPTER-2

Theory of Solar Cells

2.1 Introduction

In this chapter the theory of operation of photovoltaic materials. The types of semiconductors (intrinsic and extrinsic) and the behavior of junctions is discussed.

2.2Intrinsic and Extrinsic Semiconductors:

Extrinsic semiconductors are those to which donor or acceptor atoms have been added to turn them into n-type or p-type semiconductors respectively. This process of adding impurities to increase the number of available charge carriers is called doping. Intrinsic semiconductors are pure semiconductors that have not undergone such doping.

Silicon (Si) is the most common material used in solar cells, so it can be used to explain the theory of extrinsic semiconductors. Si is a Group IV (tetravalent) element, each Si atom forming covalent bonds with four other Si atoms in the lattice, leaving no unbounded electrons in its valence shell. If it is doped with a Group V (pentavalent) element such as phosphorus (P), [7]each phosphorus atom can form covalent 4 bonds but there is a fifth electron which, not being used in a covalent bond, can be freed from its atom as low energy (even at room temperature) and can thus move through the structure and act as a charge carrier. Thus P is an example of a donor impurity since it donates an electron and Si in P has replaced some of the Si atoms in the lattice is known as an n-type extrinsicsemiconductor due to the presence of negative charge carriers (electrons).

If Si is doped with a Group III (trivalent) element such as Boron (B),each B atom can form three covalent bonds with Si atoms, but the lack of a fourth electron leads to the formation of a hole. Electrons from Si atoms can attempt to occupy this empty slot, causing the hole to appear in that electron's slot. Thus the hole can be taken as a moving positive charge as it 'moves' in the opposite direction of electrons. Thus B is known as an acceptor impurity as it accepts electrons to replace the hole and due to the presence of positive holes, Si where B has replaced some of the SI atoms in the lattice is known as a p-type extrinsic semiconductor. It is important to note that semiconductor materials are still electrically neutral after doping as the total number of protons and electrons in the material are still equal to one another.

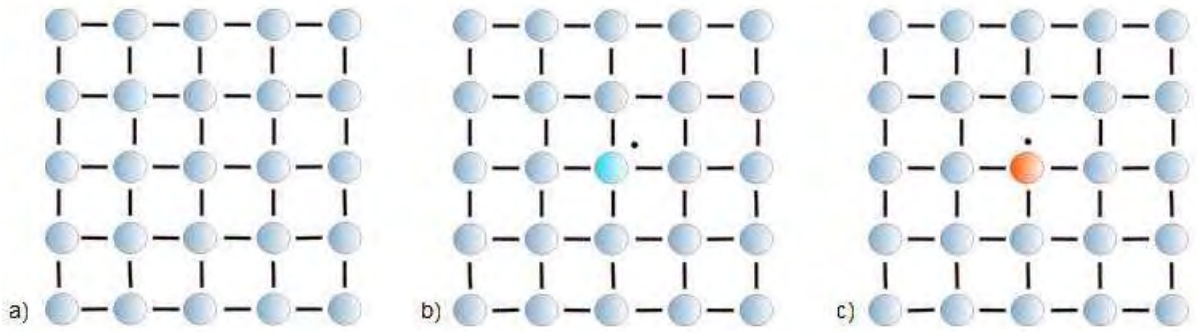

Fig: 2.1 a) intrinsic, b) n-type and c) p-type Si

2.3 Fermi Level, conduction band and valence band:

In theory a crystal lattice is composed of infinite repetitions of its basic structure. This theoretical infinite structure contains theoretically limitless energy levels which form energy bands, due to the energy levels coming very close together and forming quasi-continuous bands. The Fermi Level is the highest energy level that can be occupied by electrons. The valence band is the highest band that contains electrons at 0 Kelvin and the conduction band is the lowest band that does not contain electrons. The difference between the conduction and valence band energies is known as the energy bandgap (Eg). In an insulator the bandgap is comparatively large (3 eV or greater) so a large amount of energy is needed for electrons to move to the conduction band which does not occur at room temperature. In a conductor there is some overlap between the conduction and valence bands so electrons form the valence band can enter the conduction band in large numbers at room temperature. In semiconductors, the bandgap is low enough that some electrons gain sufficient energy to move form he valence band to the conduction band.

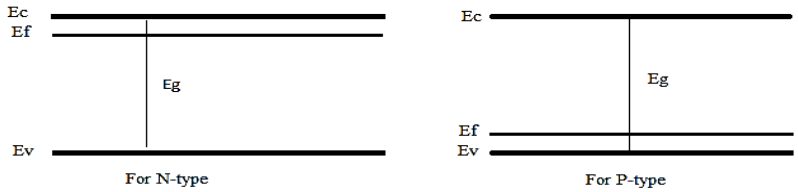

Fig 2.2 Energy band diagrams for n-type (left) and p-type (right) semiconductors.Conduction band, valence band and Fermi Level are shown.

2.4 Depletion region formation, drift and diffusion currents:

When a p-type material is connected to an n-type material a p-n junction is formed. Diffusion current will arise in this scenario. The diffusion current (J_{diff}) involves the movement of majority charge carriers (electrons in the n-side and holes in the p-side) form areas where their concentrations are high across the junction to the area where their concentrations are low. Thus electrons move to the p-side and holes to the n-side. This leaves a number of donor atoms that have lost electrons and become positive ions in the n-side and acceptor atoms that have lost holes (or gained electrons) and become negative ions in the p-side. This ion-containing region on both sides of the junction is known as the depletion region. The positive ions in the p-side and the negative ions on the n-side exert and electric field in the depletion region due to the potential

difference between them. This electric field is the cause of another current known as the drift current. The drift current (J_{drift}) involves minority charge carriers (electrons in the p-side and holes in the n-side) which travel to the depletion region via diffusion. Due to the action of electron field on the charged particles, they cross the junction. Holes move with the electron field and electrons move against the electric field. At equilibrium the drift and diffusion currents cancel each other out so there is no net current. In terms of energy bands, the position of the bands relative to the Fermi Level does not change so there is band bending [4] of the conduction and valence bands, where the conduction and valence bands of the p-type and n-type material come together via bending in the depletion region.

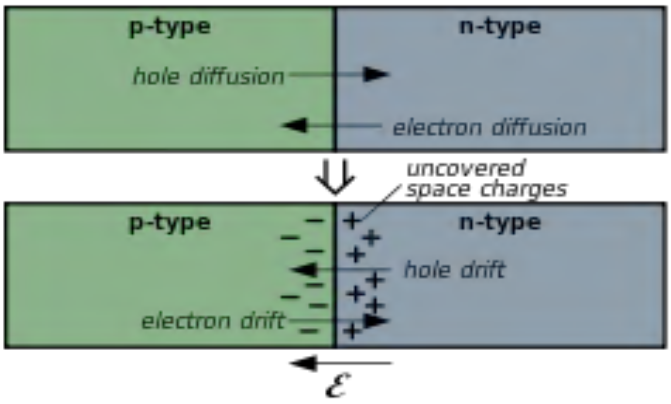

Fig 2.3 p-n junction before (top) and after (bottom) equilibrium

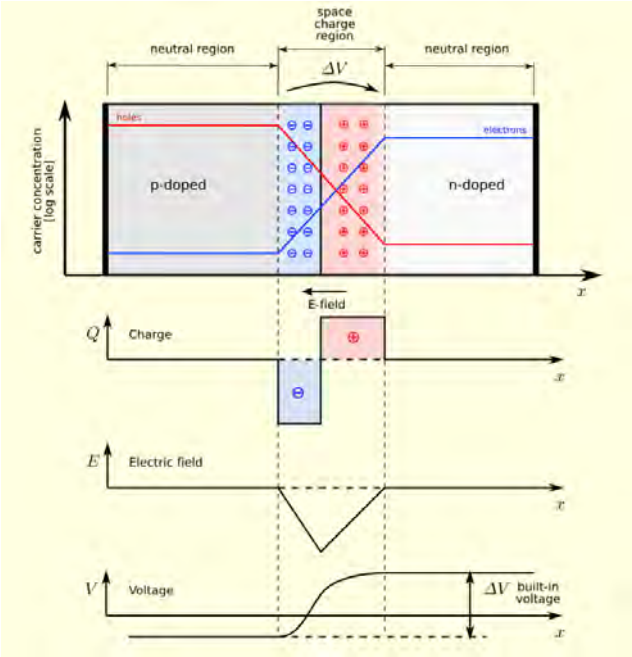

Fig 2.4 Top to bottom: diagram of p-n junction and its charge densities, electric field and potential difference

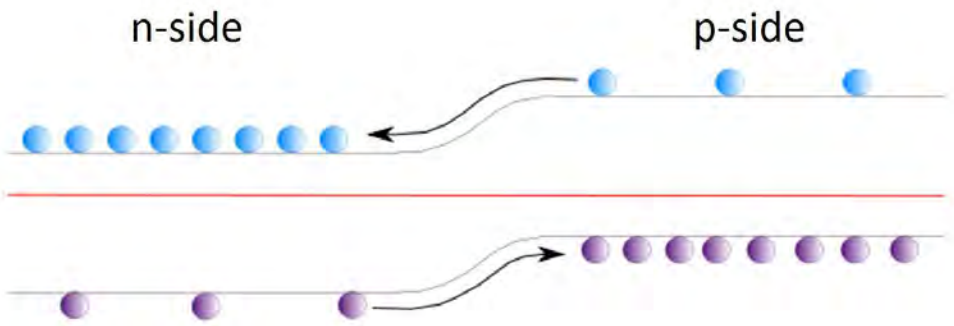

Fig 2.5 Band bending and drift current. Drift of electrons (blue) from is from p-side to n-side and drift of holes (purple) is from p-side to n-side. The red line is the Fermi Level.

2.5 J-V Characteristics of P-N junction:

When a voltage is applied to the system, it is no longer at equilibrium. [4] This allows a net current to flow through the system. The system can either be in forward biased or reverse biased condition.

In reverse biased condition, the positive pole of the voltage is connected to the n-side and the negative pole is connected to the p-side. The p-side diffusion region gains more electrons from the negative pole and the n-side depletion region loses more electrons to the positive pole. This leads to increased numbers of negative acceptor ions the p-side and positive donor ions in n-side depletion regions, causing them to become more negative and positive respectively, increasing the potential difference between them, and also the depletion region width. This increased potential barrier restricts the flow of diffusion current and may eliminate it altogether. The drift current will still flow. Thus the following formula can be applied:

$J(V)=J_{drift\text{-}n}+J_{drift\text{-}p}$ where J is the current due to voltage V and $J_{drift\text{-}n}$ and $J_{drift\text{-}p}$ are the drift currents of electrons (at conduction band) and holes (at valence band) respectively.

In forward biased condition, the p-side is connected to the positive pole of the voltage and n-side is connected to the negative pole. Holes in the p-side and electrons in the n-side are repelled by the positive and negative poles, respectively, and enter the depletion region where the holes combine with negative acceptor ions and the electrons combine with positive donor ions. This reduces the potential difference and the width of the depletion regions. Thus, the potential barrier to diffusion current is reduced and the current can increase exponentially: $J = J_{diff}\exp(\frac{qV}{kT})$ where q is the charge of an electron, k is the Boltzmann constant and T is the temperature in Kelvin.

The drift current becomes less prominent as the voltage drop decreases and the diffusion current increases, leading to the following formula:$J = (J_{diff-n} + J_{diff-n})\exp(\frac{qV}{kT})$ where J is the current

due to voltage V and $J_{diff\text{-}n}$ and $J_{diff\text{-}p}$ are the drift currents of electrons (at conduction band) and holes (at valence band) respectively.

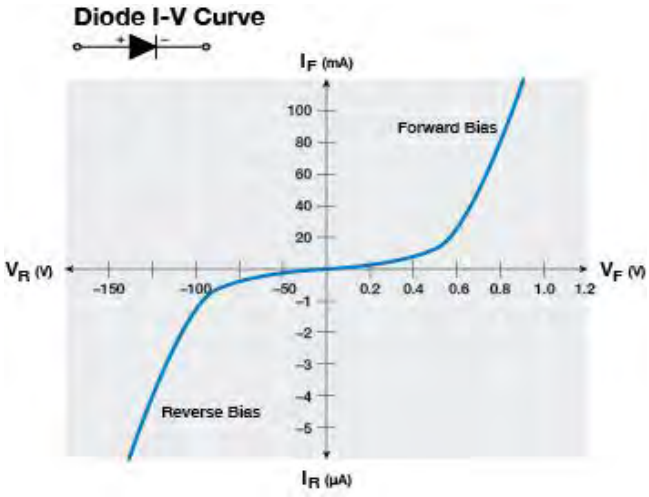

Fig 2.6 I-V characteristics of semiconductor diode. Since J is simply current per unit area, I can be replaced by J without other alterations to the equation

Under illumination, the junction is not at equilibrium. Electron-hole pairs are formed due to abruption of photons as previously stated. The minority carriers (holes in n-type material and electrons in p-type material) drift to the depletion region where they contribute to the current. Therefore to maximize current density, the depletion region must be as close to the surface as possible to allow as many photons as possible to reach the depletion region (many photons are already absorbed at the surface), the depletion region must be as wide as possible to allow as many EHPs as possible to reach it and contribute to the photocurrent. The number of defects should be kept to a minimum as well, as this will lead to a higher diffusion length of minority carriers, allowing more of these charge carriers to reach the depletion region and increase the photocurrent.

The equivalent circuit of a solar cell is given below:

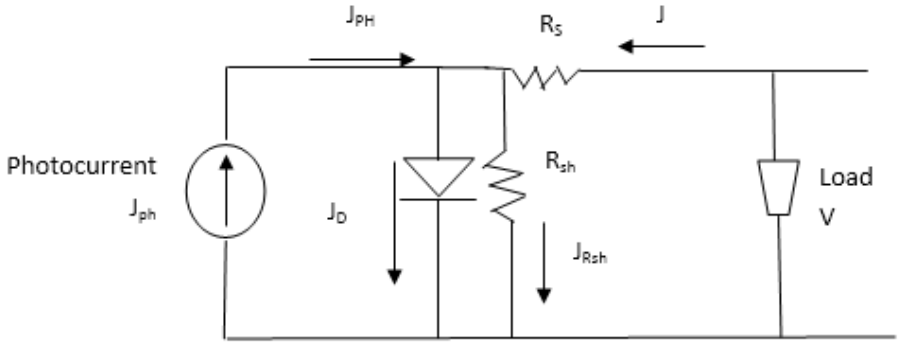

Fig 2.7 Equivalent circuit of a real solar cell

From this circuit, we can see J_D, which is the current density of the dark current and increases exponentially, and $J_{ph,}$ whichis the current density of photocurrent, are both present at illumination and affect the current J that flows through the load with voltage V. The components of the dark current (which includes the diffusion current mentioned above as well as other sources of loss) and their formulae as well as the formulae of the different components of the photocurrent (n-side, p-side and depletion region photocurrents) are elaborated on later in this text. In a real solar cell, unlike in ideal conditions, we must consider resistance in the circuit, which is represented by the series resistance (R_s), which is preferably low, and the shunt resistance (R_{sh}), which is higher. Series resistance is the resistance that current encounters when it flows through the system. Shunt is caused by defects such as impurities, defects in the crystal structure and precipitates which create a short circuit in the p-n junction and this represented by the shunt resistance. Using Kirchhoff's Current Law (KCL) it can be seen that:

$$J_{pH} = J_D \left[exp\left(\frac{q(V - JR_S)}{2kT} \right) - 1 \right] + J_{Rsh} - J$$

The voltage across R_s is V_{Rs}=JR_s and using Kirchhoff's Voltage Law (KVL) the current through shunt resistance is: $J_{Rsh} = \frac{V - JR_S}{R_{Sh}}$

Therefore the current density voltage relationship of the solar cell can be given as:

$$J = J_D \left[exp\left(\frac{q(V - JR_S)}{2kT} \right) - 1 \right] + \frac{V - JR_S}{R_{Sh}} - J_{PH}$$

Chapter 3

Dark Current, Photocurrent and J-V calculations of CZTS

3.1 Introduction

In this chapter the equations required to determine J-V characteristics of a particular solar cell structure which uses p-CZTS as the absorber layer are discussed. The band diagrams of the junction, the sources of loss, and the photocurrent are th focus of this chapter.

3.2 Solar Cell Structure:

Here a solar cell with structure Mo/CZTS/CdS/i-ZnO/TCO, where CZTS is the p-type material and is also known as the absorber, Cadmium Sulphide(CdS) is as n-type material, is to be considered.

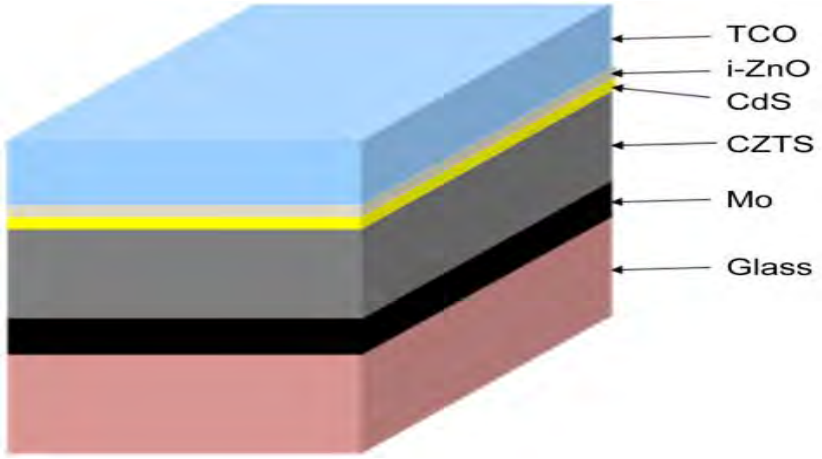

Fig 3.1 A typical schematics representation of CZTS, CdS solar cell

The initial stepis to sputter an 800nm thick Mo layer (which will be the back contact for the CZTS layer) on the glass substrate. The back contact is for required to improve conductivity.Then, CZTS layer is deposited on the Mo layer. At first, CZTS nanoparticlesare formed. [13]Next, annealing occurs, either in an inert atmosphere to initiate nucleation or a reactive atmosphere to initiate grain growth of CZTS. A 100-nm thick n-CdS layer is used in CZTS-based solar cells to form a p-n junction with p-CZTS. A 110 nm thick window layer,in this case intrinsic zinc oxide or i-ZnO deposited by sputtering. Thei-ZnO reduces shunting pathways and prevents the absorber from mixing with the transparent conductive oxide (TCO) when the thin CdS layer does not completely cover for the CZTS layer. Then the aforementioned TCO layer e.g. ITO or AZO of 110 nm thicknessis deposited via sputtering. Finally, Ni/Al metal contactsare formed on the TCO.These contacts collect the photo generated electrons for the external circuit with minimal resistive losses.

3.3 Energy-band Diagrams:

The energy band diagrams for the n-CdS/p-CZTS junction before the junction is formed, at thermal equilibrium and under illumination are shown.

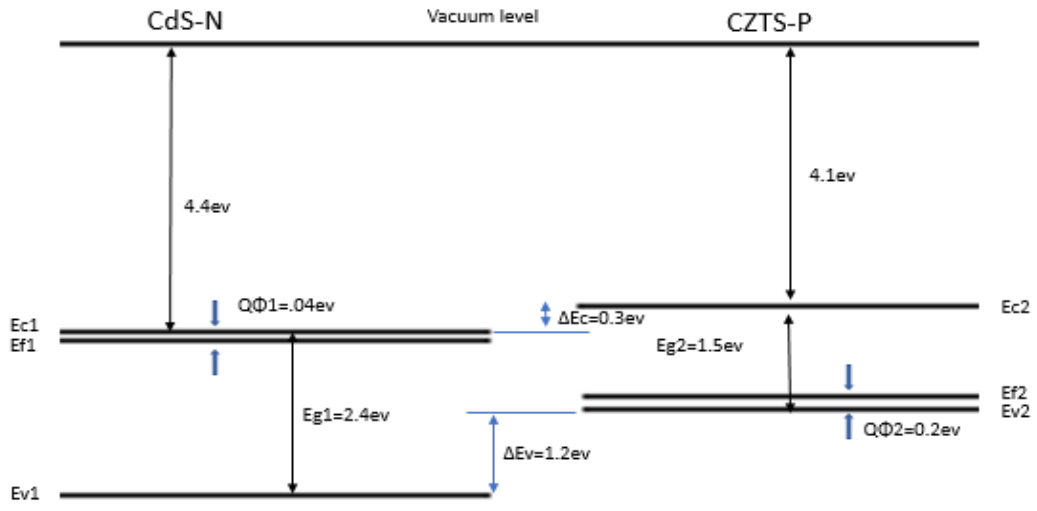

Fig 3.2 Energy band diagram before junction formation

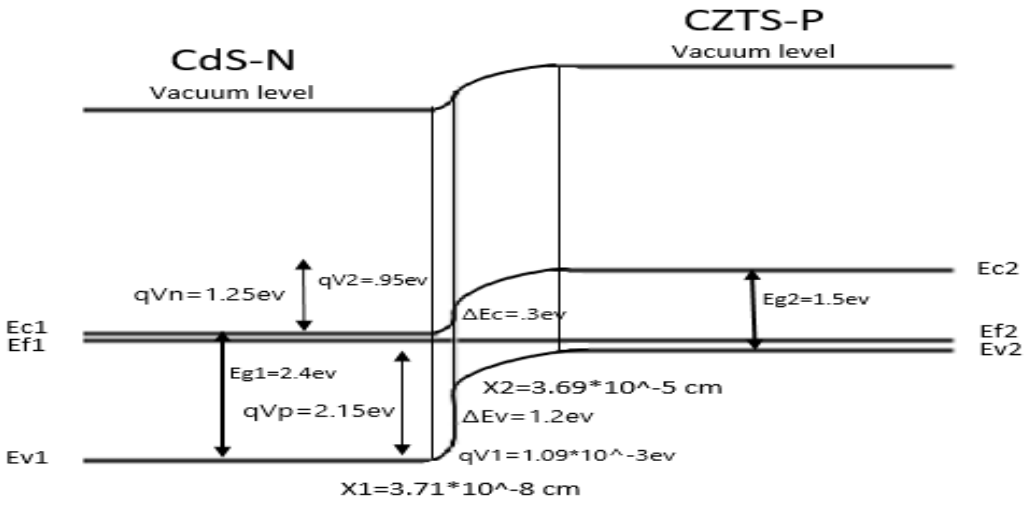

Fig 3.3 Energy band diagram at thermal equilibrium. Note the band bending to accommodate constant Fermi Level. Example values of depletion width and depletion region voltage components are shown for clarification purposes

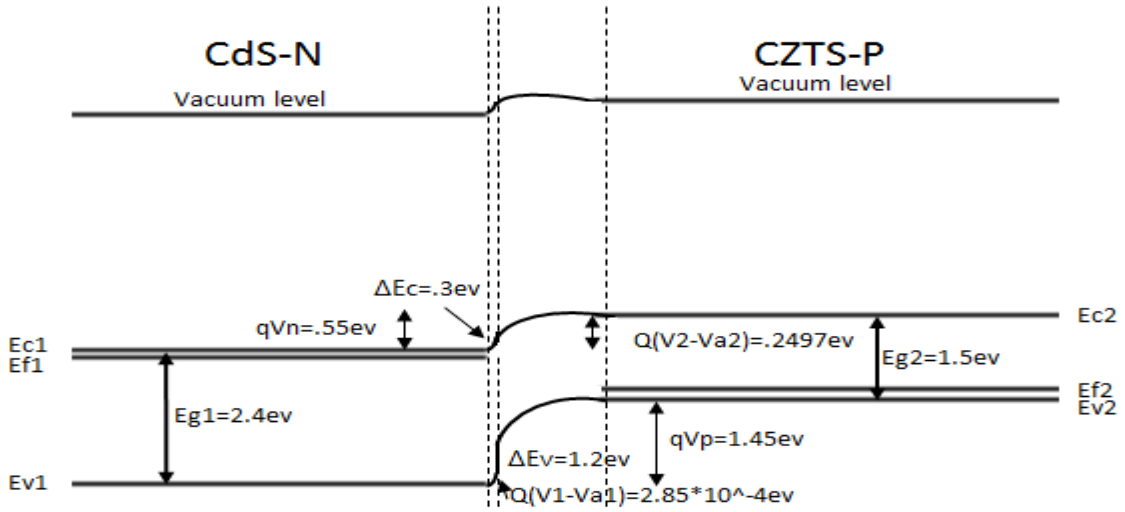

Fig 3.4 Energy band diagram at illumination. Example values of depletion width and depletion region voltage components are shown for clarification purposes

Under illumination, it is observed the potential barrier impeding current flow is reduced, allowing the EHPs generated by photon absorption to flow through the system.

3.4 Dark Current:

Various mechanisms resulting in current loss are potentially present in kesterite solar cells, namely: Diffusion (D), thermionic emission (TE), radiative recombination (RR), non-radiative recombination (NRR), trap-assisted tunneling (TATR) and CdS/CZTS interface recombination (IR). These constitute the dark current.J-V relationship of a kesterite solar cell has already been noted:

$$J = J_D\left[exp\left(\frac{q(V-JR_S)}{2kT}\right)-1\right]+\frac{V-JR_S}{R_{Sh}}-J_{PH}\ldots\ldots\ldots\ldots\ldots\text{eq}^{n}\ (1)$$

Where

J_D (is the dark current) $=J_{RR}+J_{diff}+J_{TE}+J_{TATR}+J_{IR}$

Here,

J_{RR}=Reverse-saturation current density due to radiative recombination

J_{diff} =Reverse-saturation current density due to diffusion

J_{TE}=Reverse-saturation current density due to thermionic emission

J_{TATR} = Reverse-saturation current density due to trap-assisted tunneling recombination

J_{IR}= Reverse-saturation current density due to CdS/CZTS interface recombination

J_{PH}=Photocurrent

R_S=Series resistance

R_{Sh}=Shunt resistance

q=Charge of electron/hole

k=Boltzmann constant

T=Temperature

V=voltage

3.4.1 Trap-assisted tunneling recombination

Electrons travelling between energy bands sometimes enter localized energy states formed due to impurities or defects in the material. These energy states are called traps. From the trap, the electron can move to the valence band. This can be seen as electron-hole recombination within the trap and is known as Shockley-Read-Hall (SRH) recombination. Quantum tunneling is the process where charge carriers can 'pass through' a potential barrier (e.g. the cliff in the CdS/CZTS junction) by obtaining energy from the surroundings.[10]This is considered due to the Heisenberg Uncertainty Principle which limits the precision with which the position and momentum of a particle can be determined. [2] This principle posits that there is a non-zero probability of any solution. Probability of quantum tunneling of charge carriers from energy bands to traps and vice versa increases due to large electric fields in depletion region and tunneling is prominent in heterojunctions due to the large number of energy states in the bandgap. [11] Trap-assisted tunneling occurs when the energy barrier is split by the traps. Thus the charge carrier can tunnel through a number of thinner barriers instead of thicker ones, increasing the probability of tunneling. [4]

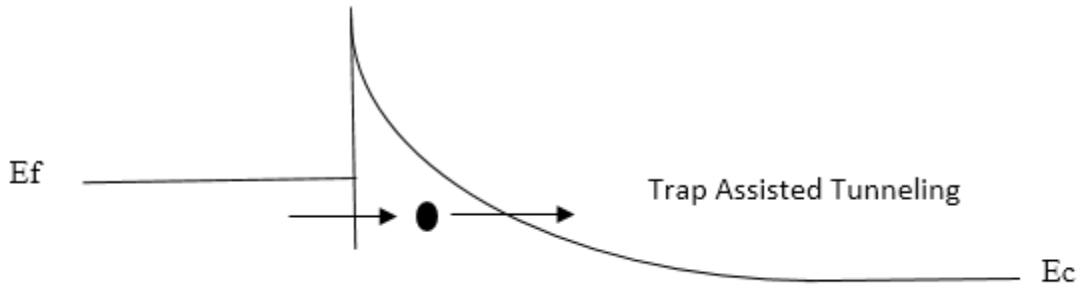

Fig 3.5 Trap-assisted tunneling mechanism

The following expression can be used to obtain the reverse saturation current due to trap-assisted tunneling recombination. It encompasses both SRH recombination and tunneling through traps and was developed by Hurx et al.

$$J_{TATR} = q\left[\frac{x_n n_{i-CdS}(1+F_{CdS})}{\tau_n} + \frac{x_p n_{i-CZTS}(1+F_{CZTS})}{\tau_p}\right] \text{…….. eq}^{n}\ (2)$$

Here,

x_n=Depletion width (CdS)

x_p=Depletion width (CZTS)

n_{i-CdS}=Intrinsic carrier concentration (n-CdS)

n_{i-CZTS}=Intrinsic carrier concentration (p-CZTS)

τ_n=Minority carrier (hole) lifetime (n-CdS)

τ_p=Minority carrier (electron) lifetime (p-CZTS)

F_{CdS}=Effect of tunneling (n-CdS)

F_{CZTS}=Effect of tunneling (p-CZTS)

The intrinsic carrier concentrations for CdS and CZTS were calculated using the formula:

$$n_{i-CdS} = \sqrt{N_{c-CdS}N_{V-CdS}}exp\left(\frac{-Eg_{CdS}}{2kT}\right) \text{…….eq}^{n}\ (3)$$

$$n_{i-CZTS} = \sqrt{N_{c-CZTS}N_{V-CZTS}}exp\left(\frac{-Eg_{CZTS}}{2kT}\right) \text{…….eq}^{n}\ (4)$$

Where,

N_{c-CdS}=Effective density of states of Conduction Band (n-CdS)

N_{V-CdS}=Effective density of states of Valence Band (n-CdS)

Eg_{CdS} =Energy band gap (n-CdS)

Eg_{CZTS}= Energy band gap (p-CZTS)

Effective density of states of conduction and valence bands of CZTS were found using the equations:

$$N_{c-CZTS} = 2\left[\frac{2\pi m^*_{e\,(CZTS)} kT}{h^2}\right]^{3/2} \quad \text{.....eq}^{n}\ (5)$$

And

$$N_{V-CZTS} = 2\left[\frac{2\pi m^*_{h\,(CZTS)} kT}{h^2}\right]^{3/2} \quad \text{.....eq}^{n}\ (6)$$

Where

$m^*_{e\,(CZTS)}$ =Electron effective mass (p-CZTS)

$m^*_{h\,(CZTS)}$ = Hole effective mass (p-CZTS)

h= Planck's constant

The depletion widths of n-CdS (x_n) and p-CZTS (x_p) were calculated using the formulae:

$$x_n = \sqrt{\frac{2\varepsilon_n V_n}{qN_D}} \quad \text{.....eq}^{n}\ (7)$$

$$x_p = \sqrt{\frac{2\varepsilon_p V_p}{qN_A}} \quad \text{.....eq}^{n}\ (8)$$

Where

ε_n =Dielectric permittivity (n-CdS)

ε_p = Dielectric permittivity (p − CZTS)

V_n =Component of built in and applied voltage (n-CdS)

V_p = Component of built in and applied voltage (p − CZTS)

N_D =Donor concentration (n-CdS)

N_A =Acceptor concentration (p-CZTS)

To find $V_n$and V_p we need to find to find built-in voltage and apply the following formulae:

$qV_{bi} = Eg_{CZTS} - \Delta E_C - q\Phi_{CZTS} - q\Phi_{CdS}$…….eq^n (9)

$qV_{bi} = \left(1 + \frac{\varepsilon_n N_D}{\varepsilon_p N_A}\right)(qV_n)$…….eq^n (10)

$qV_p = qV_{bi} - qV_n$…….eq^n (11)

Where,

V_{bi}= Built in voltage of the junction

Eg_{CZTS} =Energy band gap (p-CZTS)

ΔE_C =Conduction band offset

Φ_{CdS} =Difference between conduction band edge and Fermi level (n-CdS)

Φ_{CZTS} =Difference between valence band edge and Fermi level (p-CZTS)

To find Φ_{CdS} and Φ_{CZTS} we need to apply the followign formulae:

$q\Phi_{CdS} = kTln(\frac{N_{c-CdS}}{N_D})$…….eq^n (12)

$q\Phi_{CZTS} = kT\ ln\left(\frac{N_{V-CZTS}}{N_A}\right)$…….eq^n (13)

To find minority carrier lifetime of n-CdS(τ_n) the following equation was used:

$\frac{1}{\tau_n} = \frac{1}{\tau_B} + \frac{1}{\tau_S}$…….eq^n (14)

Where,

τ_B = Bulk lifetime

τ_S= Surface lifetime

To find these two values we use the following equations:

$\tau_B = \frac{1}{\sigma v_{th} N_A}$…….eq^n (15)

$\tau_S = \frac{1}{2\sigma v_{th} N_{it}}$…….eq^n (16)

Where

σ=Capture cross section of holes (n-CdS)

v_{th} = Hole thermal velocity (n − CdS)

N_{it}= Interface trap density

F,the effect of tunneling, affects the density of carrier captured in traps as well as emission rate of the carriers in traps. F_{CdS} and F_{CZTS}can be found from the equations:

$$F_{CdS} = 2\sqrt{3\pi}\frac{E_n q\hbar}{\sqrt{24 m^*_{e(CdS)}(kT)^3}} exp\left(\frac{E_n q\hbar}{\sqrt{24 m^*_{e(CdS)}(kT)^3}}\right)^2$$ …….eq^n (17)

$$F_{CZTS} = 2\sqrt{3\pi}\frac{E_p q\hbar}{\sqrt{24 m^*_{h\,(CZTS)}(kT)^3}} exp\left(\frac{E_p q\hbar}{\sqrt{24 m^*_{h\,(CZTS)}(kT)^3}}\right)^2$$ …….eq^n (18)

Where

$m^*_{e(CdS)}$ = Electron effective mass (n − CdS)

E_n = Built − in field (n − CdS)

E_p = Built − in field (p − CZTS)

To find built in field E of n-CdS and p-CZTS we need to use the following equations:

$E_n = \frac{qN_D x_n}{\varepsilon_n}$…….eq^n (19)

$E_p = \frac{qN_A x_p}{\varepsilon_p}$…….eq^n (20)

3.4.2 CdS/CZTS Interface Recombination

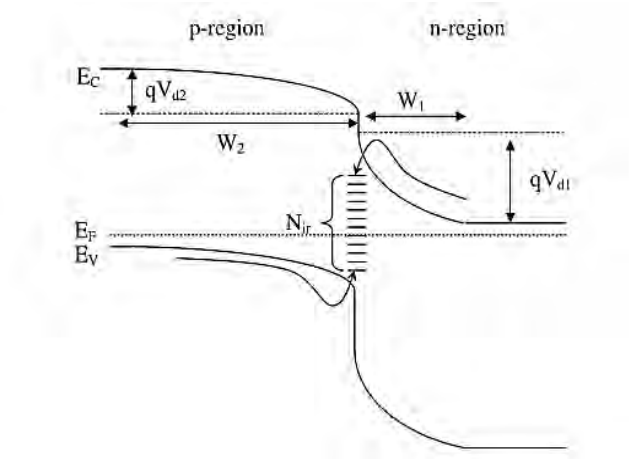

Fig 3.6 Interface recombination. Note the interface defect energy states (Nir)

CdS/CZTS interface contains many defects which arise due to the lattice terminating abruptly leaving large numbers of dangling bonds which act as recombination centersas well as thermal expansion mismatches i.e. bond length changes with respect to the energy of the bond, but when the bond energy vs. bond length curve is asymmetric, and thus thermal expansion coefficient is nonzero (bond length changes with respect to temperature). Thus temperature has an effect on interface recombination, and so do the conduction and valence band offsets. Interface recombination is modeled by the equation:

$$J_{IR} = qS\mathrm{n}_{\mathrm{i-CZTS}}\left(1 + \gamma DOS e^{-(\Delta E_C + \Delta E_V)/2kT}\right)$$.....eq^{n} (21)

Where,

γDOS =Density of states enhancement factor

$\mathrm{S} =$ Interface recombination speed

$\Delta \mathrm{E_C} =$ Conduction band offset

$\Delta \mathrm{E_V} =$ Valence band offset

To find γDOS the equation required is:

$$\gamma DOS = \frac{N_{c-CdS}}{N_{V-CZTS}}$$.....eq^{n} (22)

3.4.3 Diffusion

Diffusion current occurs due to the movement of charge carriers (electrons and holes) down a concentration gradient. In equilibrium, the diffusion current is cancelled out by the drift current (due to electric field acting on charge carriers) as the two currents flow in opposite directions. Under illumination, a forward bias is applied to the junction, which reduces the electric field across it, so the diffusion current is greater than the drift current.[8] Diffusion current itself is not dependent on the electric field and does not obey Ohm's Law. Diffusion current depends on the concentration gradient instead of the charge carrier concentration itself.

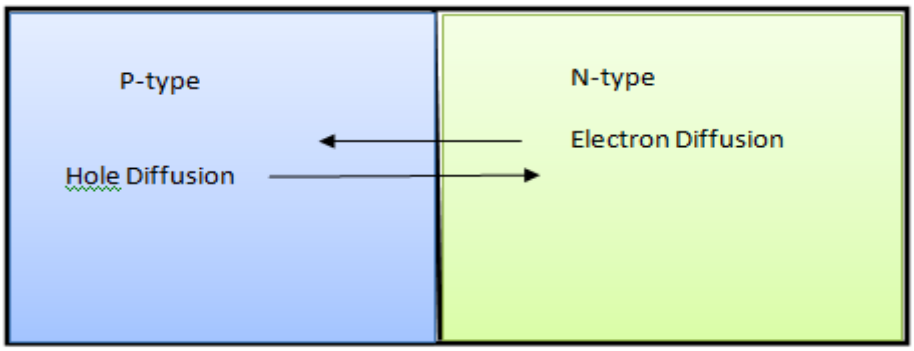

Fig 3.7 Diffusion

Electrons diffuse from the n-side (CdS) where they are present in higher concentration across the potential barrier to the p-side where they recombine with holes either in the bulk or at the surface. Holes diffuse from the p-side to the n-side and recombine with electrons. However the diffusion current due to hole diffusion is much lower than that due to electrons because of the much larger valence band offset, resulting in reduced current density-voltage characteristic. The action of these minority carriers is described by the continuity equations. Current density-voltage dependence is less sensitive to temperature for diffusion than it is for thermionic emission.

The diffusion currents are as follows:

Electron diffusion current (p-CZTS)

$J_{diff-CZTS} = qD_n \frac{d\Delta n_p}{dx} = \frac{q*Dn*n_{po}}{Ln}$.....eq^n (23) at x=$x_p$

Where D_n= Diffusion coefficient of electrons (p-CZTS)

n_{po}=Minority electron concentration(p-CZTS)

L_n =Minority electron diffusion length (p-CZTS)

To find D_n and L_n we use:

$D_n = \left(\frac{kT}{q}\right)\mu_n$…….eq^n (24)

$L_n = \sqrt{D_n \tau_n}$…….eq^n (25)

Where μ_n=Mobility of electron (p-CZTS)

And to find n_{po} we use:

$n_{po} = \frac{n_{i-CZTS}{}^2}{N_A}$…….eq^n (26)

Hole diffusion current (n-CdS):

$J_{diff-CdS} = -qD_p \frac{d\Delta p_n}{dx} = -\frac{q*Dp*p_{no}}{Lp}$…….eq^n (27) at x=-$x_n$

Where

D_p= Diffusion coefficient of holes (n-CdS)

p_{no}=Minority hole concentration(n-CdS)

L_p =Minority hole diffusion length (n-CdS))

To find D_p and L_p we use:

$D_p = \left(\frac{kT}{q}\right)\mu_p$…….eq^n (28)

$L_p = \sqrt{D_p \tau_p}$…….eq^n (29)

μ_p=Mobility of hole (n-CdS)

And to find p_{no} we use:

$p_{no} = \frac{n_{i-Cds}{}^2}{N_D}$…….eq^n (30)

Thus total Diffusion current J_D is found by adding the diffusion currents of n-CdS and p-CZTS:

$J_{diff} = J_{diff-CZTS} + J_{diff-CdS}$…….eq^n (31)

3.4.4 Thermionic Emission

Thermionic emission depends on the assumption that a probability exists for majority charge carriers to gain sufficient energy to overcome the potential barrier and this probability is proportional to temperature. The barrier height is more important than the barrier shape. Per Fermi Dirac Statistics the density of electrons (for n-type substrate) decreases exponentially as a function of their energy above the conduction band edge.[9] At any finite (non-zero) temperature, the carrier density at any energy is not zero. The integrated number of carriers exists above the barrier height and these carriers are not contained by the barrier so they can contribute to the thermionic emission current. Thermionic emission is more prominent at lower doping concentrations.

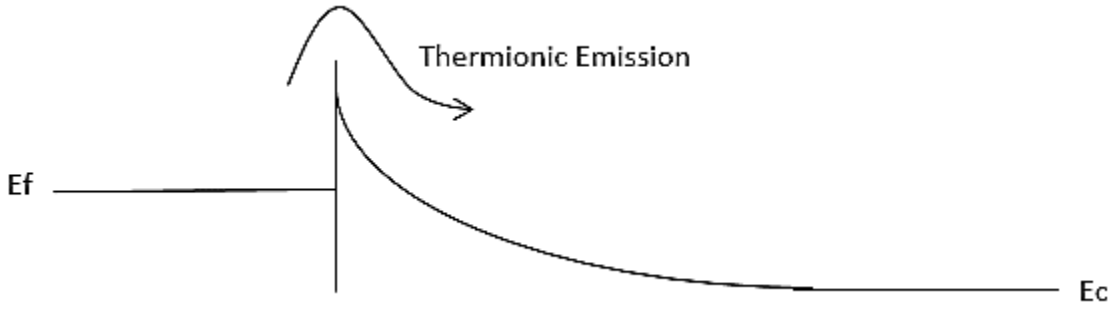

Fig 3.8 Thermionic emission

Total thermionic emission current over the barrier due to electrons is given by:

$J_{TE} = A^{*}T^{2}exp\left(-\frac{q\emptyset_B}{kT}\right)$…….eq^{n} (32)

Where

Φ_B=Barrier height

A^{*} = Effective Richardson Constant which is a function of m^{*}(effective mass)

The barrier height is given by the following equation:

$\Phi_B = \Delta E_C + V_n + V_p$…….eq^{n} (33)

And the Effective Richardson Constant is given by the equation:

$A^{*} = \frac{4\pi q m^{*}_{e(CdS)} k^2}{h^3}$…….eq^{n} (34)

3.4.5 Radiative Recombination:

This is the opposite of optical generation. An electron returns to its equilibrium energy level, recombining with a hole and thus emits a photon. As the photon has very little momentum, this type of recombination is significant in direct bandgap semiconductor materials. Direct radiative recombination has shorter carrier lifetimes than indirect radiative recombination, due to lower number of interactions, whereas indirect radiative recombination involves interactions with particles such as phonons. CZTS, like many other thin films materials such as CIGS and CdTe is a direct bandgap material which enables it to absorb light in thin regions, allowing a thin layer of material to be used. However this results in radiative recombination losses at the depletion region being a significant factor in current loss.

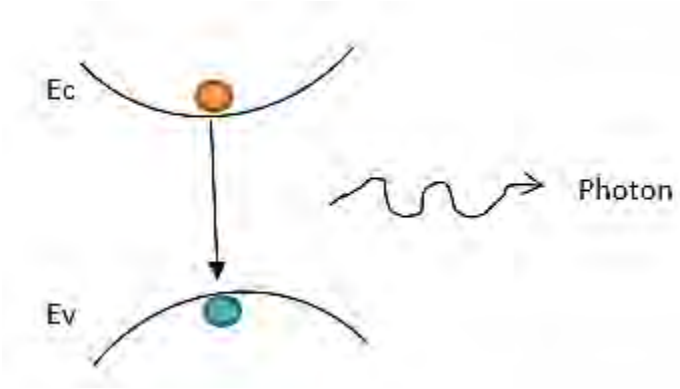

Fig 3.9 Radiative recombination

Radiative recombination losses at the depletion region can be modeled by the following equation:

$$J_{RR} = q\left(x_n * B_n * {n_{i-CdS}}^2 + x_p * B_p * {n_{i-CZTS}}^2\right)$$.....eq^n (35)

Where

x_n=Depletion width (n-CdS)

B_n=Radiative recombination coefficient (n-CdS)

x_p=Depletion width (p-CZTS)

B_p= Radiative recombination coefficient (p-CZTS)

The radiative recombination coefficients for n-CdS and p-CZTS can be calculated by the formulae:

$$B_n = \frac{8*\pi*nr_{CdS}^2}{c^2*h^3*{n_{i-CdS}}^2} * \int_{Eg_{CdS}}^{\infty} \frac{\alpha_{CdS}*E^2 dE}{exp\left(\frac{E}{k*T}\right)-1}$$.....eq^n (36)

Where

nr_{CdS}=Refractive Index (n-CdS)

α_{CdS}=Absorption coefficient (n-CdS)

$$B_p = \frac{8*\pi*nr_{CZTS}^2}{c^2*h^3*{n_{i-CZTS}}^2} * \int_{Eg_{CZTS}}^{\infty} \frac{\alpha_{CZTS}*E^2 dE}{exp\left(\frac{E}{k*T}\right)-1}$$ ……eq^n (37)

Where

nr_{CZTS}=Refractive Index (p-CZTS)

α_{CZTS}=Absorption coefficient (p-CZTS)

3.5Photocurrent:

In this section, we derive the equation for photocurrent of p-n heterojunction solar cell. Figure 1 shows a basic cross section of CZTS solar cell. As thin film solar cell is very thin so we have to deposit it in a substrate. The most common type of substrate is glass but if we use flexible substrate then it would have some new application.

When a monochromatic light of wavelengthλ is incident on the front surface of solar cell the photocurrent and spectral response, that is, the number of carriers collected per incident photon at each wavelength. [12]

The generation rate of electron – hole pair at a distance x from the semiconductor surface shown in fig 3.10.

$G(\lambda,x)=\alpha_1(\lambda)\emptyset(\lambda)[1-R(\lambda)]exp[-\alpha_1(\lambda)x]$ …….eq^n (38)

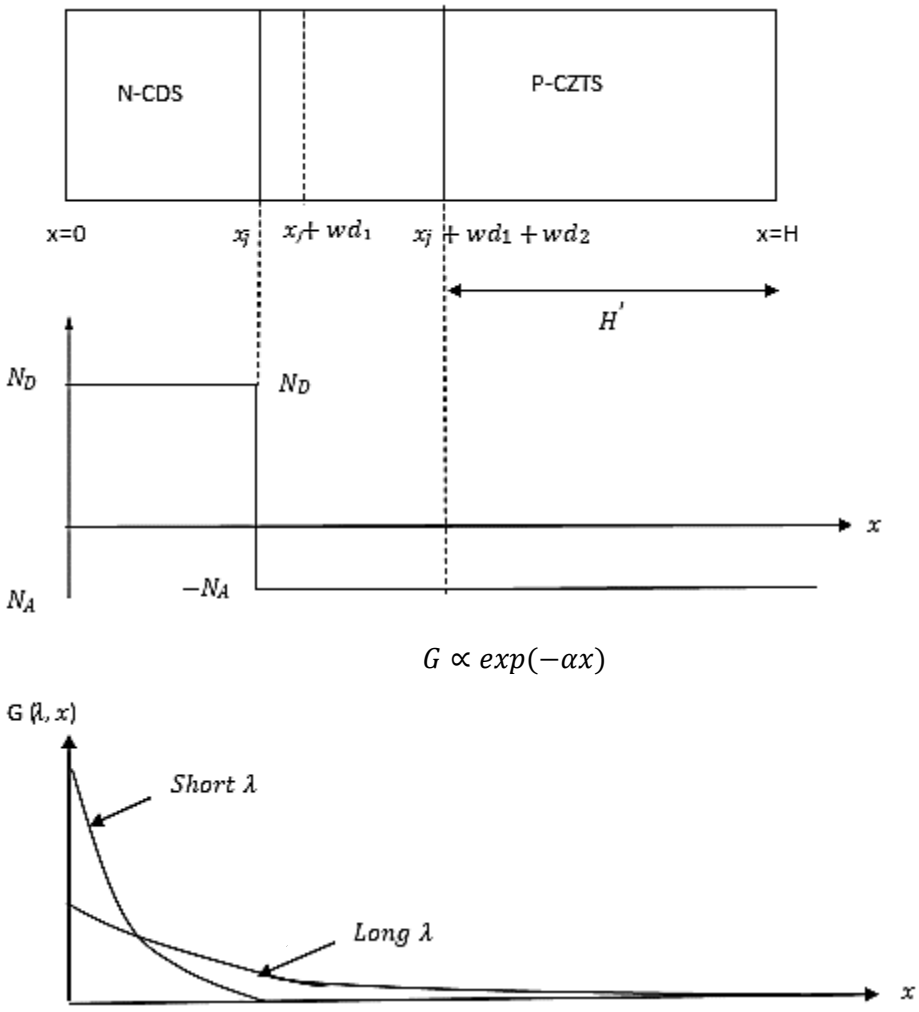

Fig 3.10 (top) Solar cell dimensions under consideration (middle) Assumed abrupt doping profiles ND >> NA (bottom) Generation rate as a function of distance for long and short wavelengths.

Here,

$\alpha_1(\lambda)$ = Absorption Co-efficient of CDS

$\emptyset(\lambda)$ =Number of incident photons per area per time per unit bandwidth

R (λ) =Function of these photons reflected from the surface

For an abrupt p-n junction solar cell with constant doping on each side, Fig. 2, there are no electric fields outside the depletion region. Photo generated carriers in these regions are collected by a diffusion process while that in the depletion region by drift process.

Under low injection condition, steady state continuity equation-

G_n-($\frac{n_p-n_{po}}{\tau_n}$)+$\frac{1}{q}\frac{d_{jn}}{dx}$ = 0 …….eq^n (39)

For electrons in the p-type substrate are-

G_p-($\frac{p_n-p_{no}}{\tau_p}$)-$\frac{1}{q}\frac{d_{jp}}{dx}$ = 0…….eq^n (40)

For holes in the n-type layer, the current density equations are-

$J_n = q\mu_n n_p \varepsilon + qD_n(\frac{d_{np}}{dx})$…….eq^n (41)

$J_p = q\mu_p p_n \varepsilon - qD_p(\frac{d_{pn}}{dx})$…….eq^n (42)

3.5.1 N-Side Photocurrent:

For the top n-side of the junction, Equations. 1, 3, and 5 can be combined to yield an expression:

$\alpha_1(\lambda)\ \emptyset(\lambda)$ [1-R (λ)] exp[-$\alpha_1(\lambda)x$]-($\frac{p_n-p_{no}}{\tau_p}$)-$\frac{1}{q}\frac{d}{dx}(q\mu_p p_n\varepsilon - qD_p(\frac{d_{pn}}{dx}))$=0

$\Rightarrow \alpha_1(\lambda)\emptyset(\lambda)$[1-R($\lambda$)]exp[-$\alpha_1(\lambda)x$]-($\frac{p_n-p_{no}}{\tau_p}$)+$D_p.\frac{d^2p_n}{dx^2}$ = 0

$\Rightarrow D_p.\frac{d^2p_n}{dx^2}$+ $\alpha_1\emptyset(\lambda)$[1-R]exp[-$\alpha_1(\lambda)x$]-($\frac{p_n-p_{no}}{\tau_p}$)=0…….eq^n (43)

The general solution of equation (43) is

$p_n - p_{no}$=$C_2\cosh\left(\frac{x}{L_p}\right) + C_3\sinh\left(\frac{x}{L_p}\right) - \frac{\alpha_1\emptyset[1-R]\tau_p}{\alpha_1{}^2Lp^2-1}$. exp (-$\alpha_1 x$)…….eq^n (44)

Where, $L_p = \sqrt{D_p\tau_p}$ is the diffusion length, and C_2 and C_3 are constants.

There are two Boundary conditions. At the surface, we have surface recombination with a recombination velocityS_p:

1st boundary condition:

$D_p.\frac{d}{dx}(p_n - p_{no}) = S_p(p_n - p_{no})$ at x=0

At the depletion edge, the excess carrier density is small due to the electric field in the depletion region.

2nd Boundary condition-

$p_n - p_{no} = 0$ At $x = x_j$

By using these two boundary condition we get the values of C_2 and C_3. And substituting the values of C2 and C3 in equation (44) we get,

$$P_n - P_{no} = \left[\frac{\alpha_1 \emptyset[1-R]\tau_p}{(\alpha_1{}^2 L_p{}^2 - 1)}\right] * \left[\frac{\left(\frac{S_P L_P}{Dp} + \alpha_1 L_P\right)\sinh\left(\frac{x_j - x}{Lp}\right) + \exp(-\alpha_1 x_j)\left(\frac{S_P L_P}{Dp} sinh\left(\frac{x}{Lp}\right) + \cosh\left(\frac{x}{Lp}\right)\right)}{\left(\frac{S_P L_P}{Dp}\right) sinh\left(\frac{x_j}{Lp}\right) + cosh\left(\frac{x_j}{Lp}\right)} - \exp(-\alpha_1 x)\right] \quad \text{.....eq}^{\text{n}} (45)$$

Hole photocurrent density at the depletion edge is –

$$J_p = -q.D_p\left(\frac{dp_n}{dx}\right)_{x_j}$$

$$J_p = \left[\frac{q\emptyset(1-R)\alpha_1 L_P}{(\alpha_1{}^2 L_p{}^2 - 1)}\right]\left[\frac{\left(\frac{S_P L_P}{Dp} + \alpha_1 L_P\right) - \exp(-\alpha_1 x_j)\left(\left(\frac{S_P L_P}{Dp}\right) cosh\left(\frac{x_j}{Lp}\right) + sinh\left(\frac{x_j}{Lp}\right)\right)}{\left(\frac{S_P L_P}{Dp}\right) sinh\left(\frac{x_j}{Lp}\right) + cosh\left(\frac{x_j}{Lp}\right)} - \alpha_1 L_P \exp(-\alpha_1 x_j)\right] \quad \text{.....eq}^{\text{n}} (46)$$

3.5.2 P-side photocurrent:

For P side of junction (CZTS) eq^n38, 39& 41 can be combined to yield the expression-

$\alpha_2(\lambda)\emptyset(\lambda)$[1-R($\lambda$)] exp[-$\alpha_2(\lambda)x'$]=$\frac{n_p-n_{po}}{\tau_n}-\ D_n\frac{d^2n_p}{dx^2}$

$\Rightarrow D_n\frac{d^2n_p}{dx^2}+\alpha_2\emptyset$[1-R] exp [-$\alpha_2x'$] $-\frac{n_p-n_{po}}{\tau_n}=0$ …….eq^n (47)

The general solution of equation (47) is-

n_p-n_{po}=C_2cosh$(\frac{x'}{Ln})$+C_3sinh$\left(\frac{x'}{Ln}\right)-\frac{\alpha_2\emptyset[1-R]\tau_n}{(\alpha_2{}^2Ln^2-1)}$ exp [-α_2x']…….eq^n (48)

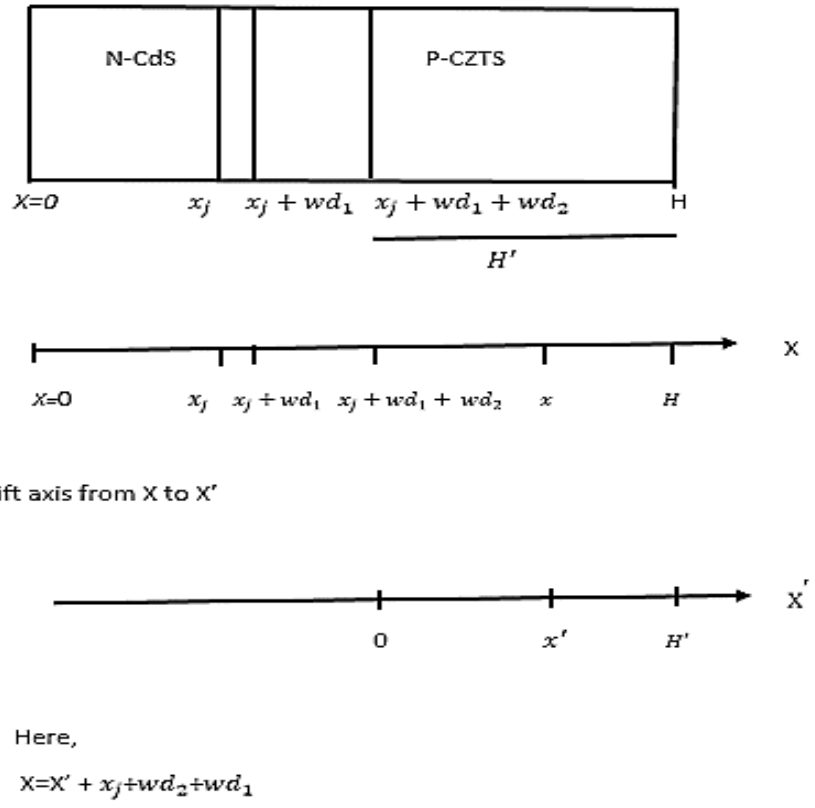

Fig 3.11 Depletion region and shifting axis

1st boundary Condition:

n_p-n_{po}=0 at $x'=0$

2nd boundary Condition:

$S_p(n_p - n_{po}) = -D_n \frac{dn_p}{dx}$; at x=H'

By using these boundary conditions we get the values for C_2 and C_3 and putting the values in Equation (48) we get the electron density,

$$n_p - n_{po} = \frac{\alpha_2 \emptyset[1-R]\tau_n}{{\alpha_2}^2 Ln^2 - 1} \exp[-\alpha_1 (x_j + wd_1)] \left[\cosh\left(\frac{x'}{Ln}\right) - \exp(-\alpha_2 x_p) - \frac{\left(\frac{S_n Ln}{Dn}\right)\left[cosh\left(\frac{H'}{Ln}\right) - \exp(\alpha_2 H')\right] + \sinh\left(\frac{H'}{Ln}\right) + \alpha_2 Ln \exp(-\alpha_2 H')}{\left(\frac{S_n Ln}{Dn}\right)\sinh\left(\frac{H'}{Ln}\right) + \cosh\left(\frac{H'}{Ln}\right)} * sinh\left(\frac{x'}{Ln}\right) \right] \ldots\ldots\ldots\ldots\ldots\text{eq}^{\text{n}}\ (49)$$

Here,

$$x' = x - x_j - wd_1 - wd_2$$

The photocurrent due to electrons collected at the depletion edge, $x = x_j + wd_1 + wd_2$ is-

$$J_n = q.D_n \left(\frac{dn_p}{dx}\right)_{x_j + wd_2}$$

$$= \frac{q\emptyset[1-R]\alpha_2 Ln}{{\alpha_2}^2 Ln^2 - 1} \exp[-\alpha_1 (x_j + wd_1)] * \exp(-\alpha_2 x_p) * \left[\alpha_2 Ln - \frac{\left(\frac{S_n Ln}{Dn}\right)\left[\cosh\left(\frac{H'}{Ln}\right) - \exp(-\alpha_2 H')\right] + \sinh\left(\frac{H'}{Ln}\right) + \alpha_2 Ln \exp(-\alpha_2 H')}{\left(\frac{S_n Ln}{Dn}\right)\sinh\left(\frac{H'}{Ln}\right) + \cosh\left(\frac{H'}{Ln}\right)} \right] \ldots\ldots\ldots\ldots\ldots\text{eq}^{\text{n}}\ (50)$$

$H' = H - x_j - wd_2$Shown in Fig 3.11.

3.5.3 Depletion Region Photocurrent

Some photocurrent generation takes place within the depletion region as well. Theelectric field in this region is generally high, and the photo generated carriers areaccelerated out of the depletion region before they can recombine. The quantum efficiency in this region is near 100% [3] and the photocurrent per unit bandwidth is equal tothe number of photons absorbed:

$$J_{dr_1} = q\emptyset(1-R)\exp(-\alpha x)\Big|_{x_j + wd_1}^{x_j}$$

$$\Rightarrow q\emptyset(1-R)\exp(-\alpha_1 x_j)[1 - \exp(-\alpha_1 wd_1)]$$

$$J_{dr_2} = q\emptyset(1-R)\exp(-\alpha x)\Big|_{x_j+wd_1+wd_2}^{x_j+wd_1}$$

$$\Rightarrow q\emptyset(1-R)\exp\left[-\alpha_1\left(x_j+wd_1\right]\right[1-\exp(-\alpha_2 wd_2)]$$

$$J_{dr} = J_{dr_1} + J_{dr_2} \ldots\ldots\ldots\ldots\ldots \text{eq}^{\text{n}}\ (51)$$

So, the total photocurrent at a given wavelength is then the sum of Eqns. 46, 50, and 51:

$$J_{PH}(\lambda) = J_p(\lambda) + J_n(\lambda) + J_{dr}(\lambda) \ldots\ldots\ldots\ldots\ldots \text{eq}^{\text{n}}\ (52)$$

Chapter 4

Calculation and Results

4.1 Introduction

In this chapter, the equations provided in Chapter 3 for the J-V relation of the solar cell, along with the equations for photocurrent and the dark current will be applied in order to determine the

effect of doping density, CdS and CZTS thicknesses and temperature on the electrical output of the solar cell. This will entail finding not only the photocurrent, dark current and the J-V relation, but also the efficiency and fill factor of the solar cell. These latter two are important criteria used to judge solar cell performance.

4.2 Efficiency and Fill Factor

The formula for the solar cell efficiency (Efficiency) is:

$$Efficiency = \frac{P_{max}}{P_{in}} * 100\% \ldots\ldots\ldots\ldots\ldots \text{eq}^{n}\ (53)$$

Where,

P_{max}=Maximum output power density which is taken from the maximum power point of the J-V curve ($P_{max}=V_{max}*J_{max}$)…….eq^{n} (54)

P_{in}=Maximum input power density which is found by integrating the standard terrestrial solar spectral irradiance at ai mass 1.5 (AM 1.5) with respect to the wavelength

The formula for fill factor (FF) is:

$$FF = \frac{P_{max}}{V_{oc}*J_{sc}} \ldots\ldots\ldots\ldots\ldots \text{eq}^{n}\ (55)$$

Where,

V_{oc}= Open circuit voltage (x-intercept of J-V graph)

J_{sc}= Short circuit current density (y-intercept of J-V graph)

Thus maximum efficiency gives the maximum percentage of the input solar power that can be converted to output electrical power. The fill factor gives a ratio that compares the maximum output power to the theoretical limit of $V_{oc}*J_{sc}$, Thus the higher these two values are, the better the performance of the solar cell.

4.3 Model Parameters

The following parameters required for electrical analysis of the considered n-CdS/p-CZTS heterojunction solar cell structure are listed below. These were kept constant during calculations.

Table 1 n-CdS thin film parameters

Variable/Constant	Description	Value
μ_n	Mobility of hole	50 $cm^2 V^{-1}s^{-1}$
ε_n	Dielectric permittivity	$9\varepsilon_o = 7.969 * 10^{-13}$ Fcm^{-1}
Eg_{CdS}	Energy band gap	2.4 eV
N_{c-CdS}	Effective density of states of conduction band	$1.8*10^{19}cm^{-3}$
N_{V-CdS}	Effective density of states of Valence Band	$2.4*10^{18}cm^{-3}$
N_{it}	Interface trap density	$5*10^{13}cm^{-3}$
σ	Capture cross section of holes	10^{-13} cm^2
v_{th}	Hole thermal velocity	$10^7 cms^{-1}$
$m^*_{e(CdS)}$	Electron effective mass	$0.25m_o=2.2775*10^{-31}kg$
$m^*_{h\ (CdS)}$	Hole effective mass	$0.7m_o=6.377*10^{-31}kg$

Table 2 p-CZTS thin film solar cell parameters

Variable/Constant	Description	Value
τ_p	Minority electron lifetime	$1.7*10^{-9}s$
μ_p	Mobility of electron	620 $cm^2 V^{-1}s^{-1}$
N_A	Acceptor concentration	10^{15} cm^{-3}
Eg_{CZTS}	Energy band gap	1.5 eV
$m^*_{e(CZTS)}$	Electron effective mass	$0.18\ m_o=1.6398*10^{-31}kg$
$m^*_{h\ (CZTS)}$	Hole effective mass	$0.71m_o=6.4681*10^{-31}kg$
ε_p	Dielectric permittivity	$10\varepsilon_o = 8.854 * 10^{-13}F/cm$
ΔE_C	Conduction band offset	-0.3 eV
ΔE_V	Valence band offset	1.2 eV
S	Interface recombination speed	$10^4 cms^{-1}$
R_S	Series resistance	5.8 Ωcm^2
R_{Sh}	Shunt resistance	$2.2*10^4$ Ωcm^2

In addition, the values of certain constants are also required:

$k=1.3806*10^{-23}$ JK^{-1}or$8.617*10^{-5}$ eVK^{-1}

$h=6.626*10^{-34}$Js or $4.136*10^{-15}$ eVs

$\hbar = 1.05 * 10^{-34}$Js or $6.582 * 10^{-16}$eVs

And to find permittivity and effective mass we needpermittivity of free space (ε_o) and free electron rest mass (m_o)

$\varepsilon_o = 8.854 * 10^{-14}$Fcm^{-2}

$m_0 = 9.11 \times 10^{-31}$kg

Here the constants with units in cm and eV were taken instead of the SI m as the former two are more helpful to our calculations as all other units are in cm or eV.

The absorption spectrums of CdS and CZTS and the standard terrestrial solar spectral irradiance at AM 1.5 used in these calculations are given below:

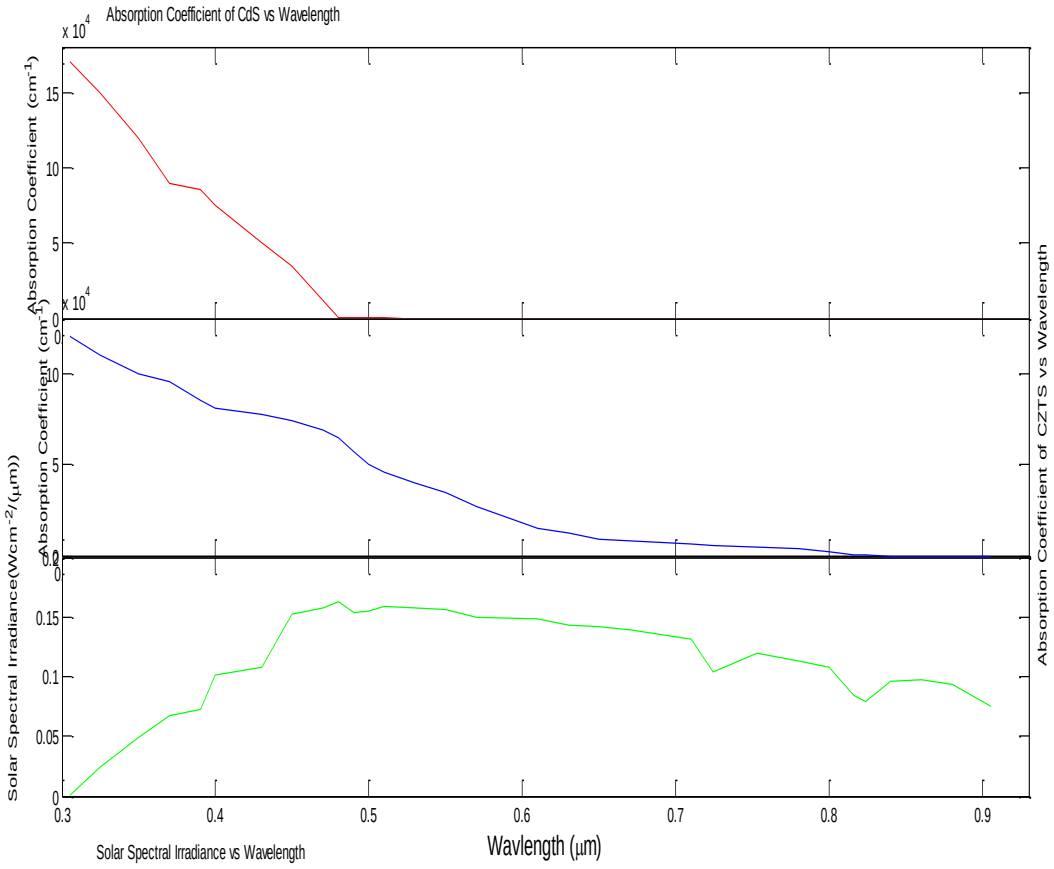

Fig 4.1 Absorption coefficient of CdS, absorption coefficient of CZTS, Standard terrestrial solar spectral irradiance at AM 1.5 v vs Wavelength

4.4 Doping Density and Thickness Optimization

Optimization of donor and acceptor concentrations and CdS and CZTS thickness were carried out step-by-step. Initially a constant CdS and CZTS thickness were taken, and values of donor and acceptor concentrations were changed. The concentrations that give the highest efficiency were noted and these values were constant as CdS and CZTS thicknesses were changed to find the values that provided the highest efficiency.

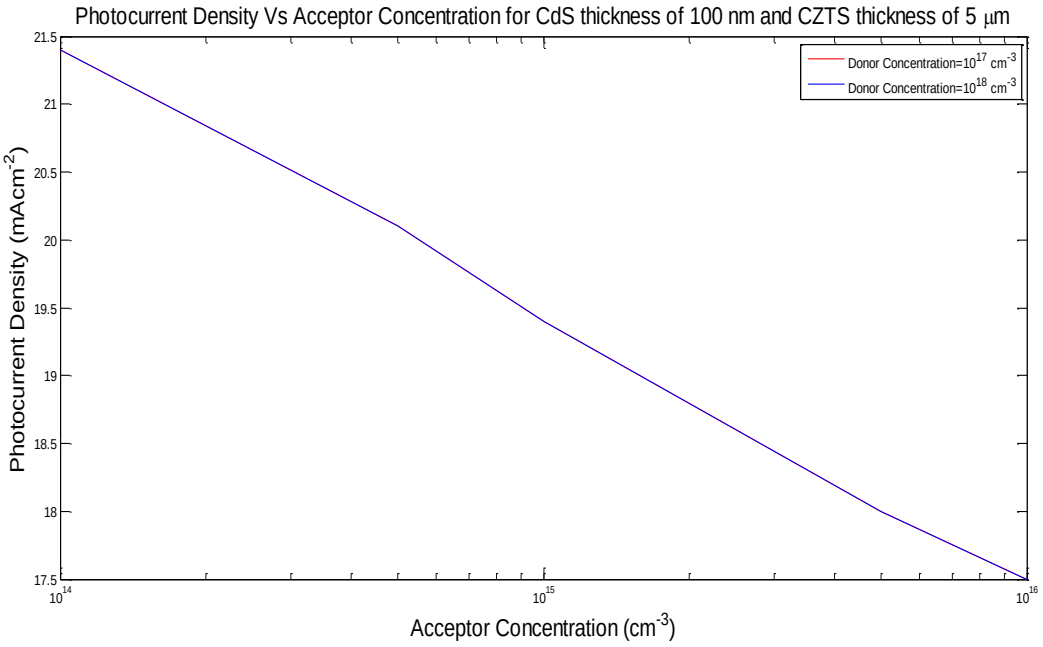

Fig 4.2 Photocurrent Density vs Acceptor Concentration. The current densities for donor concentration 10^{17} and $10^{18}cm^{-3}$ overlap.

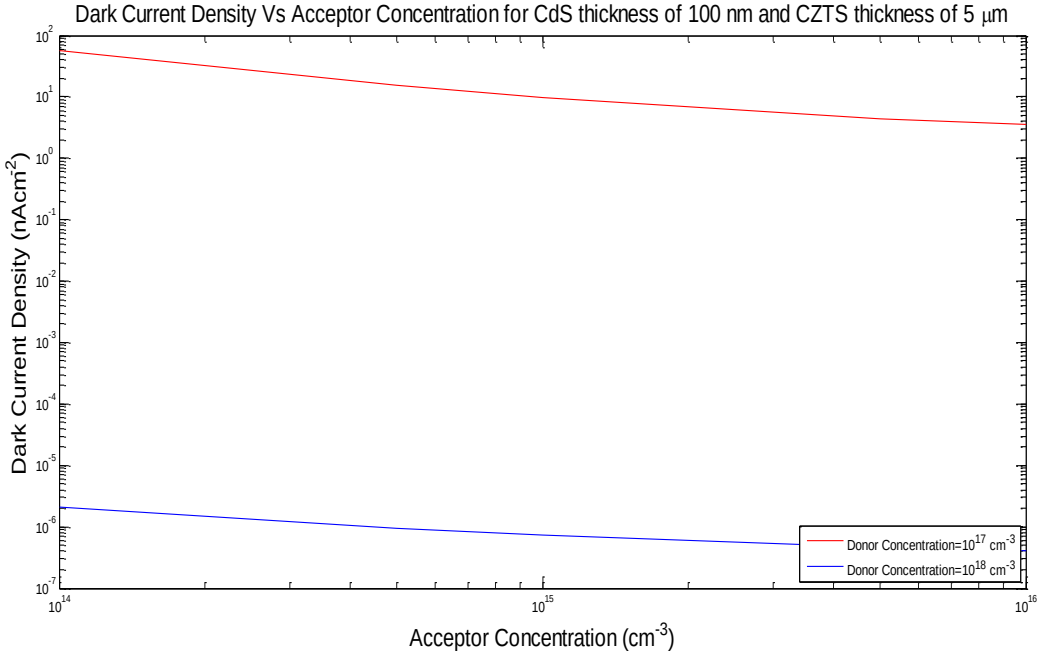

Fig 4.3 Dark Current Density vs Acceptor Concentration

These values of photocurrent and dark current are used to find the J-V graph. The photocurrent is identical for both donor densities but is several orders of magnitude lower for donor concentration 10^{18} cm^{-3} than for 10^{17} cm^{-3}.

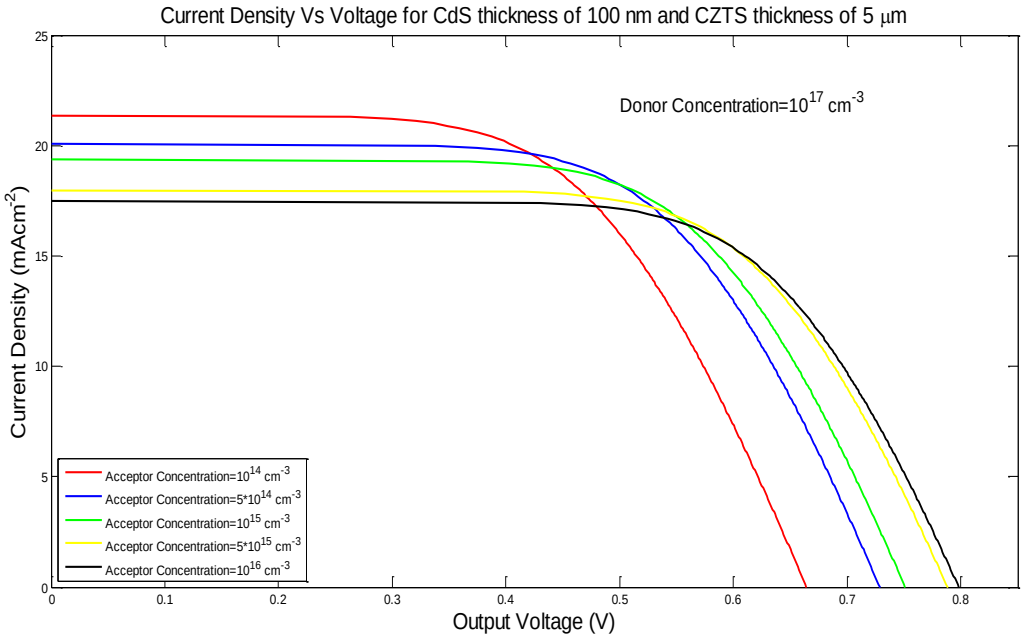

Fig 4.4 Current Density vs Output Voltage for Donor Concentration 10^{17} cm^{-3} and varying acceptor concentration

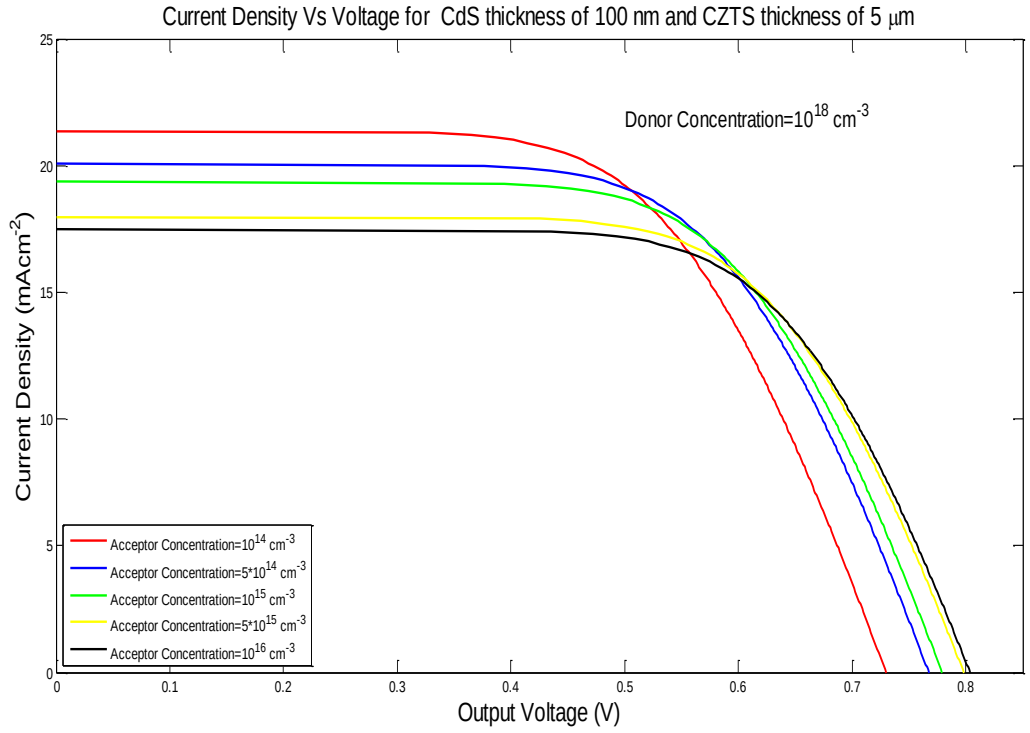

Fig 4.5 Current Density vs Output Voltage for Donor Concentration 10^{18} $cm^{-3}$and varying acceptor concentration

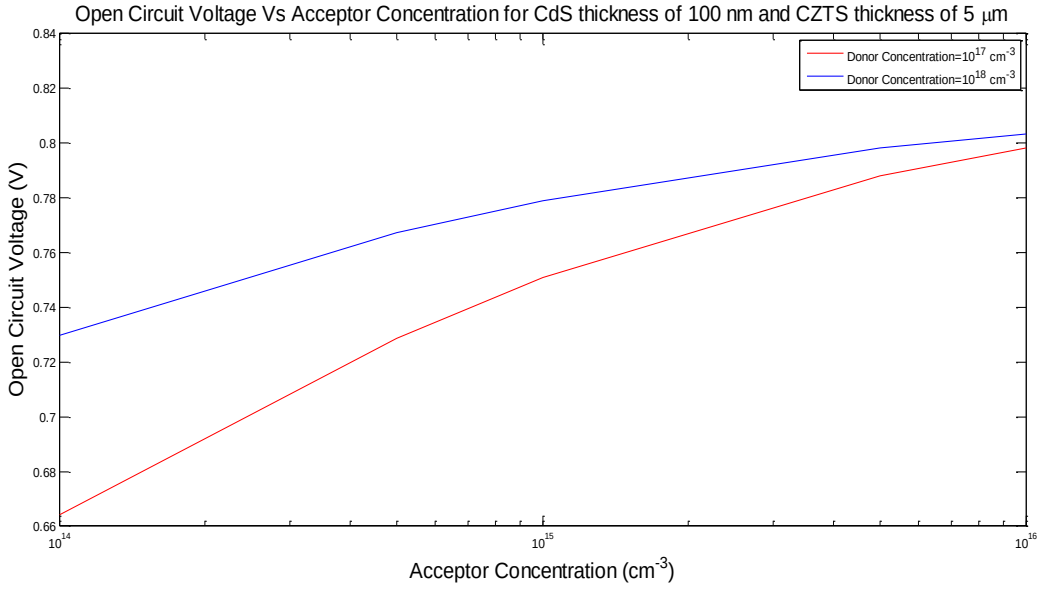

Fig 4.6 Open Circuit Voltage vs Acceptor Concentration

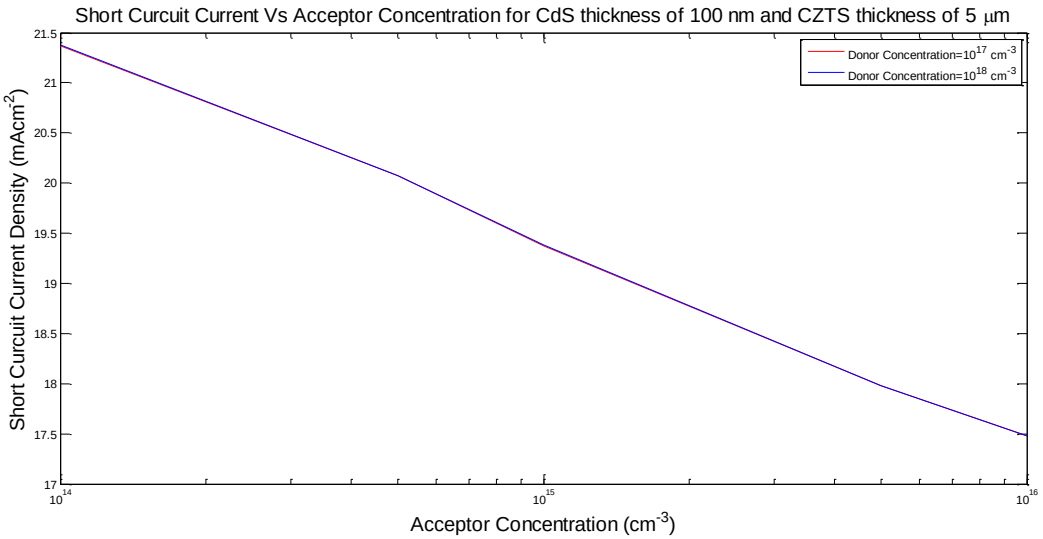

Fig 4.7 Short Circuit Current vs Acceptor Concentration

From the current density-voltage (J-V) graphs as well as the open circuit voltage (V_{oc}) and short circuit current (J_{sc}) graphs it can be seen that as acceptor concentration increases the open circuit voltage increases but the short circuit current decreases. We can also see that the J-V characteristics are very similar for both 10^{17} and 10^{18} cm^{-3} donor concentrations, with no difference in short-circuit current (the two short circuit current vs acceptor concentration graphs overlap) and the difference in open circuit voltage is very low (around 0.1 V for the lowest acceptor concentration 10^{14} cm^{-3} and decreasing to almost 0 at $10^{16}cm^{-3}$).

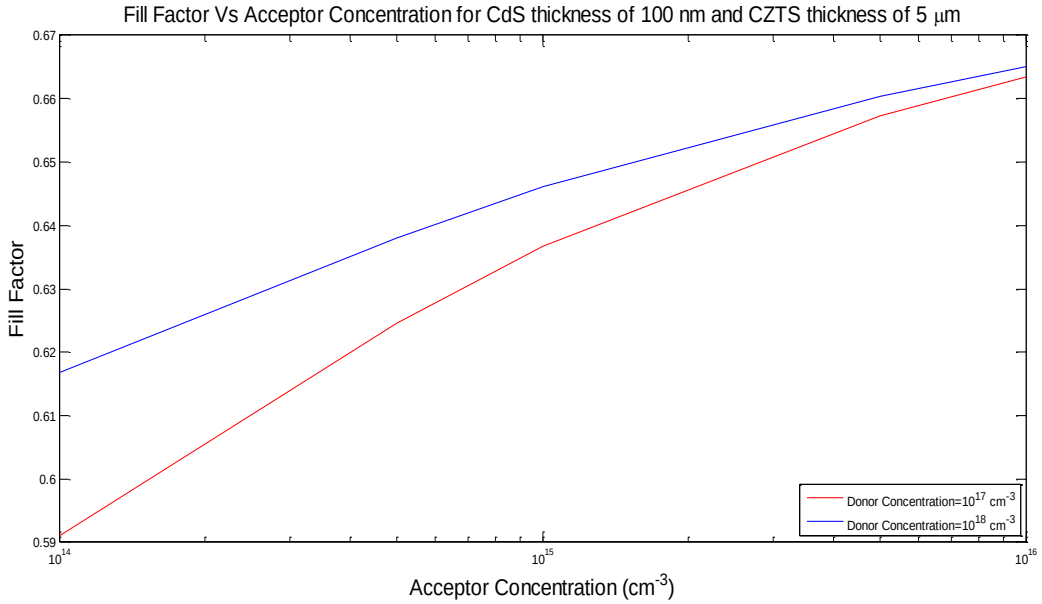

Fig 4.8 Fill Factor vs Acceptor Concentration

The fill factor is observed to rise with increasing acceptor concentration. It is higher for donor concentration of 10^{18} cm^{-3} than for 10^{17} cm^{-3} but this difference decreases as acceptor concentration increases.

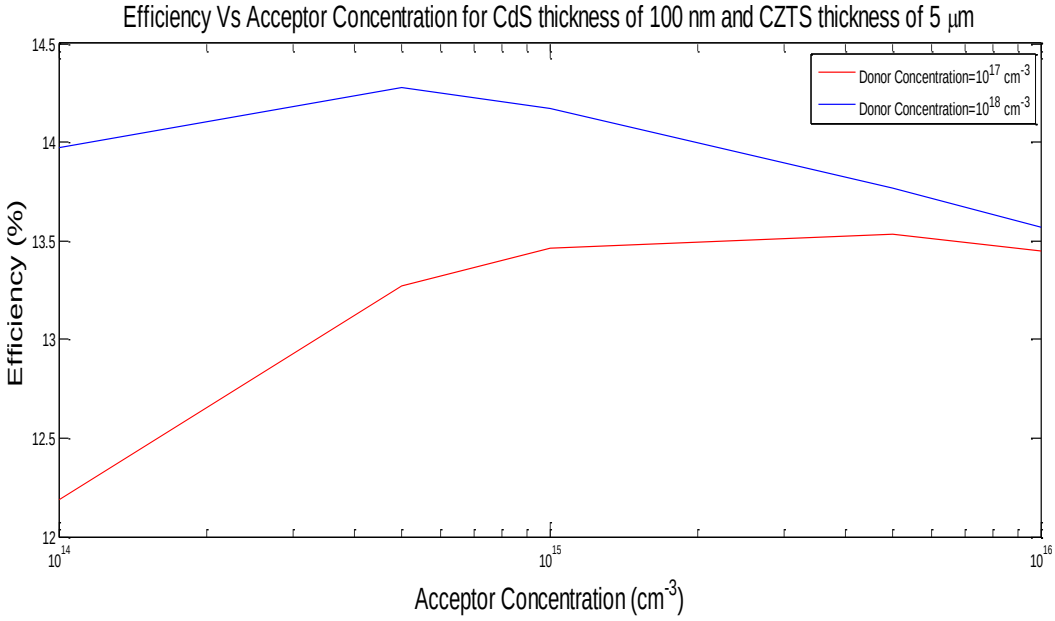

Fig 4.9 Efficiency vs Acceptor Concentration

To optimize donor and acceptor doping densities, a constant CdS thickness of 100 nm and a constant CZTS thickness of 5 μm were taken. Acceptor density (N_A) was varied, taking values of 10^{14}, $5*10^{14}$, 10^{15},$5*10^{15}$ and10^{16} cm^{-3} for donor densities (N_D) of 10^{17} and 10^{18} cm^{-3}.From the graph below it can be seen that efficiency was highest (14.3%) for $N_D=10^{18}$ cm^{-3} and $N_A=5*10^{14}$ cm^{-3}. This fits the theoretical observation that a high donor density, compared to acceptor density, increases the depletion width in the absorber side, thus allowing more photo generated EHPs to reach the depletion region and be separated by the voltage, increasing the photocurrent and efficiency.

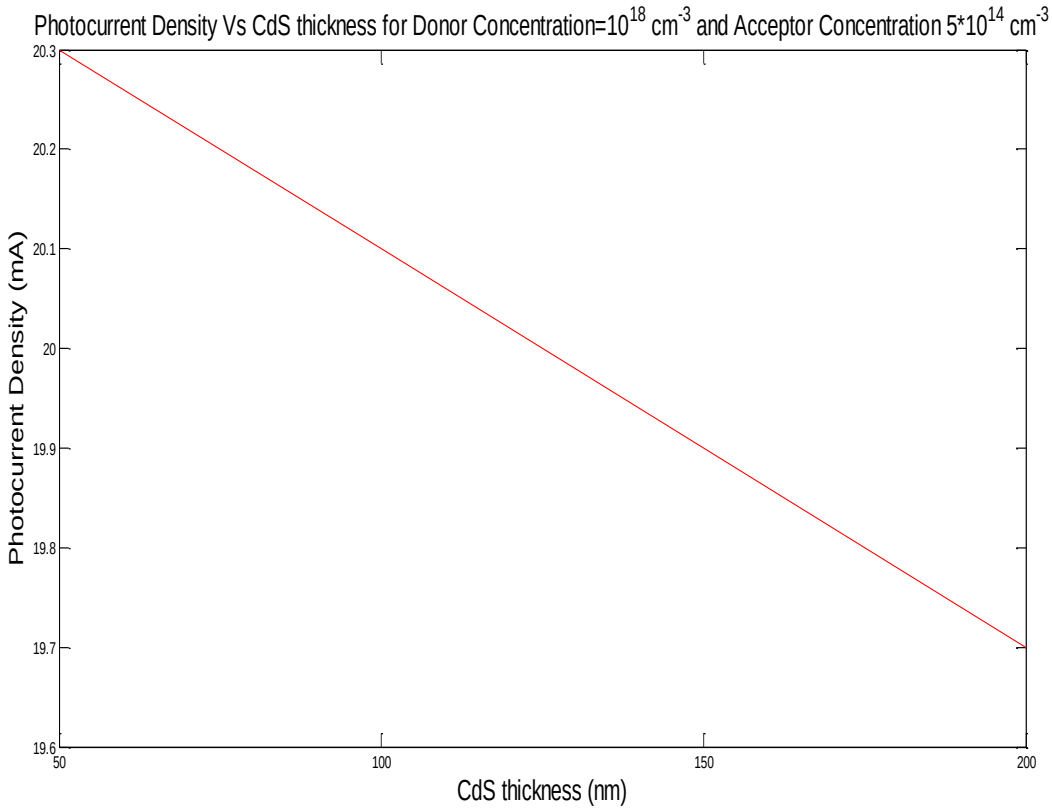

Fig 4.10 Photocurrent Density vs. CdS thickness

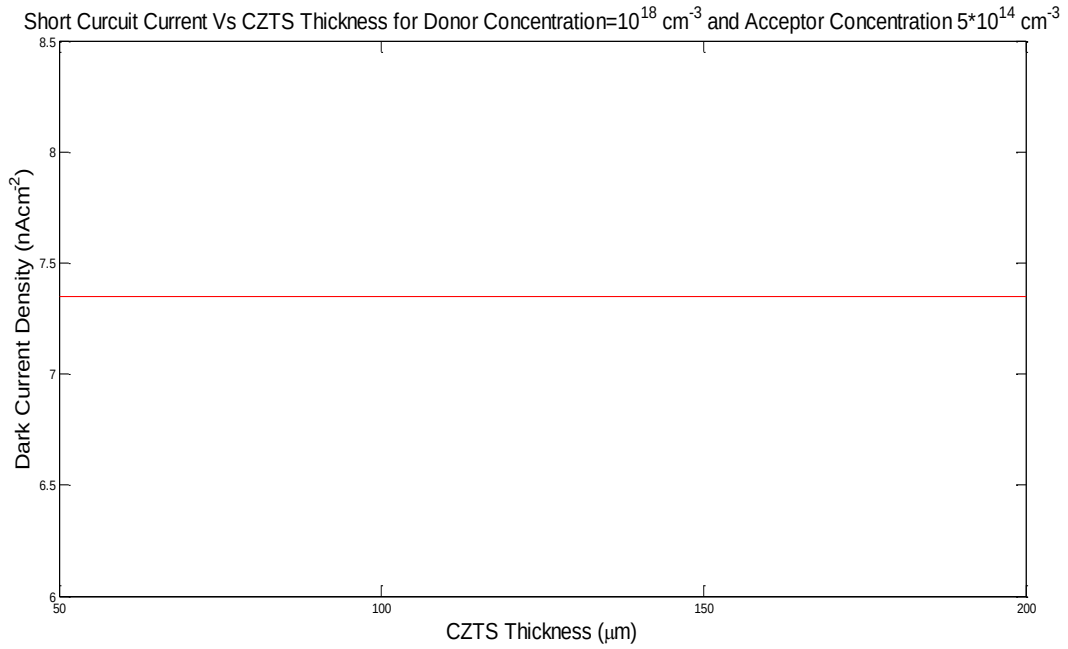

Fig 4.11 Dark Current Density vs. CZTS thickness

Dark current is not dependent on CdS thickness so it stays constant but photocurrent decreases as CdS thickness increases, which is consistent with the theoretical observation that a less thick n-CdS layer allows more photons to penetrate to the depletion region and be absorbed to generate more electron-hole pairs which contribute to the photocurrent.

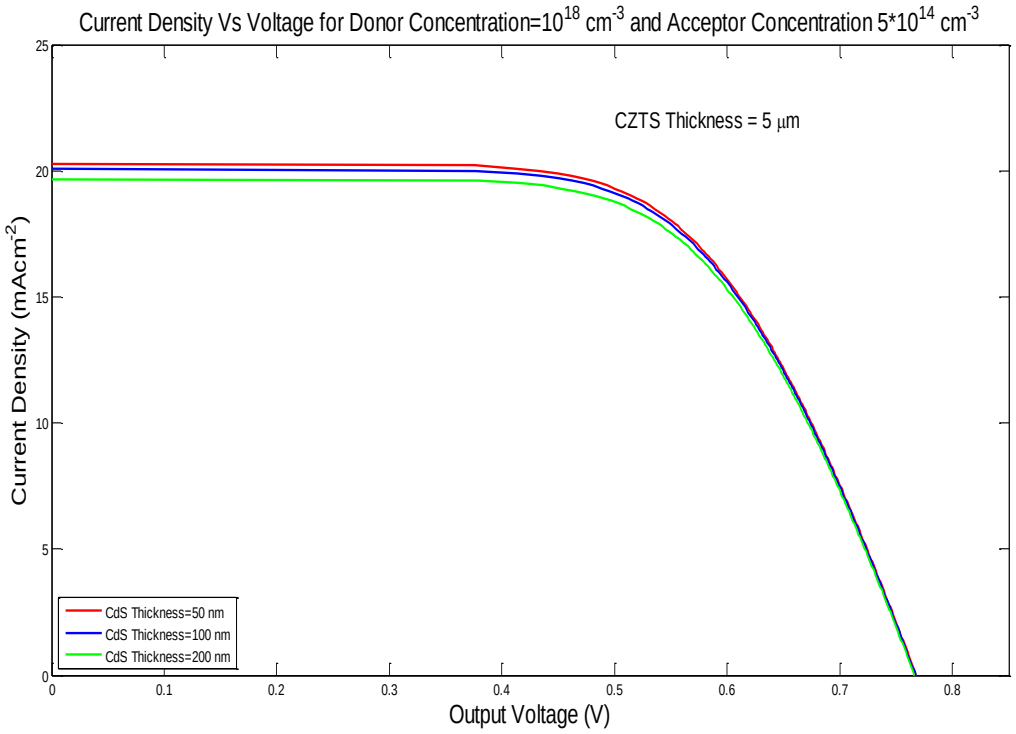

Fig 4.12 Current Density vs. Output Voltage for constant CZTS thickness5 μm and varying CdS thickness

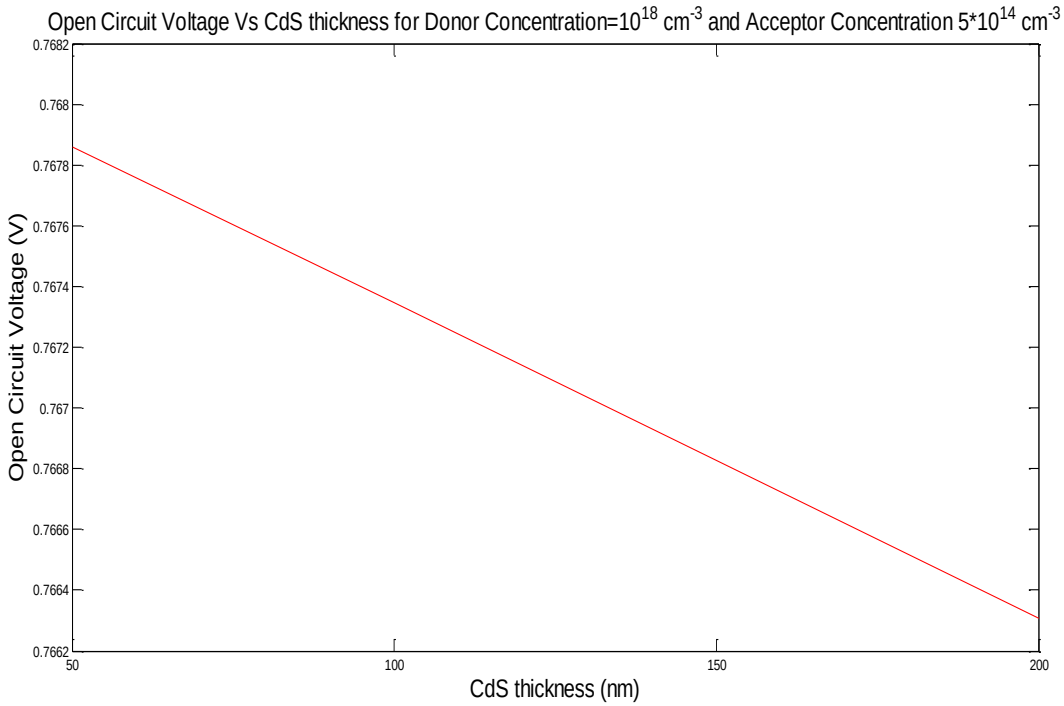

Fig 4.13 Open Circuit Voltage vs. CdS thickness

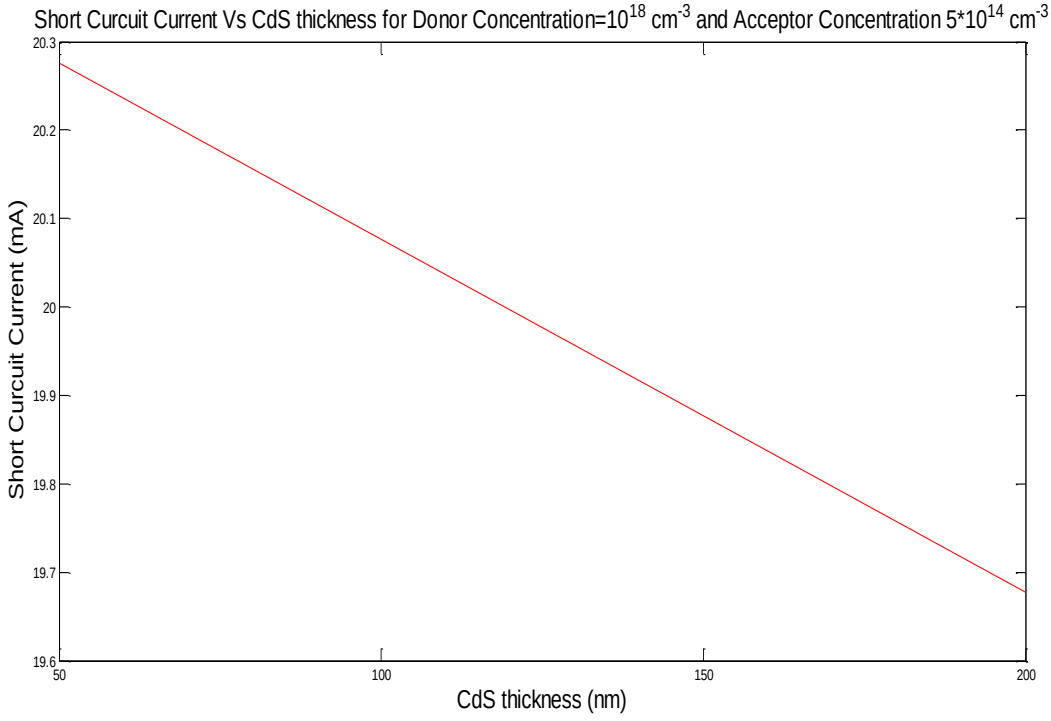

Fig 4.14 Short Circuit Current vs. CdS thickness

From the above graphs, it can be seen that there is very little change in the J-V characteristics with respect to CdS thickness. The change in V_{oc}due to CdS thickness from 50 to 200 nm is around 0.01 V and the change in J_{sc} is less than 1 $mAcm^{-3}$.

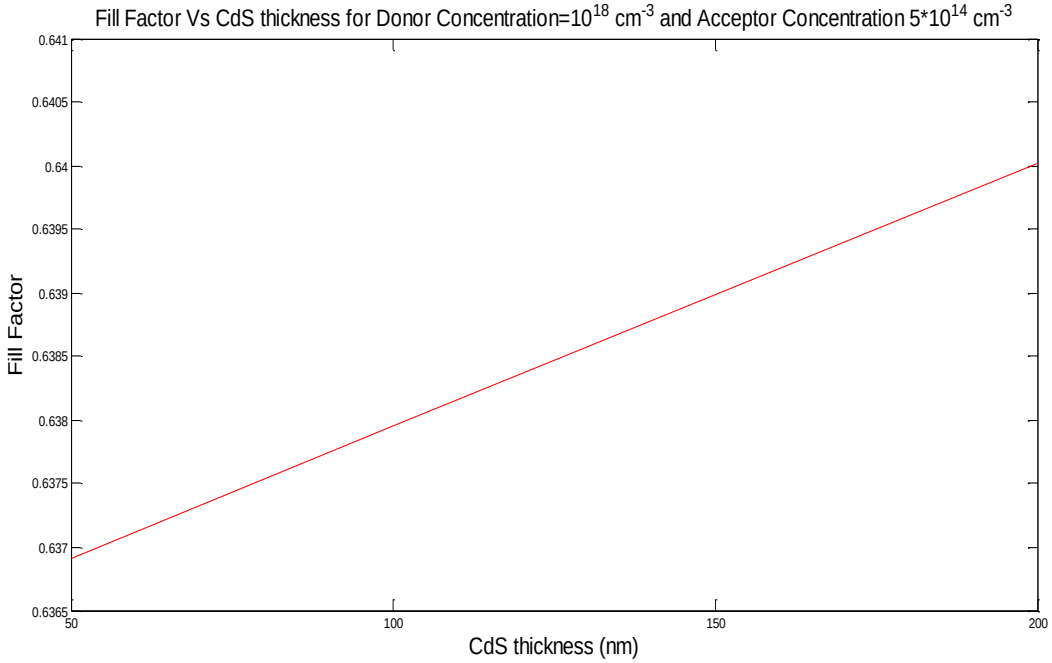

Fig 4.15 Fill Factor vs. CdS thickness

The Fill Factor increases as CdS thickness increases since both V_{oc} and J_{sc} are falling with increasing CdS thickness.

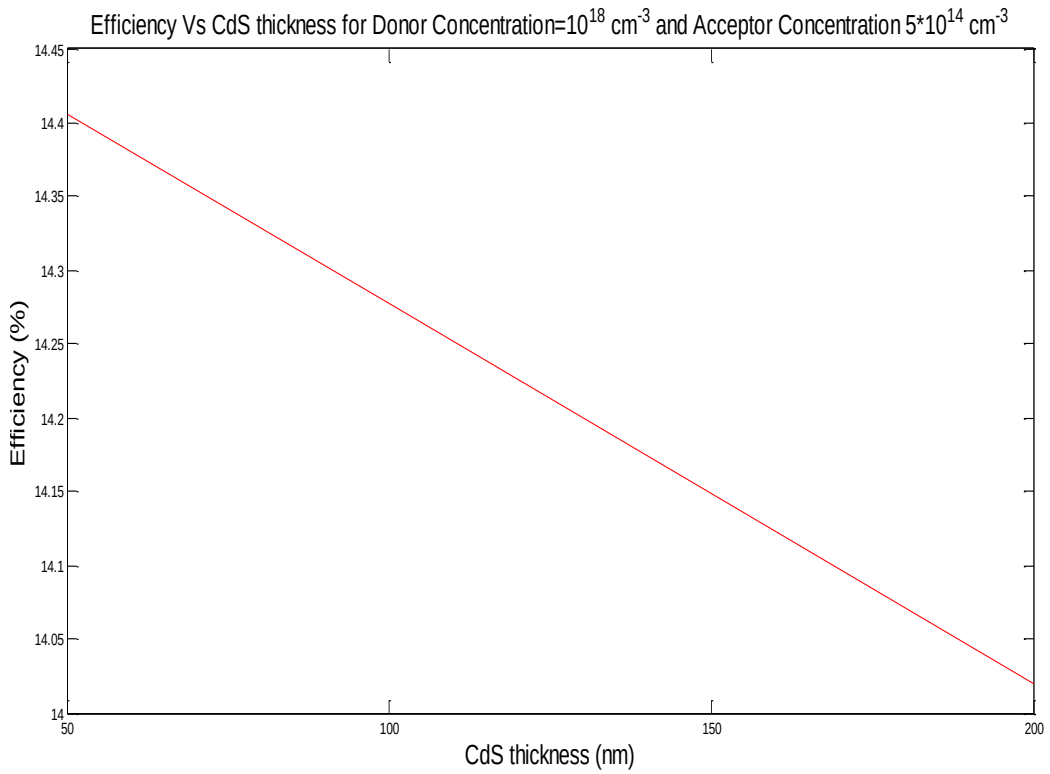

Fig 4.16 Efficiency vs. CdS thickness

Thus, the aforementioned maximum efficiency doping densities were taken, along with CZTS thickness of 5 μm in order to optimize CdS thickness. CdS thicknesses of 50,100 and 200 nm were taken and from the resulting efficiency graph it can be noted that the efficiency was highest (14.4%) for the lowest CdS thickness (50 nm). This can be attributed to the highest photocurrent being for the lowest thickness. Therefore, this CdS thickness of 50 nm was taken alongside $N_D=10^{18}$ cm^{-3} and $N_A=5*10^{14}$ cm^{-3} to find optimal CZTS thickness.

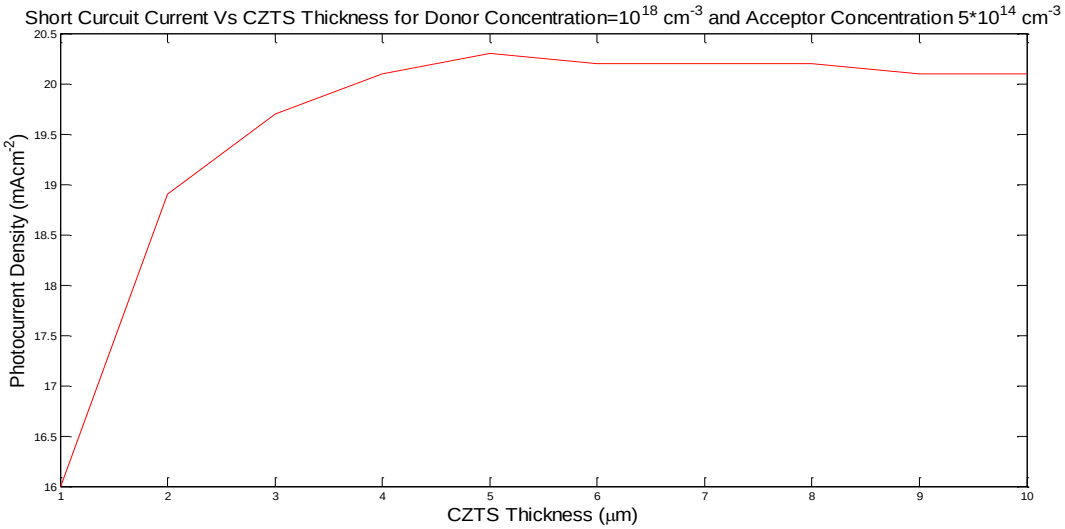

Fig 4.17 Photocurrent density vs CZTS thickness

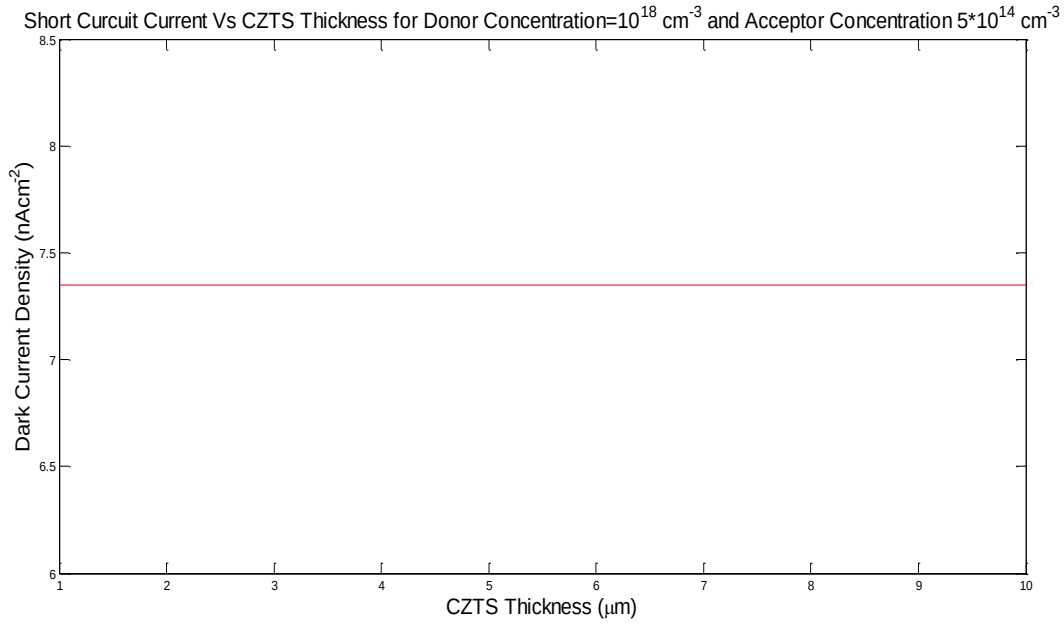

Fig 4.18 Dark Current Density vs CZTS thickness

The photocurrent reaches a peak at 5 μm before decreasing slightly. The dark current is unchanged regardless of CZTS thickness.

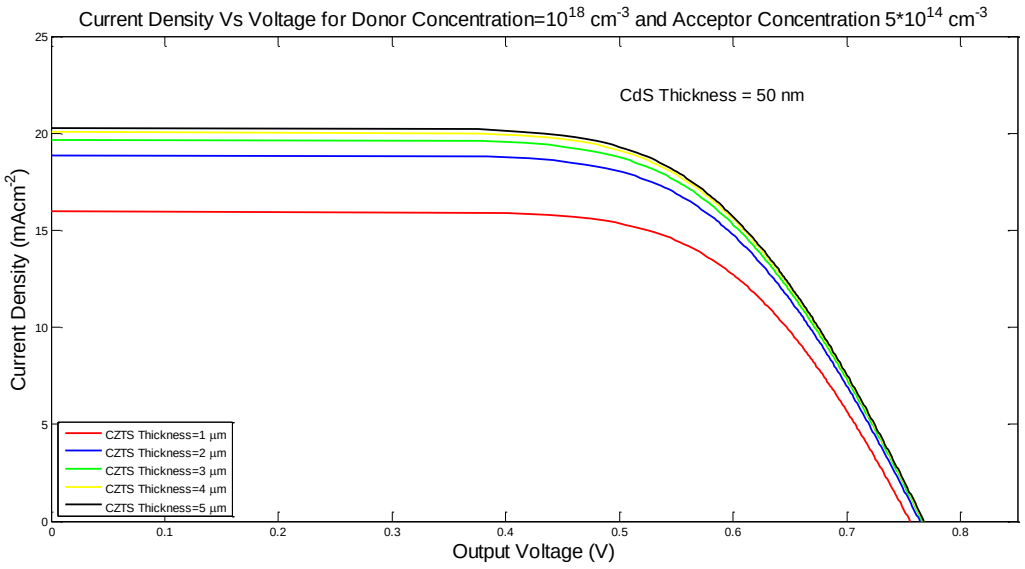

Fig 4.19 Current Density vs Output Voltage for constant CdS thickness 50 nm and CZTS thickness varying from1 to 5 µm

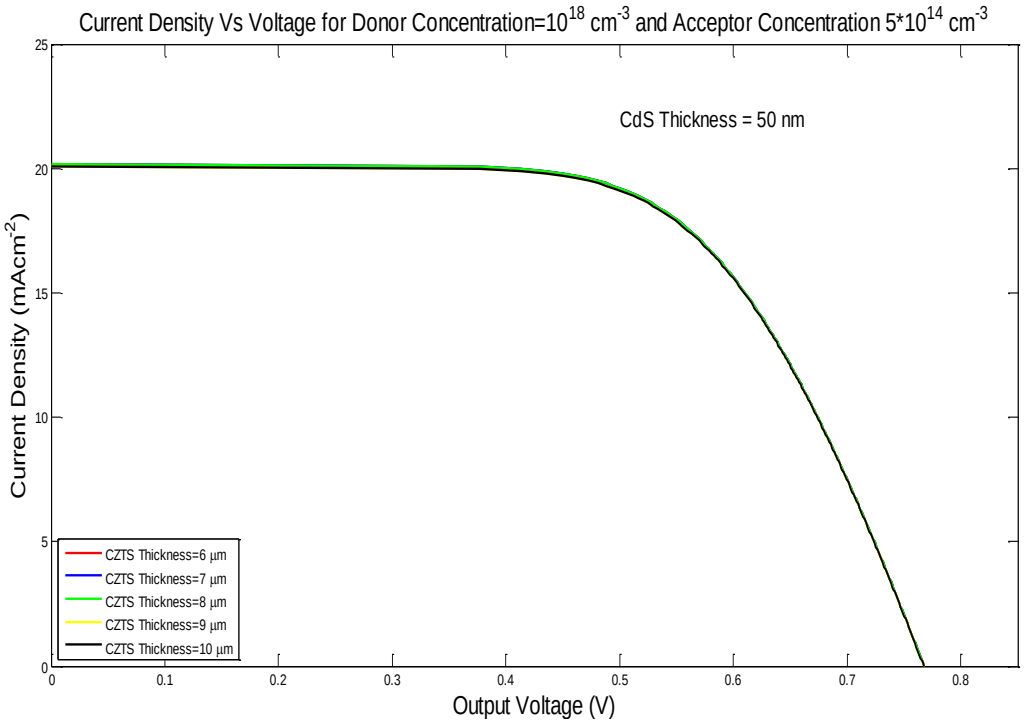

Fig 4.20 Current Density vs Output Voltage for constant CdS thickness 50 nm and CZTS thickness varying from 6 to 10 µm

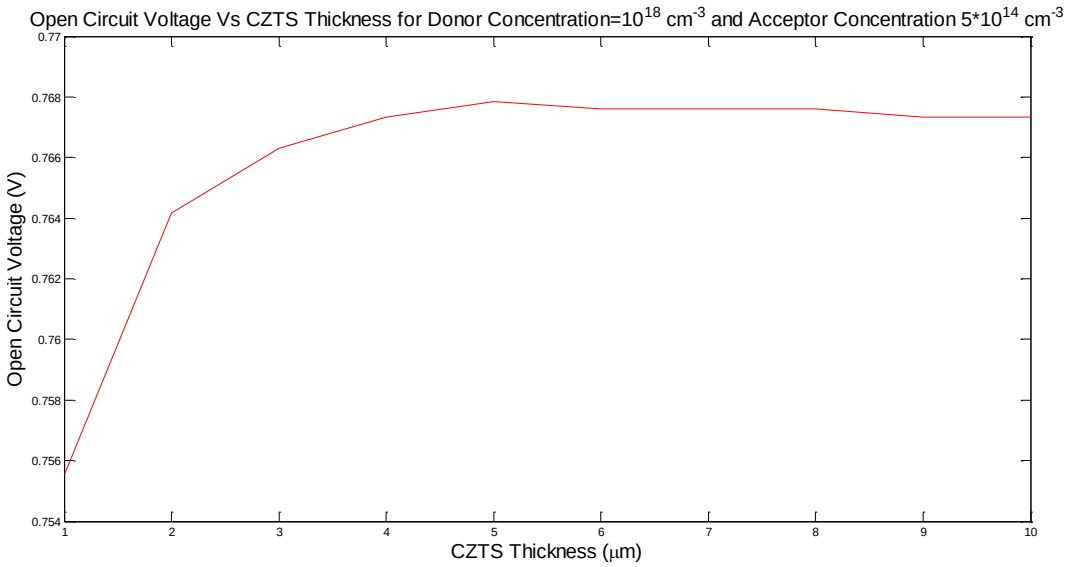

Fig 4.21 Open Circuit Voltage vs CZTS thickness

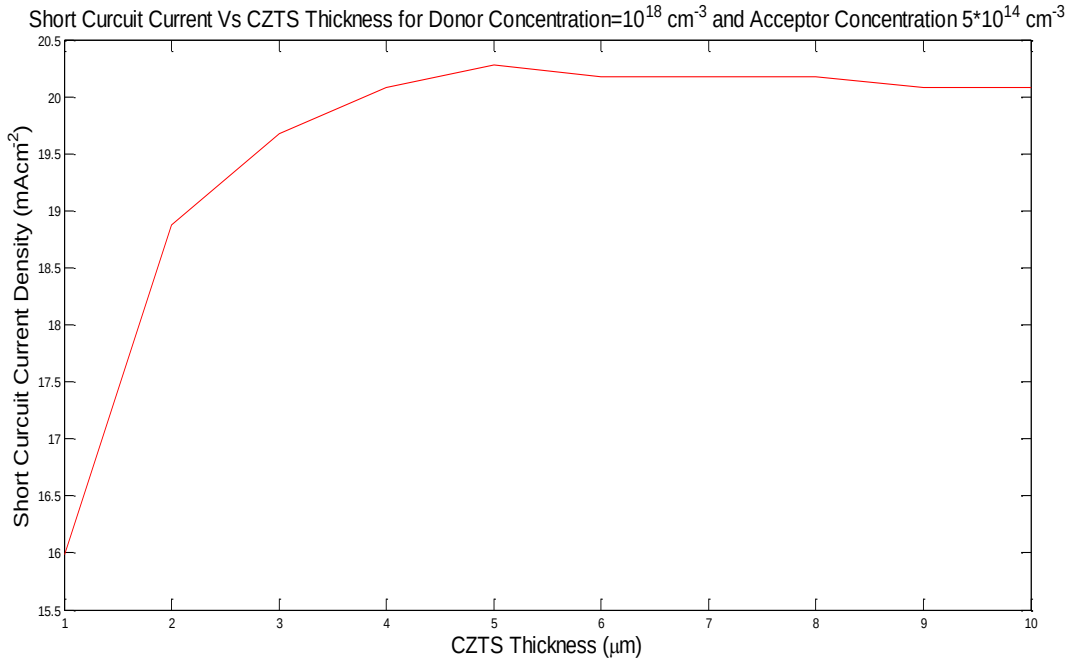

Fig 4.22 Short Circuit Current vs CZTS thickness

It is observed that there is greater variation in the J-V characteristics with varying CZTS thickness than with changing CdS thickness. While change in V_{oc} is only around 0.1 V, the change in J_{sc} is over 4 $mAcm^{-3}$. Both V_{oc} and J_{sc} peak at 5 μm.

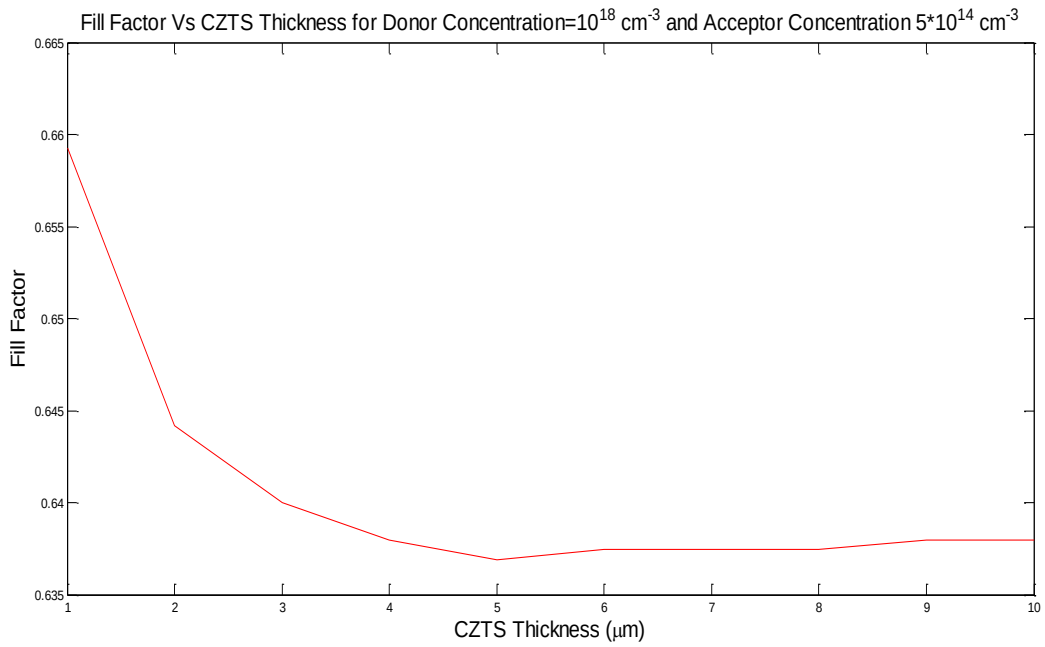

Fig 4.23 Fill Factor vs CZTS Thickness

The fill factor reaches its lowest point at 5 μm as both V_{oc} and J_{sc} peak at this thickness.

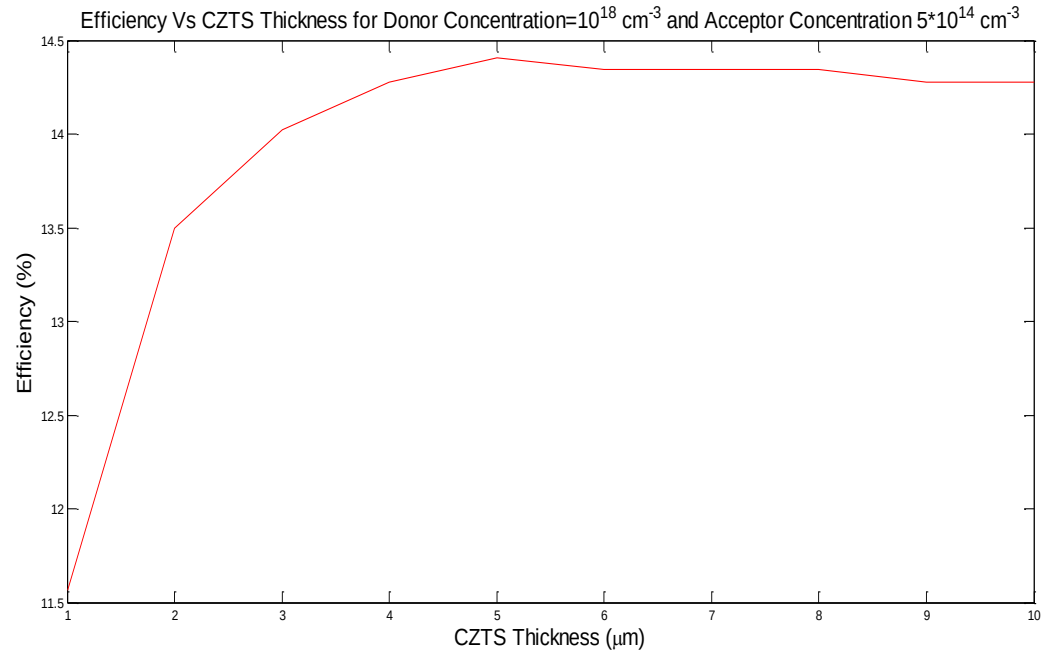

Fig 4.24Efficiency vs CZTS Thickness

Over the range of CZTS thickness used, (from 1 to 10μm) it was found that maximum efficiency reached its peak of 14.4 % at CZTS thickness of 5 μm before decreasing slightly. As the highest

photocurrent was also recorded at 5 µm this is expected. A larger absorber layer increases the number of potential EHPs that can be generated but it must not be so large that EHPs recombine before they can reach the depletion region and contribute to the photocurrent. Thus the conclusion is that donor and acceptor concentrations of 10^{18} and $5*10^{14}$ cm^{-3} along with CdS and CZTS thickness of 50 nm and 5 µm are the most desirable doping and thickness parameters among those tested as they give the highest efficiency.A thinner surface layer, an absorber layer that is not too thick and a more heavily doped n-side compared to the p-side give the most desirable results, consistent with the theory. The variations of fill factor with changing parameters have been noted but the value has stayed above 0.6 and below 0.7, the latter being a FF value seen in 'good' solar cells, due to the series resistance value.

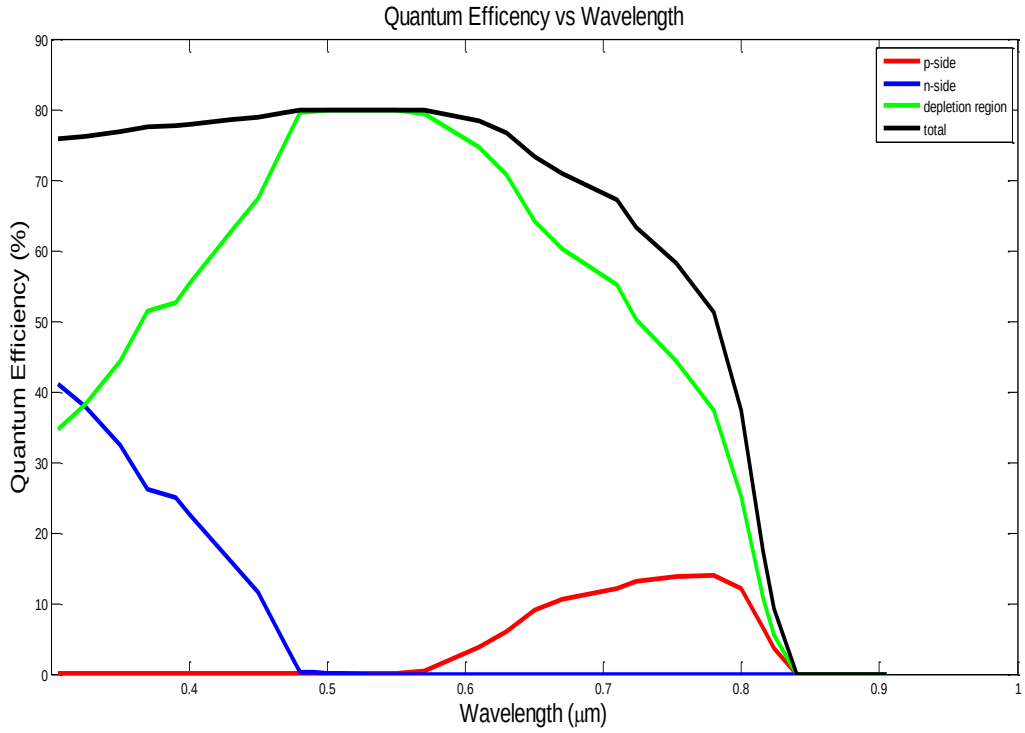

Fig 4.25Quantum Efficiency (QE) at optimized doping density and thickness parameters.

From the QE graph it can be seen that n-side absorbs photons of lower wavelengths while p-side absorbs higher wavelength photons. This is consistent with the theoretical observation. Maximum QE of around 80% (due to 20% reflectance) is obtained in the depletion region.

4.5 Effect of Temperature on Efficiency and Fill Factor

In addition the effect of temperature on electrical characteristics of the n-CdS/p-CZTS junction was noted. In operation, the temperature of the solar cell is higher than the surrounding environment by as much as 20 C. Thus for a hot environment of around 40 C, the operating temperaturecan be as high as 60 C. Thus it is important to evaluate the performance of the solar cell over a temperature range that encompasses possible operating temperatures. The optimal values of doping density and thickness found in the previous section were used in the following calculations while temperature was varied over a range of 5-75 C.

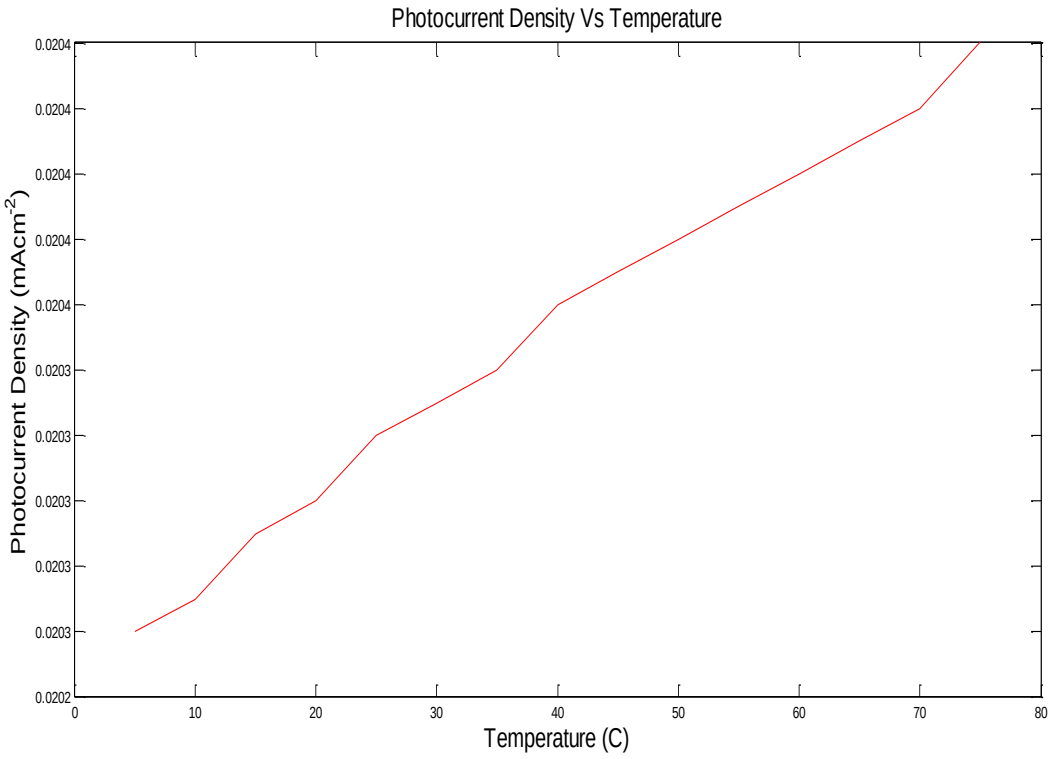

Fig 4.26 Photocurrent Density vs Temperature

A very slight increase in photocurrent density (1 $mAcm^{-2}$) is observed as temperature increases, which will not contribute greatly to any efficiency change.

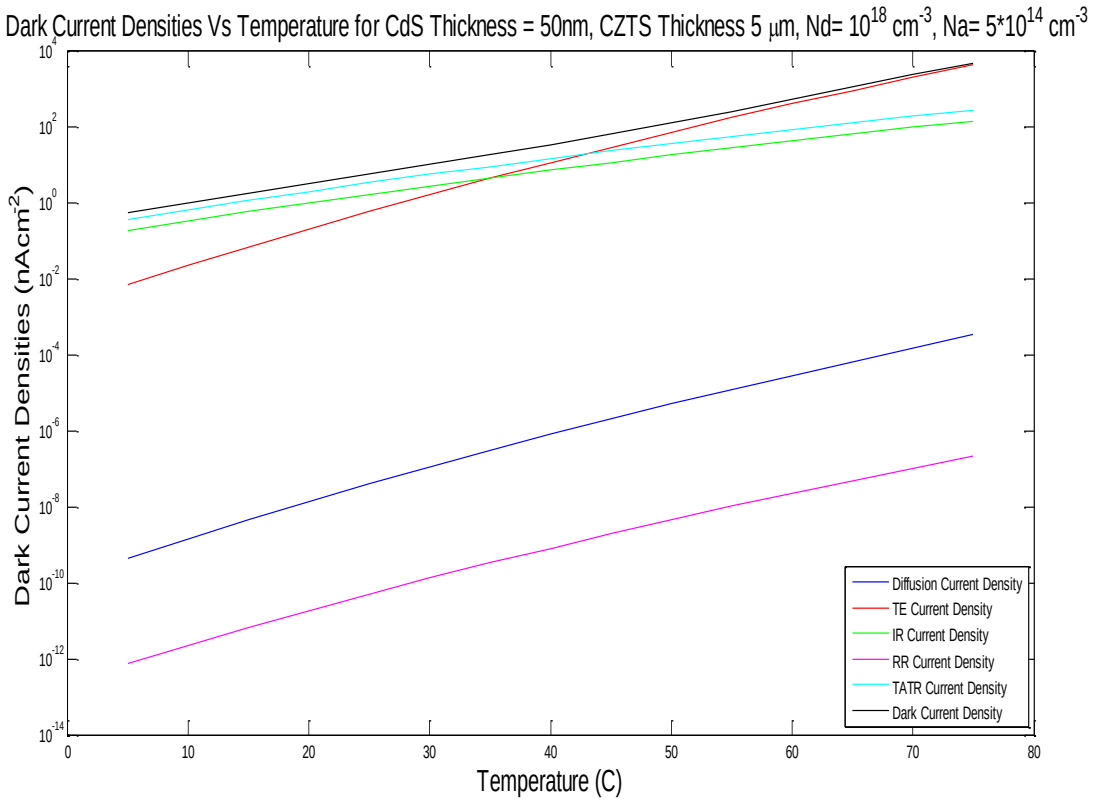

Fig 4.27 Dark Current and its components vs Temperature

From this graph it is observed that the dark current and all its components rise as temperature rises. At lower temperatures including room temperature, trap assisted tunneling recombination and interface recombination are the largest contributors to the dark current but as temperature increases above 40 C, thermionic emission overtakes them to become the largest single component of the dark current. From eq^{n} (32) we can see that this is because thermionic emission current increases with the square of the temperature. Diffusion current and radiative recombination current have a much smaller effect on dark current as they are several orders of magnitude lower. Since, the dark current is rising greatly, it will effect solar cell performance to a larger extent at higher temperatures.

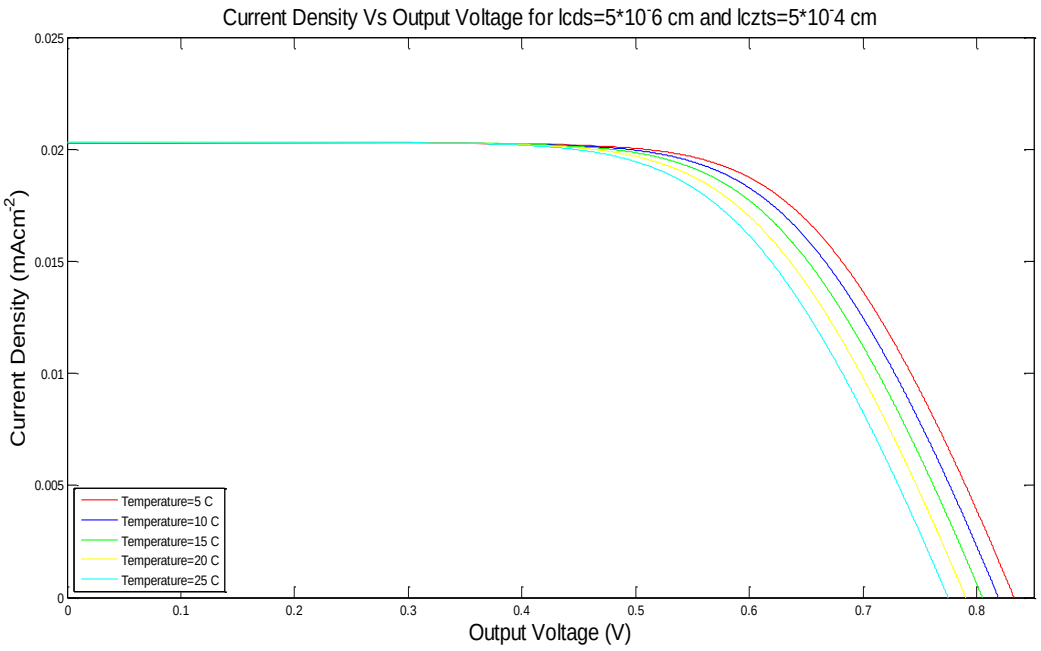

Fig 4.28 Current Density vs Output Voltage for temperatures 5-25 C

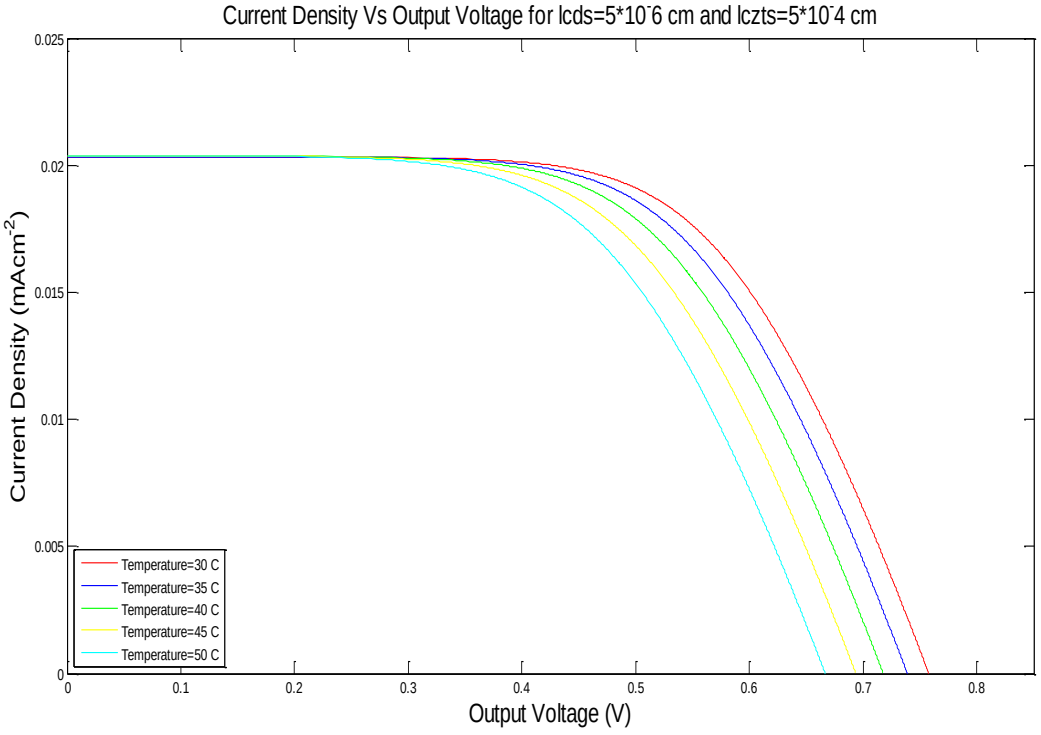

Fig 4.29 Current Density vs Output Voltage for temperatures 30-50 C

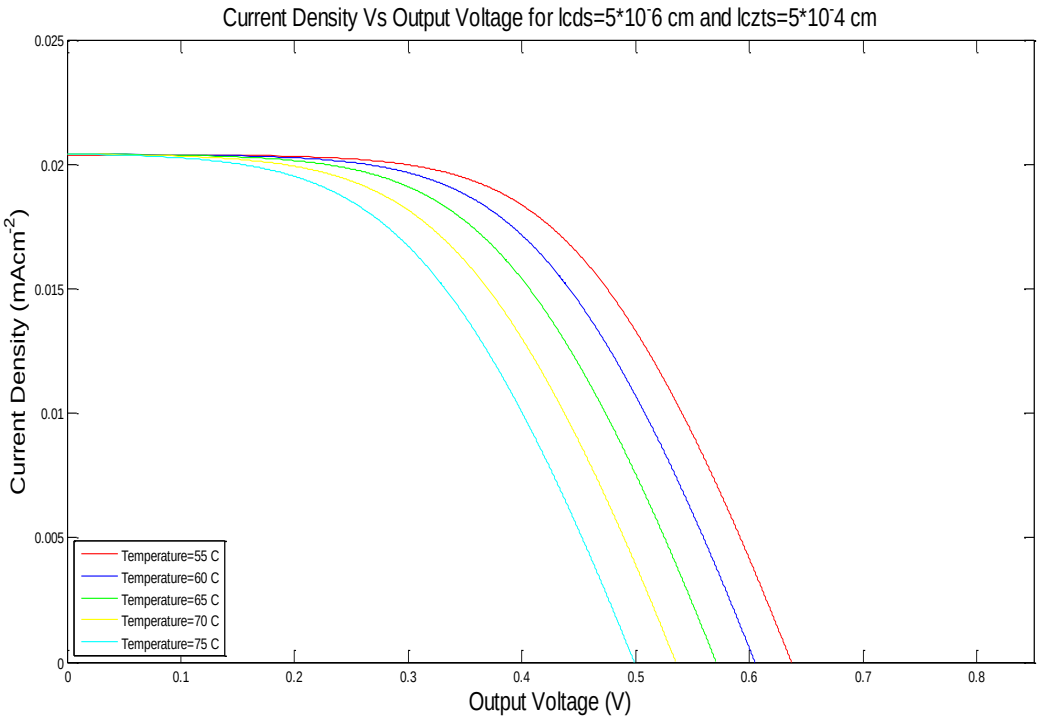

Fig 4.30 Current Density vs Output Voltage for temperatures 55-75 C

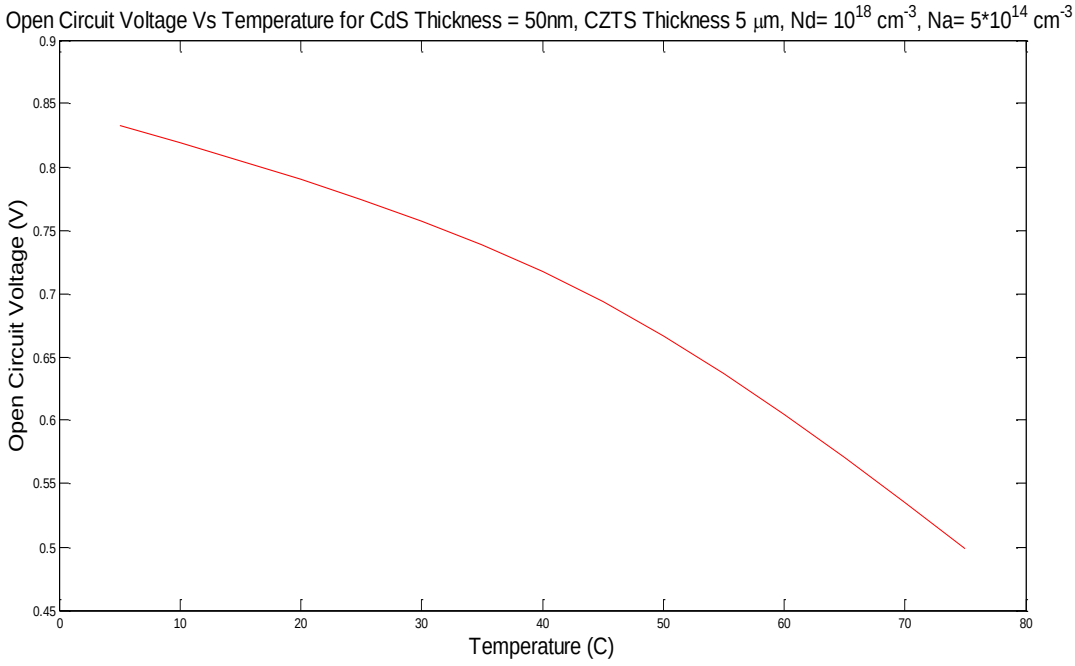

Fig 4.31 Open Circuit Voltage vs Temperature

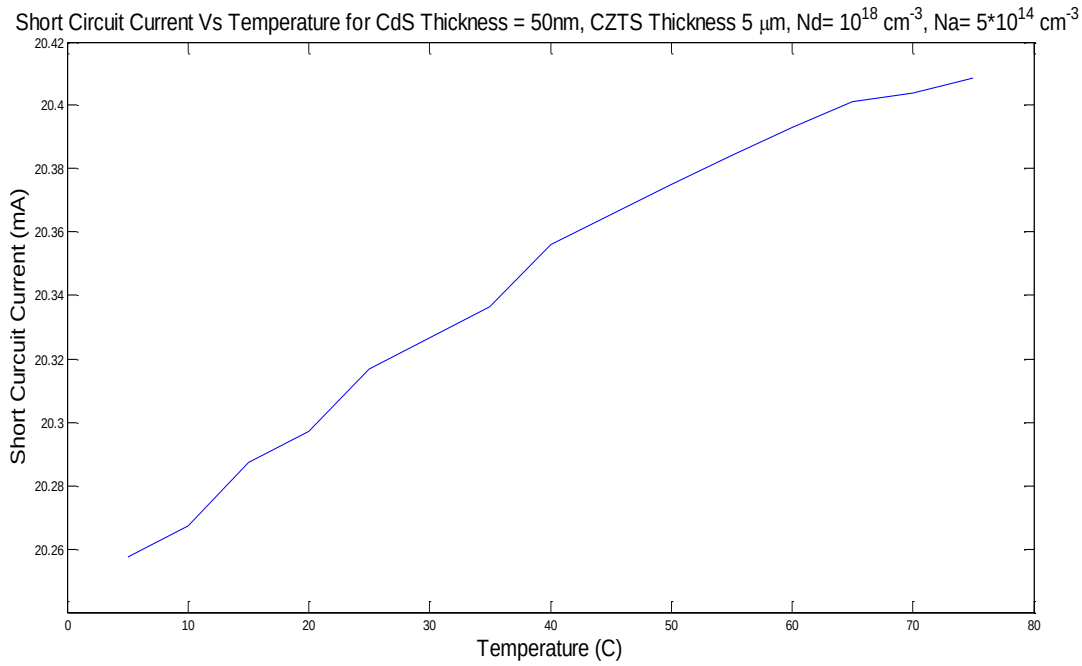

Fig 4.32Short Circuit Current vs Temperature

J_{sc}increases by a very small amount, less than 0.2 $mAcm^{-2}$ over a temperature range covering 5 to 75 C, while V_{oc} falls by around 0.3 V over this range.

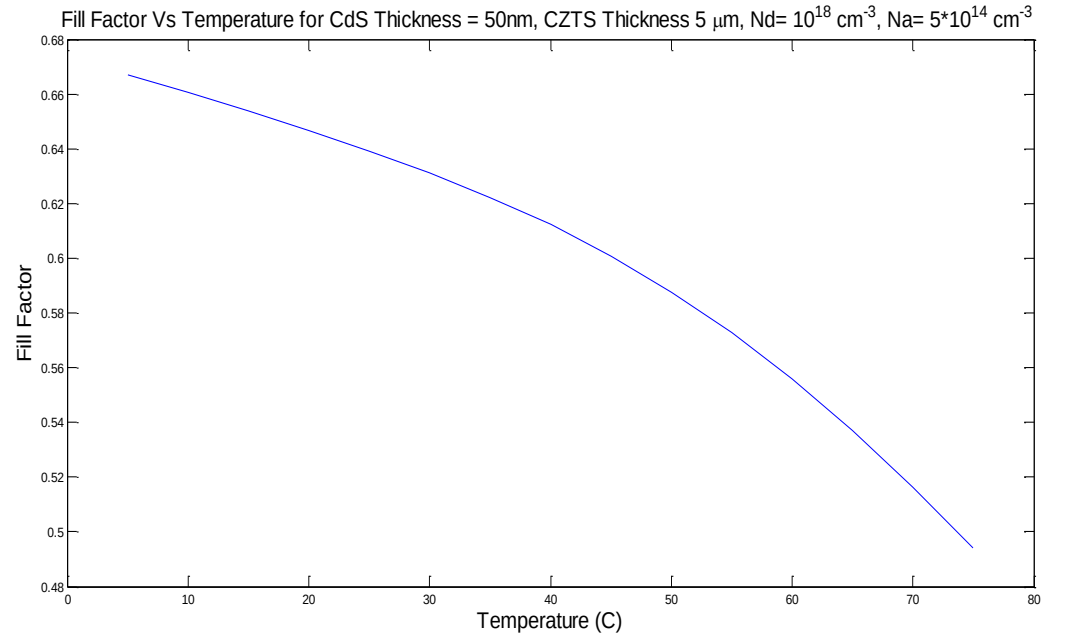

Fig 4.33 Fill Factor vs Temperature

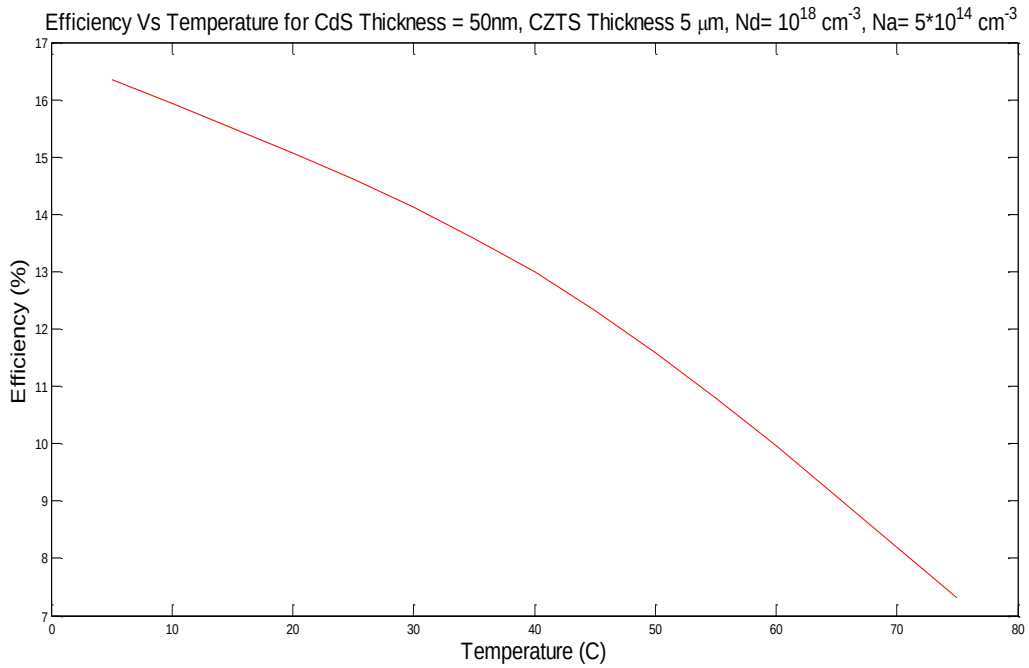

Fig 4.34 Efficiency vs Temperature

Table 3 Temperature coefficients of solar cell performance parameters

Parameter	Temperature Coefficient
Open-Circuit Voltage(V_{oc})	-4.77 mV/C
Short-Circuit Current Density (J_{sc})	2.14 $\mu Acm^{-2}/C$
Fill Factor	$-2.47*10^{-3}/C$
Efficiency (%)	-0.13%/C

Efficiency and fill factor also decrease over this range, with low temperatures around 5 C give efficiencies of around 16% while 25 C gives the previously mentioned efficiency of above 14%. High temperatures of around 70 C give efficiencies of around 8%. At 60 C, the efficiency is around10%. Fill factor falls from around 0.67 to around 0.49 and is around 0.55 at 60 C(compared to around 0.64 at 25 C) despite the large fall in V_{oc} since maximum output power density decreases which can be inferred from the efficiency graph. Thus solar cell performance is higher at lower temperatures and it is much reduced at higher operating temperatures. These negative temperature coefficients indicate that the solar cell is sensitive to temperature which is a drawback of our system.

4.6 Limitations and Future Work

When calculating current density, electrical activity arising from n-CdS and p-CZTS layers were taken into account but those from the i-ZnO and TCO layers and the Mo back-contact were not. The effect of optical phenomena affecting solar cell performance such as shading, the changing position of the Sun throughout the day (sun-tracking loss) and dust and dirt collecting on the solar cells were not considered. Neither was the relatively small variation of reflectance with respect to wavelength of solar radiation. Investigation of the model parameters of the i-ZnO and TCO layers and the Mo back-contact and their effect on current density and efficiency could be performed in the future in order to improve the accuracy of results. Modifying photocurrent equations to account for shading from grid as well as evaluating the effect of sun-tracking loss and dust on solar cell performance is another area in which future work could be done. In addition, since many of the model parameters of CZTS and CdS change depending on the fabrication method of the thin films, comparison of n-CdS/p-CZTS junctions fabricated via differing methods can be used to determine which gives the best performance, especially related to production cost.

References

1. Lewerenz, H.-J. ; Jungblut, H.: *Photovoltaik - Grundlagen und Anwendungen*. Springer-Verlag, 1995
2. Experimental study of Cu2ZnSnS4 thin films for solar cells *Hendrik Flammersberger*
3. Green, M. A. ; Emery, K. ; Hishikawa, Y. ; Warta, W.: Solar cell efficiency tables
4. (version 35). In: *Progress in photovoltaics: Research and applications* 18 (2010), S. 144–150
5. "Cadmium Telluride: Advantages & Disadvantages". *Solar-facts-and-advice.com*. N.p., 2017. Web. 5 Apr. 2017.
6. Ramsurn, Hema, and Ram B. Gupta. "Nanotechnology In Solar And Biofuels". *ACS Sustainable Chemistry & Engineering* 1.7 (2013): 779-797. Web. 4 Apr. 2017
7. Werner Heisenberg, *The Physical Principles of the Quantum Theory*, p. 20
8. "Equal Probability and Nonzero Probability | Emathzone". *eMathZone*. N.p., 2017. Web. 4 Apr. 2017.
9. "Trap Assisted Tunneling (TAT) Processes". *Diegm.uniud.it*. N.p., 2017. Web. 4 Apr. 2017.
10. Courel, Maykel, J. A. Andrade-Arvizu, and O. Vigil-Galán. "Towards A Cds/Cu2znsns4 Solar Cell Efficiency Improvement: A Theoretical Approach". *Applied Physics Letters* 105.23 (2014): 233501. Web. 4 Apr. 2017.
11. A. Polizzotti, I. Reping, R. Noufi, S. Huai Wei, and D. Mitzi, Energy Environ. Sci. 6, 3171–3182 (2013).
12. Dhakal, Tara P. et al. "Characterization Of A CZTS Thin Film Solar Cell Grown By Sputtering Method". *Solar Energy* 100 (2014): 23-30. Web. 16 Apr. 2017.
13. Shi, Chengwu et al. "Deposition Of Cu2znsns4 Thin Films By Vacuum Thermal Evaporation From Single Quaternary Compound Source". *Materials Letters* 73 (2012): 89-91. Web. 16 Apr. 2017.
14. Kumar, Arepalli Vinaya, Nam-Kyu Park, and Eui-Tae Kim. "A Simple Chemical Approach For The Deposition Of Cu2znsns4thin Films". *physica status solidi (a)* 211.8 (2014): 1857-1859. Web. 16 Apr. 2017
15. Yan, Xia et al. "Surface Texturing Studies Of Bilayer Transparent Conductive Oxide (TCO) Structures As Front Electrode For Thin-Film Silicon Solar Cells". *Journal of Materials Science: Materials in Electronics* 26.9 (2015): 7049-7058. Web.

Appendix-A

Photocurrent Equation Derivation

Photocurrent:

In this section, we derive the equation for photocurrent of p-n heterojunction solar cell. A typical schematics representation of solar cell is shown in fig: 1.

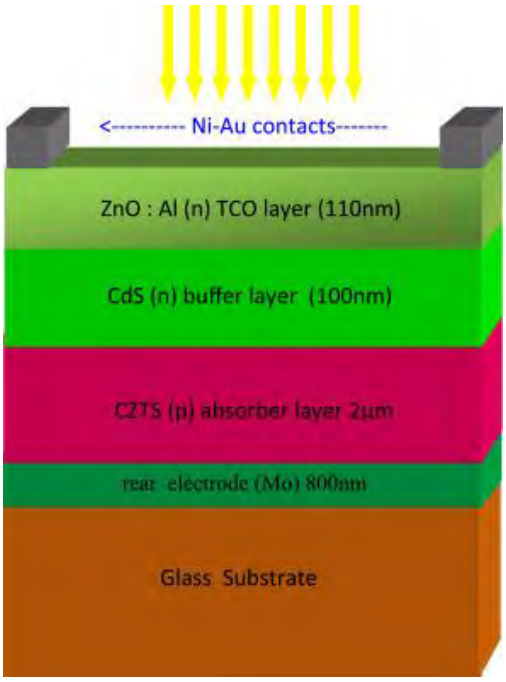

Fig-1:A typical schematics representation of CZTS, CdS solar cell is shown in fig: 1.

When a monochromatic light of wavelengthλ is incident on the front surface of solar cell the photocurrent and spectral response, that is, the number of carriers collected per incident photon at each wavelength.

The generation rate of electron – hole pair at a distance x from the semiconductor surface shown if fig:2 .

G(λ, x)=$\alpha_1(\lambda)$Ø(λ)[1-R(λ)]exp[-$\alpha_1(\lambda)x$]……eq^n (1)

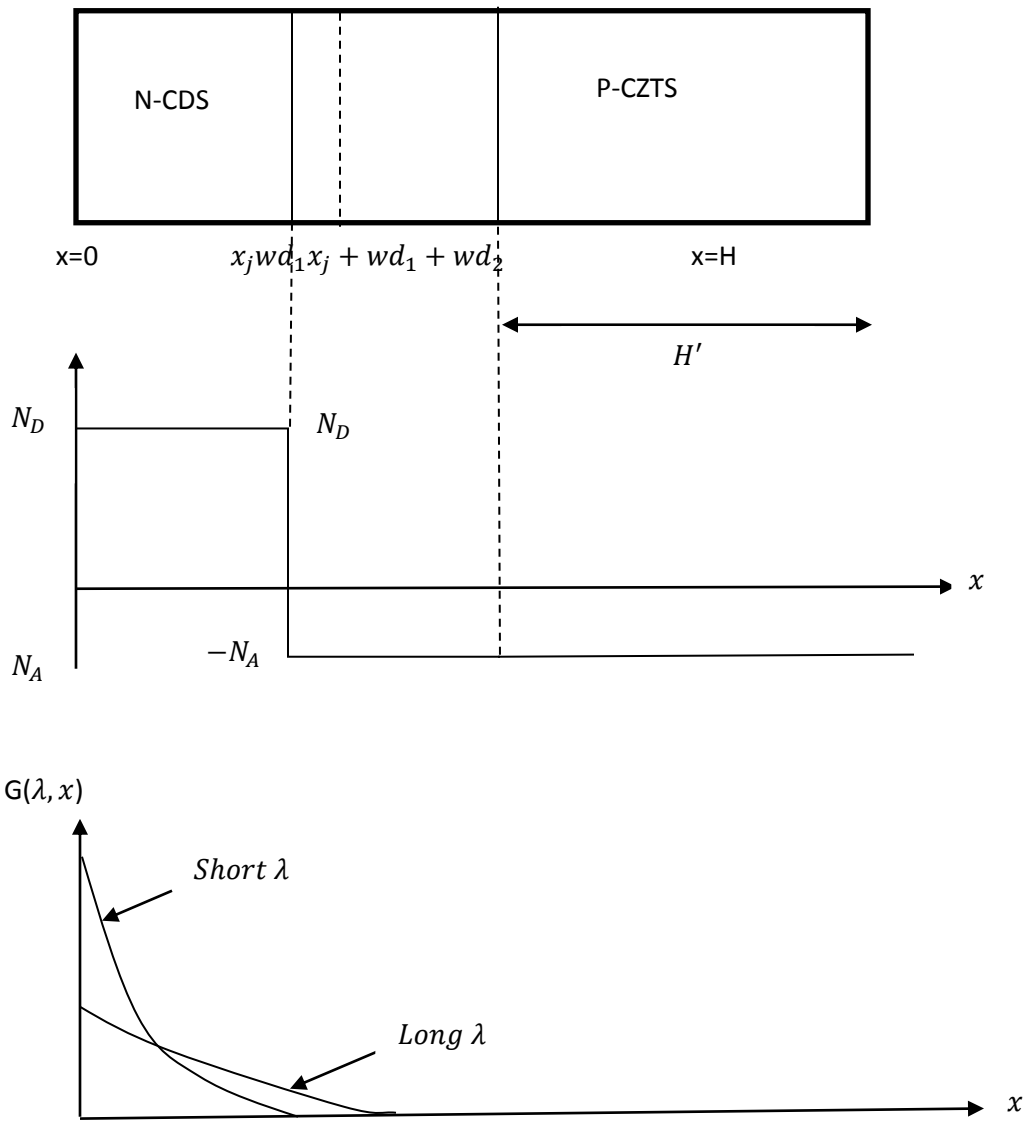

Fig. 2: (a) Solar cell dimensions under consideration (b) Assumed abrupt doping profiles ND >> NA. (c) Generation rate as a function of distance for long and short wavelengths.

Here,

$\alpha_1(\lambda)$ = Absorption Co-efficient of CDS

$\emptyset(\lambda)$=Number of incident photons per area per time per unit bandwidth

R(λ)=Function of these photons reflected from the surface

For an abrupt p-n junction solar cell with constant doping on each side, Fig. 2 ,there are no electric fields outside the depletion region. Photo generated carriers in these regions are collected by a diffusion process while that in the depletion region by drift process.

Under low injection condition, steady state continuity equation-

G_n-$(\frac{n_p-n_{po}}{\tau_n})$+$\frac{1}{q}\frac{d_{jn}}{dx}$ = 0 …….eq^n (2)

For electrons in the p-type substrate are-

G_p-$(\frac{p_n-p_{no}}{\tau_p})$-$\frac{1}{q}\frac{d_{jp}}{dx}$ = 0…….eq^n (3)

For holes in the n-type layer, the current density equations are-

$J_n = q\mu_n n_p \varepsilon + qD_n(\frac{d_{np}}{dx})$……$eq^n$ (4)

$J_p = q\mu_p p_n \varepsilon - qD_p(\frac{d_{pn}}{dx})$……$eq^n$ (5)

For the top n-side of the junction, Equations. 1, 3, and 5 can be combined to yield an expression:

$\alpha_1(\lambda)\ \emptyset(\lambda)$ [1-R (λ)] exp[-$\alpha_1(\lambda)x$]-$(\frac{p_n-p_{no}}{\tau_p})$-$\frac{1}{q}\frac{d}{dx}(q\mu_p p_n \varepsilon - qD_p(\frac{d_{pn}}{dx}))$=0

$\Rightarrow \alpha_1(\lambda)\emptyset(\lambda)$[1-R($\lambda$)]exp[-$\alpha_1(\lambda)x$]-$(\frac{p_n-p_{no}}{\tau_p})$+$D_p.\frac{d^2p_n}{dx^2}$ = 0

$\Rightarrow D_p.\frac{d^2p_n}{dx^2}$+ $\alpha_1\emptyset(\lambda)$[1-R]exp[-$\alpha_1(\lambda)x$]-$(\frac{p_n-p_{no}}{\tau_p})$=0……..$eq^n$ (6)

Homogeneous solution of equation (6) is-

$D_p . D^2(p_n - p_{no}) - (\frac{p_n - p_{no}}{\tau_p})$=0

$\Rightarrow D^2 - \frac{1}{Lp^2}$=0

$\Rightarrow$D = $\pm \frac{1}{L_p}$

$p_n - p_{no}$=C_2cosh$\left(\frac{x}{L_p}\right) + C_3$sinh$\left(\frac{x}{L_p}\right)$……..$eq^n$ (7)

Particular solution of equation (6) is:

$D_p . \frac{d^2}{dx^2} p_n$+$\alpha_1(\lambda)\emptyset(\lambda)$[1-R]exp[-$\alpha_1(\lambda)x$]-($\frac{p_n - p_{no}}{\tau_p}$)=0

$\Rightarrow D_p . \frac{d^2}{dx^2}(p_n - p_{no})$-($\frac{p_n - p_{no}}{\tau_p}$)= $-\alpha_1(\lambda)\emptyset(\lambda)$[1-R]exp [-$\alpha_1(\lambda)x$]

$\Rightarrow \left(\frac{d^2}{dx^2} - \frac{1}{Lp^2}\right)(p_n - p_{no})$=−B exp (-$\alpha_1 x$)

Here, B=$\frac{\alpha_1(\lambda)\emptyset(\lambda)[1-\mathrm{R}]}{D_p}$

$\Rightarrow(\alpha^2 - \frac{1}{Lp^2})(p_n - p_{no})$= −B exp (-$\alpha_1 x$)

$\Rightarrow p_n - p_{no}$ =k. exp (-$\alpha_1(\lambda)x$)

Here, K=$-\frac{\alpha_1\emptyset[1-\mathrm{R}]}{D_p} * \frac{Lp^2}{\alpha^2 Lp^2 - 1}$……..eq(8)

By adding equation 7 & 8 we get the general solution ->

$p_n - p_{no}$=C_2cosh$\left(\frac{x}{L_p}\right) + C_3$sinh$\left(\frac{x}{L_p}\right) - \frac{\alpha_1\emptyset[1-\mathrm{R}]\tau_p}{{\alpha_1}^2 Lp^2 - 1}$. exp (-$\alpha_1 x$)……$eq^n$ (9)

Where,L_p = $\sqrt{D_p\tau_p}$is the diffusion length, and C_2 and C_3 are constants.

There are two Boundary conditions. At the surface, we have surface recombination with a recombination velocityS_p:

1st boundary condition:

$D_p . \frac{d}{dx}(p_n - p_{no})$ =$S_p(p_n - p_{no})$ at x=0

$\frac{d}{dx}(p_n - p_{no})$=$\frac{C_2}{L_p}$sinh$\left(\frac{x}{L_p}\right) + \frac{C_3}{L_p}$cosh$\left(\frac{x}{L_p}\right)$-k(-α)exp (-$\alpha_1 x$)

$D_p \frac{d}{dx}(p_n - p_{no})|_{x=0}$=$S_p(p_n - p_{no})$ at x=0

$D_p[\frac{C_3}{L_p} + \alpha k]$=$S_p[C_2 - k]$

$\frac{C_3}{L_p} + \alpha k$=$\frac{S_p}{D_p}[C_2 - k]$

⇒ C_3=$\frac{S_p L_p}{D_p}[C_2 - k]$- $\alpha k L_p$

⇒ C_3=$\frac{S_p L_p}{D_p} C_2 - k(\frac{S_p L_p}{D_p} + \alpha L_p))$……$eq^n$(10)

Here k =$\frac{\alpha \emptyset [1-\mathrm{R}]\tau_p}{\alpha^2 Lp^2 - 1}$

At the depletion edge, the excess carrier density is small due to the electric field in the depletion region.

2nd Boundary condition-

$p_n - p_{no} = 0$ at $x = x_j$

$0 = C_2 cosh\left(\frac{x_j}{L_p}\right) + C_3 sinh\left(\frac{x_j}{L_p}\right) - \frac{\alpha \emptyset [1-\mathrm{R}]\tau_p}{\alpha^2 Lp^2 - 1}$exp (-$\alpha x_j$)

⇒ $C_2 cosh\left(\frac{x_j}{L_p}\right) + \left[\frac{S_p L_p}{D_p} C_2 - k\left(\frac{S_p L_p}{D_p} + \alpha L_p\right)\right] sinh\left(\frac{x_j}{L_p}\right) = \frac{\alpha \emptyset [1-\mathrm{R}]\tau_p}{\alpha^2 Lp^2 - 1}$exp (-$\alpha x_j$)

$$C_2 = \frac{\frac{\alpha\emptyset[1-R]\tau_p}{\alpha^2 Lp^2-1}\left[\exp(-\alpha x_j)+sinh\left(\frac{x_j}{L_p}\right)\left(\frac{S_p L_p}{D_p}+\alpha L_p\right)\right]}{\frac{S_p L_p}{D_p}sinh\left(\frac{x_j}{L_p}\right)+cosh\left(\frac{x_j}{L_p}\right)} \ldots\ldots\ldots eq^n(11)$$

Now, putting the value of equation (11) to (10), we get

$$C_3 = \frac{S_p L_p}{D_p}\left[\frac{\frac{\alpha\emptyset[1-R]\tau_p}{\alpha^2 Lp^2-1}\left[\exp(-\alpha x_j)+sinh\left(\frac{x_j}{L_p}\right)\left(\frac{S_p L_p}{D_p}+\alpha L_p\right)\right]}{\frac{S_p L_p}{D_p}sinh\left(\frac{x_j}{L_p}\right)+cosh\left(\frac{x_j}{L_p}\right)}\right] - k\left(\frac{S_p L_p}{D_p}+\alpha L_p\right) \ldots\ldots\ldots eq^n(12)$$

By substituting the values of C2 and C3 in equation (9) we get,

$$P_n - P_{no} = \left[\frac{\alpha_1\emptyset[1-R]\tau_p}{({\alpha_1}^2 {L_p}^2-1)}\right]*\left[\frac{\left(\frac{S_P L_P}{Dp}+\alpha_1 L_P\right)\sinh\left(\frac{x_j-x}{Lp}\right)+\exp(-\alpha_1 x_j)\left(\frac{S_P L_P}{Dp}sinh\left(\frac{x}{Lp}\right)+\cosh\left(\frac{x}{Lp}\right)\right)}{\left(\frac{S_P L_P}{Dp}\right)sinh\left(\frac{x_j}{Lp}\right)+cosh\left(\frac{x_j}{Lp}\right)} - \exp(-\alpha_1 x)\right] \ldots\ldots\ldots eq^n(13)$$

Hole photocurrent density at the depletion edge is –

$$J_p = -q.D_p\left(\frac{dp_n}{dx}\right)_{x_j}$$

$$J_p = \left[\frac{q\emptyset(1-R)\alpha_1 L_P}{(\alpha_1{}^2 L_p{}^2-1)}\right]\left[\frac{\left(\frac{S_P L_P}{Dp}+\alpha_1 L_P\right)-\exp\left(-\alpha_1 x_j\right)\left(\left(\frac{S_P L_P}{Dp}\right)cosh\left(\frac{x_j}{Lp}\right)+sinh\left(\frac{x_j}{Lp}\right)\right)}{\left(\frac{S_P L_P}{Dp}\right)sinh\left(\frac{x_j}{Lp}\right)+cosh\left(\frac{x_j}{Lp}\right)} - \alpha_1 L_P \exp\left(-\alpha_1 x_j\right)\right] \ldots\ldots\ldots eq^n(14)$$

For P side of junction (CZTS) eq^n 1, 2&4 can be combined to yield the expression-

$\alpha_2(\lambda)\emptyset(\lambda)$[1-R($\lambda$)] exp[-$\alpha_2(\lambda)x'$]=$\frac{n_p-n_{po}}{\tau_n} - D_n\frac{d^2 n_p}{dx^2}$

$\Rightarrow D_n\frac{d^2 n_p}{dx^2} + \alpha_2\emptyset$[1-R] exp[-$\alpha_2 x'$] $-\frac{n_p-n_{po}}{\tau_n}$ = 0$\ldots\ldots\ldots eq^n$(15)

Homogeneous solution of equation (15) is:

$D_n D^2(n_p - n_{po}) - \frac{n_p-n_{po}}{\tau_n}$ =0

D^2- $\frac{1}{Ln^2}$=0

D=$\pm\frac{1}{Ln}$

$n_p - n_{po}$=C_2cosh($\frac{x'}{Ln}$)+C_3sinh($\frac{x'}{Ln}$)$\ldots\ldots\ldots eq^n$ (16)

Particular solution of equation (15) is:

$D_n\frac{d^2}{dx^2}n_p + \alpha_2\emptyset$[1-R] exp[-$\alpha_2 x'$]-$\frac{n_p-n_{po}}{\tau_n}$ = 0

$n_p - n_{po}$=K.exp $(-\alpha_2 x')$;$\ldots\ldots\ldots eq^n$ (17)

Where, K=$-\frac{\alpha_2\emptyset[1-\mathrm{R}]}{D_p} * \frac{Lp^2}{(\alpha_2{}^2 Lp^2-1)}$

By adding the eq^n(16) & (17), we get the general solution:

$n_p - n_{po}$=C_2cosh($\frac{x'}{Ln}$)+C_3sinh$\left(\frac{x'}{Ln}\right) - \frac{\alpha_2 \emptyset[1-\mathrm{R}]\tau_n}{(\alpha_2{}^2 Ln^2-1)}$ exp [-$\alpha_2 x'$].....eq^n (18)

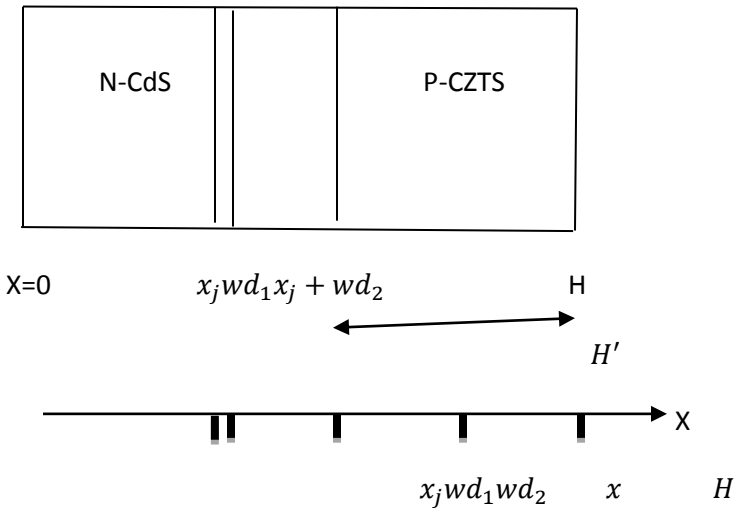

Shift axis from X to X'

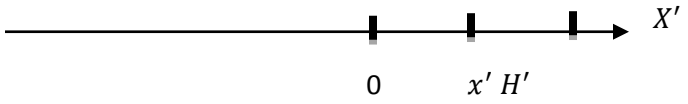

Here,

X=X' + x_j+wd_2

Fig:3 Axis shifting

1st Condition:

$n_p - n_{po}$=0 at $x' = 0$

C_2=K ;……..eq^n (19)

Here, K=$\frac{\alpha_2 \emptyset[1-\mathrm{R}]}{{\alpha_2}^2 Ln^2-1}$exp [-α $(x_j + wd_2)$]

2nd Condition:

$S_p(n_p - n_{po}) = -D_n \frac{dn_p}{dx}$; at x=H'

$\Rightarrow -D_n[\frac{C_2}{Ln} sinh\left(\frac{H'}{Ln}\right) + \frac{C_3}{Ln} cosh\left(\frac{H'}{Ln}\right)$ +k$\alpha_2$exp (-$\alpha_2 x'$)]

$\Rightarrow S_n[C_2 \cosh(\frac{H'}{Ln})+C_3 \sinh\left(\frac{H'}{Ln}\right) - kexp$ [-$\alpha_2 H'$]

$C_3=\frac{-k\left[sinh\left(\frac{H'}{Ln}\right)+\frac{S_n Ln}{Dn} cosh\left(\frac{H'}{Ln}\right)+\left(\frac{S_n}{Dn}-\alpha_2\right) \exp(-\alpha_2 H')Ln\right]}{cosh\left(\frac{H'}{Ln}\right)+\frac{S_n Ln}{Dn}\sinh\left(\frac{H'}{Ln}\right)}$……..$eq^n$ (20)

By putting the values of equation (19) and (20) into equation (18) we get the electron density,

$n_p - n_{po}$=K. $\cosh\left(\frac{x'}{Ln}\right) - k\frac{\left[sinh\left(\frac{H'}{Ln}\right)+\frac{S_n Ln}{Dn} cosh\left(\frac{H'}{Ln}\right)+\left(\frac{S_n}{Dn}-\alpha_2\right) \exp(-\alpha_2 H')Ln\right]}{\cosh(\frac{H'}{Ln})+\frac{S_n Ln}{Dn}\sinh\left(\frac{H'}{Ln}\right)} * \sinh\left(\frac{x'}{Ln}\right) - \frac{\alpha_2 \emptyset[1-\mathrm{R}]}{{\alpha_2}^2 Ln^2-1}$exp ($\alpha_2 x'$)

$n_p - n_{po}=\frac{\alpha_2 \emptyset[1-\mathrm{R}]\tau_n}{{\alpha_2}^2 Ln^2-1}$exp [-$\alpha_1$ $(x_j + wd_1)$]$\left[\cosh\left(\frac{x'}{Ln}\right) - \exp\left(-\alpha_2 x_p\right) - \frac{\left(\frac{S_n Ln}{Dn}\right)\left[cosh\left(\frac{H'}{Ln}\right)-\exp(\alpha_2 H')\right]+\sinh\left(\frac{H'}{Ln}\right)+\alpha_2 Ln \exp(-\alpha_2 H')}{\left(\frac{S_n Ln}{Dn}\right)\sinh\left(\frac{H'}{Ln}\right)+\cosh\left(\frac{H'}{Ln}\right)} * sinh\left(\frac{x'}{Ln}\right)\right]$ ……..eq^n (21)

Here,

$$x' = x - x_j - wd_2$$

The photocurrent due to electrons collected at the depletionedge, $x = x_j + wd_2$ is-

$$J_n = q.D_n\left(\frac{dn_p}{dx}\right)_{x_j+wd_2}$$

$$= \frac{q\emptyset[1-\mathrm{R}]\alpha_2 Ln}{{\alpha_2}^2 Ln^2-1} \exp\,[-\alpha_1\,(x_j + wd_1)] * \exp\left(-\alpha_2 x_p\right) * \left[\alpha_2 Ln - \frac{\left(\frac{S_n L_n}{Dn}\right)\left[\cosh\left(\frac{H'}{Ln}\right)-\exp(-\alpha_2 H')\right]+\sinh\left(\frac{H'}{Ln}\right)+\alpha_2 Ln\exp\,(-\alpha_2 H')}{\left(\frac{S_n L_n}{Dn}\right)\sinh\left(\frac{H'}{Ln}\right)+\cosh\left(\frac{H'}{Ln}\right)}\right] \ldots\ldots eq^n \text{ (22)}$$

$H' = H - x_j - wd_2$ shown in fig-3.

Some photocurrent generation takes place within the depletion region as well. Theelectric field in this region is generally high, and the photo generated carriers areaccelerated out of the depletion region before they can recombine. The quantum efficiency in this region is near 100% and the photocurrent per unit bandwidth is equal tothe number of photons absorbed:

$$J_{dr_1} = q\emptyset(1-R)\exp(-\alpha x)\Big|_{x_j+wd_1}^{x_j}$$

$$\Rightarrow q\emptyset(1-R)\,\exp\,(-\alpha_1 x_j)[1-\exp(-\alpha_1 wd_1)]$$

$$J_{dr_2} = q\emptyset(1-R)\exp(-\alpha x)\Big|_{x_j+wd_1+wd_2}^{x_j+wd_1}$$

$$\Rightarrow q\emptyset(1-R)\,\exp\,[-\alpha_1(x_j + wd_1\,][1-\exp(-\alpha_2 wd_2)]$$

$$J_{dr} = J_{dr_1} + J_{dr_2} \ldots\ldots eq^n \text{ (23)}$$

So, The total photocurrent at a given wavelength is then the sum of Eqs. 14, 22, and 23:

$$J_L(\lambda) = J_p(\lambda) + J_n(\lambda) + J_{dr}(\lambda)$$

Appendix B: MATLAB Code

Functions

required_val

Calculating minority hole lifetime of n-CdS, depletion widths, effective density of states of conduction and valence bands of CZTS, intrinsic carrier concentrations, built in voltage and its components, differences between conduction and valence band edges and the Fermi Level,

```
function [ Tp,xn,xp,ni_cds,ni_czts,Nc_czts,Nv_czts,Vn,Vp,b_cds,b_czts,V_bi ]
= required_val(
Nd,Na,Es_n,Es_p,Nc_cds,Nv_cds,me_czts,mh_czts,Eg_cds,Eg_czts,del_Ec,cap_cross
,NT,Nit,vth,T)
%UNTITLED Summary of this function goes here
%   Detailed explanation goes here

k=1.3806*10^-23;
q=1.6*10^-19;
h=6.626*10^-34;


Nc_czts=2*(((2*pi*me_czts*k*T)/(h^2))^(3/2))/1e6;
Nv_czts=2*(((2*pi*mh_czts*k*T)/(h^2))^(3/2))/1e6;
ni_cds=(sqrt(Nc_cds*Nv_cds))*exp(-Eg_cds/((1.7234*10^-4)*T));
ni_czts=(sqrt(Nc_czts*Nv_czts))*exp(-Eg_czts/((1.7234*10^-4)*T));
b_cds=((8.617*10^-5)*T)*log(Nc_cds/Nd);
b_czts=((8.617*10^-5)*T)*(log(Nv_czts/Na));
V_bi=Eg_czts-del_Ec-b_czts-b_cds;
Vn=V_bi/(1+(Es_n*Nd)/(Es_p*Na));
Vp=V_bi-Vn;
xn=sqrt((2*Es_n*Vn)/(q*Nd));
xp=sqrt((2*Es_p*Vp)/(q*Na));
Tb=1/(cap_cross*vth*NT);
Ts=1/(2*cap_cross*vth*Nit);
Tp=1/(1/Tb+1/Ts);
end
```

req_val_diff

Calculating diffusion coefficients, diffusion lengths, minority carrier conentrations:

```
function [ Dn,Dp,Ln,Lp,npo,pno ] = req_val_diff(
Tn,Tp,mob_p,mob_n,ni_cds,ni_czts,Nd,Na,T )
%UNTITLED4 Summary of this function goes here
%   Detailed explanation goes here
k=1.3806*10^-23;
q=1.6*10^-19;

npo=(ni_czts^2)/Na;
pno=(ni_cds^2)/Nd;


Dn=(k*T/q)*mob_n;
Dp=(k*T/q)*mob_p;
Ln=sqrt(Dn*Tn);
Lp=sqrt(Dp*Tp);

npo=(ni_czts^2)/Na;
pno=(ni_cds^2)/Nd;

end
```

tunnel

Calculating effect of tunneling and electric fields:

```
function [ F_cds,F_czts,En,Ep ] = tunnel(
Nd,Na,Es_n,Es_p,xn,xp,me_cds,mh_czts,T )
%UNTITLED Summary of this function goes here
%   Detailed explanation goes here
q=1.6*10^-19;
h_cut=1.054*10^-34;

k=1.3806*10^-23;
En=(q*Nd*xn)/Es_n;
Ep=(q*Na*xp)/Es_p;

F_cds=(2*sqrt(3*pi))*((En*q*h_cut)/(sqrt((24*me_cds)*((k*T)^3))))*exp(((En*q*
h_cut)/(sqrt((24*me_cds)*((k*T)^3))))^2);
F_czts=(2*sqrt(3*pi))*((Ep*q*h_cut)/(sqrt((24*mh_czts)*((k*T)^3))))*exp(((Ep*
q*h_cut)/(sqrt((24*mh_czts)*((k*T)^3))))^2);

end
```

cds_int_calc

Calculating radiative recombination coefficient of CdS

```
function [ Bn ] = cds_int_calc( ni_cds,T )
%UNTITLED3 Summary of this function goes here
%   Detailed explanation goes here
E=[2.4,2.5,3,3.5,4];
a1=[1.1*10^5,1.15*10^5,2.5*10^5,3*10^5,3.1*10^5];
nr_cds=[2.74,2.75,2.65,2.85,2.78];
```

```
for j=1:length(E)
    in_cds(j)=(a1(j)*(E(j)^2))/(exp(E(j)/((8.617*10^-5)*T))-1);
    I_cds(j)=((8*pi*(nr_cds(j)^2))/(((3*10^10)^2)*((4.135*10^-
15)^3)*((ni_cds)^2)))*in_cds(j);
end
Bn=trapz(E,I_cds);



end
```

czts_int_calc

Calculating radiative recombination coefficient of CZTS

```
function [ Bp ] = czts_int_calc( ni_czts, T )
%UNTITLED2 Summary of this function goes here
%   Detailed explanation goes here
E=[1.5,2,2.5,3,3.5,4];
a2=[0.4*10^5,0.75*10^5,1.7*10^5,1.8*10^5,1.8*10^5,1.8*10^5];
nr_czts=[2.15,2.15,2.2,2.25,2.3,2.3];



for j=1:length(E)
    in_czts(j)=(a2(j)*(E(j)^2))/(exp(E(j)/((8.617*10^-5)*T))-1);
    I_czts(j)=((8*pi*(nr_czts(j)^2))/(((3*10^10)^2)*((4.135*10^-
15)^3)*((ni_czts)^2)))*in_czts(j);
end
Bp=trapz(E,I_czts);


End
```

photo_len_calc

Calculating boundary lengths used in photocurrent calculation

```
function [ xj,Wd1,Wd2,H] = photo_len_calc( l_cds,l_czts,xn,xp )
%UNTITLED Summary of this function goes here
%   Detailed explanation goes here

l_tot=l_cds+l_czts;
Wd1=xn;
Wd2=xp;
xj=l_cds-xn;
H=l_tot-(xj+xn+xp);
if xj<0
    xj=0;
end
if H<0
    H=0;
end
```

```
if Wd1>l_cds
    Wd1=l_cds;
end
if Wd2>l_czts
    Wd2=l_czts;
end



end
```

Jdiff_calc
Calculating diffusion current

```
function [ J_diff ] = Jdiff_calc( Dp,Dn,Lp,Ln,npo,pno )
%UNTITLED5 Summary of this function goes here
%   Detailed explanation goes here
q=1.6*10^-19;


Jdiff_p=((q*Dp*pno)/Lp); % diffusion current n-side
Jdiff_n=((q*Dn*npo)/Ln); % diffusion current p-side
J_diff=Jdiff_p+Jdiff_n;  % total diffusion current



End
```

Jte_calc
Calculating thermionic emission current

```
function [ J_te,A_star,barr_h ] = Jte_calc( me_cds,del_Ec,Vn,Vp,T )
%UNTITLED6 Summary of this function goes here
%   Detailed explanation goes here
k=1.3806*10^-23;
h=6.626*10^-34;
q=1.6*10^-19;

barr_h=del_Ec+Vn+Vp;
A_star=(4*pi*q*me_cds*(k^2))/(h^3);
J_te=A_star*(T^2)*exp(-(barr_h)/((8.617*10^-5)*T));



end
```

Jir_calc
Calculating interface recombination current

```
function [ J_ir ] = Jir_calc( Nc_cds,Nv_czts,ni_czts,S,del_Ec,del_Ev,T )
%UNTITLED3 Summary of this function goes here
```

```
%   Detailed explanation goes here
q=1.6*10^-19;


en_fact=Nc_cds/Nv_czts;
J_ir=q*S*ni_czts*(1+(en_fact*exp((-(del_Ec+del_Ev))/((1.7234*10^-4)*T))));


end
```

Jir_calc
Calculating radiative recombination current

```
function [ J_rr ] = Jrr_calc( xn,xp,Bn,Bp,ni_cds,ni_czts )
%UNTITLED Summary of this function goes here
%   Detailed explanation goes here
q=1.6*10^-19;

J_rr=q*(xn*Bn*(ni_cds^2)+xp*Bp*(ni_czts^2));

end
```

Jtatr_calc
Calculating radiative recombination current

```
function [ J_tatr ] = Jtatr_calc( xn,xp,ni_cds,ni_czts,Tn,Tp,F_cds,F_czts)
%UNTITLED2 Summary of this function goes here
%   Detailed explanation goes here
q=1.6*10^-19;


J_tatr=q*(((xn*ni_cds*(1+F_cds))/Tn)+((xp*ni_czts*(1+F_czts))/Tp));

end
```

nside_Jp_calc
Calculating n-side photocurrent

```
function [ Jp_tot,Jp,Jp_n eV, px,n ] = nside_Jp_calc( a1, p, lam, R, Lp, Dp,
Sp, xj)
%UNTITLED Summary of this function goes here
%   Detailed explanation goes here
q=1.6*(10^-19);%c

b=length(lam);
for i=1: b
eV(i)=1.24/(lam(i));
px(i)=p(i)/(eV(i)*(1.6*10^-19));
end
```

```
for i=1: b

ST1(i)=(q*px(i)*(1-R)*a1(i)*Lp)/((a1(i)^2)*(Lp^2)-1);
ST2(i)=(((Sp*Lp)/Dp)+a1(i)*Lp)-exp(-
a1(i)*xj)*((((Sp*Lp)/Dp)*cosh(xj/Lp))+sinh(xj/Lp));
ST3=((Sp*Lp)/Dp)*sinh(xj/Lp)+cosh(xj/Lp);
ST4(i)=a1(i)*Lp*exp(-a1(i)*xj);
Jp(i)=ST1(i)*((ST2(i)/ST3)-ST4(i));
end
n=lam(1):0.005:lam(end);
Jp_n=interp1(lam,Jp,n);
Jp_tot=trapz(n,Jp_n);
end
```

pside_Jn_calc

Calculating p-side photocurrent

```
function [ Jn_tot,Jn,Jn_n eV, px,n ] = pside_Jn_calc(a1, a2, p, lam, R,
Dn,Ln, Sn,xj, H, Wd1, Wd2)
%UNTITLED2 Summary of this function goes here
%   Detailed explanation goes here
q=1.6*(10^-19);%c

b=length(lam);
for i=1:b
eV(i)=1.24/(lam(i));
px(i)=p(i)/(eV(i)*(1.6*10^-19));
end

for i=1:b

ST1(i)=((q*px(i)*(1-R)*a2(i)*Ln)/((a2(i)^2)*(Ln^2)-1))*exp(-
a1(i)*(xj+Wd1))*exp(-a2(i)*(Wd2));
ST2(i)=((Sn*Ln)/Dn)*(cosh(H/Ln)-exp(-a2(i)*H))+sinh(H/Ln)+a2(i)*Ln*exp(-
a2(i)*H);
ST3=((Sn*Ln)/Dn)*sinh(H/Ln)+cosh(H/Ln);
ST4(i)=a2(i)*Ln;
Jn(i)=ST1(i)*(ST4(i)-(ST2(i)/ST3));
end
n=lam(1):0.005:lam(end);
Jn_n=interp1(lam,Jn,n);
Jn_tot=trapz(n,Jn_n);

end
```

dep_Jdr_calc

Calculating depletion region photocurrent

```
function [ Jdr1,Jdr2,Jdr1_n,Jdr2_n,Jdr1_tot,Jdr2_tot,Jdr_tot,Jdr,Jdr_n, eV,
px ,n] = dep_Jdr_calc(a1,a2,p,lam,R,xj,Wd1,Wd2)
%UNTITLED3 Summary of this function goes here
%   Detailed explanation goes here
q=1.6*(10^-19);
b=length(lam);
for i=1: b
eV(i)=1.24/(lam(i));
```

```
px(i)=p(i)/(eV(i)*(1.6*10^-19));
end

for i=1:b
Jdr1(i)=q*px(i)*(1-R)*exp(-a1(i)*xj)*(1-exp(-a1(i)*Wd1));
Jdr2(i)=q*px(i)*(1-R)*exp(-a1(i)*(xj+Wd1))*(1-exp(-a2(i)*Wd2));
Jdr(i)=Jdr1(i)+Jdr2(i);

end
n=lam(1):0.005:lam(end);

Jdr1_n=interp1(lam,Jdr1,n);
Jdr2_n=interp1(lam,Jdr2,n);
Jdr_n=interp1(lam,Jdr,n);

Jdr1_tot=trapz(n,Jdr1_n);
Jdr2_tot=trapz(n,Jdr2_n);
Jdr_tot=trapz(n,Jdr_n);

end
```

currents_calc
Calculating total photocurrent and dark current

```
function [ J_D,Jphoto,Jph,Jph_n,n] = currents_calc(
J_rr,J_ir,J_diff,J_te,J_tatr,Jn,Jp,Jdr,lam)
%UNTITLED3 Summary of this function goes here
%   Detailed explanation goes here
J_D=J_rr+J_ir+J_diff+J_te+J_tatr;
a=length(lam);

n=lam(1):0.005:lam(end);
for i=1:a
    Jphoto(i)=Jn(i)+Jp(i)+Jdr(i);
end
Jph_n=interp1(lam,Jphoto,n);
Jph=trapz(n,Jph_n);

end
```

JvV_eq
Calculating J-V relation for 1 photocurrent and dark current value

```
function [V] = JvV_eq(Jph,JD,J,Rs,T )
%UNTITLED2 Summary of this function goes here
%   Detailed explanation goes here
k=1.3806e-23;
q=1.6e-19;

for i=1:1:length(J)
     V(i)=((2*k*T)/q)*log(((Jph-J(i))/JD)+1)-J(i)*Rs;

end
```

```
end
```

JvV_eq2

Calculating J-V relation for 5 photocurrent and dark current values

```
function [ V1,V2,V3,V4,V5,J1,J2,J3,J4,J5 ] = JvV_eq2( Jph,JD,Rs,T )
%UNTITLED2 Summary of this function goes here
%   Detailed explanation goes here
J1=0:0.0001:Jph(1);
J2=0:0.0001:Jph(2);
J3=0:0.0001:Jph(3);
J4=0:0.0001:Jph(4);
J5=0:0.0001:Jph(5);
[ V1 ] = JvV_eq(Jph(1),JD(1),J1,Rs,T );
[ V2 ] = JvV_eq(Jph(2),JD(2),J2,Rs,T );
[ V3 ] = JvV_eq(Jph(3),JD(3),J3,Rs,T );
[ V4 ] = JvV_eq(Jph(4),JD(4),J4,Rs,T );
[ V5 ] = JvV_eq(Jph(5),JD(5),J5,Rs,T );
end
```

JvV_eq3

Calculating J-V relation for 3 photocurrent, dark current and temperature values

```
function [ V1,V2,V3,J1,J2,J3  ] = JvV_eq3( Jph,JD,Rs,T )
%UNTITLED2 Summary of this function goes here
%   Detailed explanation goes here
J1=0:0.00001:Jph(1);
J2=0:0.00001:Jph(2);
J3=0:0.00001:Jph(3);
[ V1 ] = JvV_eq(Jph(1),JD(1),J1,Rs,T(1) );
[ V2 ] = JvV_eq(Jph(2),JD(2),J2,Rs,T(2) );
[ V3 ] = JvV_eq(Jph(3),JD(3),J3,Rs,T(3) );

end
```

maxpower

Calculating the maximum power at maximum power point

```
function [ P,Pmax,Vmax,Jmax ] = maxpower( V,J )
%UNTITLED Summary of this function goes here
%   Detailed explanation goes here
a=length(V);
for i=1:1:a
    P(i)=V(i)*J(i);
end
Pmax=max(P);
Vmax=interp1(P,V,Pmax);
Jmax=Pmax/Vmax;

end
```

find_Voc_Jsc

Finding the open circuit voltage and short circuit current

```
function [ Voc,Jsc ] = find_Voc_Jsc( V,J )
%UNTITLED3 Summary of this function goes here
%   Detailed explanation goes here
Voc=interp1(J,V,0);
Jsc=interp1(V,J,0);

end
```

find_Eff_FF

Finding the efficiency and fill factor

```
function [ Eff,FF ] = Find_Eff_FF(Pmax,Voc,Isc,Pin )
%UNTITLED4 Summary of this function goes here
%   Detailed explanation goes here
Eff=Pmax/Pin;
FF=Pmax/(Voc*Isc);


end
```

Jph_JD_temp_func

Calculating dark current and photocurrent for changing temperature

```
function [ JD,JD2,Jph,Jph2,Jn_tot,Jp_tot,Jdr_tot,J_diff,J_te,J_ir,J_rr,J_tatr
] = Jph_JD_temp_func(
Nd,Na,Es_n,Es_p,Nc_cds,Nv_cds,me_cds,me_czts,mh_czts,Eg_cds,Eg_czts,del_Ec,de
l_Ev,cap_cross,NT,Nit,vth,Tn,mob_p,mob_n,l_cds,l_czts,S,Sp,Sn,a1,a2,p,lam,R,T
)
%UNTITLED Summary of this function goes here
%   Detailed explanation goes here
for i=1:1:length(T)
    [ Tp,xn,xp,ni_cds,ni_czts,Nc_czts,Nv_czts,Vn,Vp,b_cds,b_czts,V_bi ] =
required_val(
Nd,Na,Es_n,Es_p,Nc_cds,Nv_cds,me_czts,mh_czts,Eg_cds,Eg_czts,del_Ec,cap_cross
,NT,Nit,vth,T(i));
    [Dn,Dp,Ln,Lp,npo,pno ] = req_val_diff(
Tn,Tp,mob_p(i),mob_n(i),ni_cds,ni_czts,Nd,Na,T(i) );
    [ F_cds,F_czts,En,Ep ] = tunnel(
Nd,Na,Es_n,Es_p,xn,xp,me_cds,mh_czts,T(i) );
    [ Bn ] = cds_int_calc( ni_cds,T(i) );
    [ Bp ] = czts_int_calc( ni_czts, T(i) );
    [ xj,Wd1,Wd2,H] = photo_len_calc( l_cds,l_czts,xn,xp );
    [ J_diff(i) ] = Jdiff_calc( Dp,Dn,Lp,Ln,npo,pno );
    [ J_te(i),A_star,barr_h ] = Jte_calc( me_cds,del_Ec,Vn,Vp,T(i) );
    [ J_ir(i) ] = Jir_calc( Nc_cds,Nv_czts,ni_czts,S,del_Ec,del_Ev,T(i) );
    [ J_rr(i) ] = Jrr_calc( xn,xp,Bn,Bp,ni_cds,ni_czts );
    [ J_tatr(i) ] = Jtatr_calc( xn,xp,ni_cds,ni_czts,Tn,Tp,F_cds,F_czts);
    [ Jp_tot(i),Jp,Jp_n eV, px,n ] = nside_Jp_calc( a1, p, lam, R, Lp, Dp,
Sp, xj);
    [ Jn_tot(i),Jn,Jn_n eV, px,n ] = pside_Jn_calc(a1, a2, p, lam, R, Dn,Ln,
Sn,xj, H, Wd1, Wd2);
```

```
    [ Jdr1,Jdr2,Jdr1_n,Jdr2_n,Jdr1_tot,Jdr2_tot,Jdr_tot(i),Jdr,Jdr_n, eV, px
,n] = dep_Jdr_calc( a1,a2,p,lam,R,xj,Wd1,Wd2);
    [ JD(i),Jphoto,Jph(i),Jph_n,n] = currents_calc(
J_rr(i),J_ir(i),J_diff(i),J_te(i),J_tatr(i),Jn,Jp,Jdr,lam);
    [ JD2(i),Jph2(i)] = currents_calc2(
J_rr(i),J_ir(i),J_diff(i),J_te(i),J_tatr(i),Jn_tot(i),Jp_tot(i),Jdr_tot(i),la
m);
end
end
```

Scripts

Jph_JD_main

Calculating dark current and its components, photocurrent for single temperature

```
mob_p=50; %minority hole mobility n-CdS cm^2 V^-1 s^-1
mob_n=620; %minority electron mobility n-CZTS cm^2 V^-1 s^-1
Tn=1.7*10^-9; %minority electron lifetime s
Es_n=7.969*10^-13; % dielectric permittivity of n-CdS F/cm     ??? -
Es_p=8.854*10^-13; % dielectric permittivity of p-CZTS F/cm    ??? -
me_czts=1.6398*10^-31; % electron effective mass p-CZTS kg
mh_czts=6.4681*10^-31; % hole effective mass p-CZTS kg
me_cds=2.2775*10^-31; % electron effective mass n-CdS kg
mh_cds=6.377*10^-31; % hole effective mass n-CdS kg
Nc_cds=1.8*10^19; % effective density of states of conduction band n-Cds cm^-
3
Nv_cds=2.4*10^18; % effective density of states of valence band n-Cds cm^-3
Nd=1e18; %Donor concentration cm^-3
Na=5e14;  %Acceptor concentration cm^-3
Eg_cds=2.4;%Energy band gap cds eV
Eg_czts=1.5;%Energy band gap czts  eV
del_Ec=-0.3;%Conduction band offset eV
del_Ev=1.2;%Valence band offset  eV
Sp=5*10^4; %Surface recombination speed n-CdS cm s^-1     ??? -
Sn=6*10^5; %Surface recombination speed p-CZTS cm s^-1
S=10^4;%Interface recombination speed cm s^-1     ??? -
cap_cross=10^-13;%Capture cross section of holes cm^2
NT=10^13;       %impurity density cm^-3
Nit=5*10^13;      %interface trap density cm^-2    ???
vth=10^7;       %Hole thermal velocity  cm s^-1     ???
l_cds=5e-6; %length of cds cm               ??? -
l_czts=5e-4;%length of czts cm                ??? -
R=0.2; %reflectance
lam=[0.305,0.325,0.350,0.370,0.390,0.400,0.430,0.450,0.470,0.480,0.490,0.500,
0.510,0.530,0.550,0.570,0.610,0.630,0.650,0.670,0.710,0.724,0.753,0.780,0.800
,0.816,0.824,0.840,0.860,0.880,0.905]; %wavelength in micro-meter       ??? -
a1=[1.7*10^5,1.5*10^5,1.2*10^5,9*10^4,8.5*10^4,7.5*10^4,5*10^4,3.5*10^4,1.2*1
0^4,9.0*10^2,6.0*10^2,1.2*10^2,50,0,0,0,0,0,0,0,0,0,0,0,0,0,0,0,0,0,0,0,0,0]; %
cds absorption coeffcient cm^-1
a2=[1.2*10^5,1.1*10^5,1*10^5,9.5*10^4,8.5*10^4,8.1*10^4,7.7*10^4,7.4*10^4,6.9
*10^4,6.5*10^4,5.7*10^4,5.0*10^4,4.6*10^4,4.0*10^4,3.5*10^4,2.7*10^4,1.5*10^4
,1.2*10^4,9*10^3,7.8*10^3,6.5*10^3,5.5*10^3,4.5*10^3,3.5*10^3,2.1*10^3,8.0*10
^2,4.0*10^2,0,0,0,0]; % czts absorption coeffcient cm^-1
p=[9.5*10^-
4,0.0247,0.0484,0.0667,0.0721,0.1013,0.1072,0.1526,0.1581,0.1628,0.1539,0.154
9,0.1587,0.1572,0.1561,0.1502,0.1485,0.1434,0.1420,0.1392,0.1317,0.1043,0.119
```

```
4,0.1131,0.1082,0.0849,0.0785,0.0959,0.0979,0.0933,0.0749]; % solar spectral
irradiance at AM 1.5 W/cm^2/micro-m

T=300; %temperature K
[ Tp,xn,xp,ni_cds,ni_czts,Nc_czts,Nv_czts,Vn,Vp,b_cds,b_czts,V_bi ] =
required_val(
Nd,Na,Es_n,Es_p,Nc_cds,Nv_cds,me_czts,mh_czts,Eg_cds,Eg_czts,del_Ec,cap_cross
,NT,Nit,vth,T);
[ Dn,Dp,Ln,Lp,npo,pno ] = req_val_diff(
Tn,Tp,mob_p,mob_n,ni_cds,ni_czts,Nd,Na,T );
[ F_cds,F_czts,En,Ep ] = tunnel( Nd,Na,Es_n,Es_p,xn,xp,me_cds,mh_czts,T );
[ Bn ] = cds_int_calc( ni_cds,T );
[ Bp ] = czts_int_calc( ni_czts, T );
[ xj,Wd1,Wd2,H] = photo_len_calc( l_cds,l_czts,xn,xp );
[ J_diff ] = Jdiff_calc( Dp,Dn,Lp,Ln,npo,pno );
[ J_te,A_star,barr_h ] = Jte_calc( me_cds,del_Ec,Vn,Vp,T );
[ J_ir ] = Jir_calc( Nc_cds,Nv_czts,ni_czts,S,del_Ec,del_Ev,T );
[ J_rr ] = Jrr_calc( xn,xp,Bn,Bp,ni_cds,ni_czts );
[ J_tatr ] = Jtatr_calc( xn,xp,ni_cds,ni_czts,Tn,Tp,F_cds,F_czts);
[ Jp_tot,Jp,Jp_n eV, px,n ] = nside_Jp_calc( a1, p, lam, R, Lp, Dp, Sp, xj);
[ Jn_tot,Jn,Jn_n eV, px,n ] = pside_Jn_calc(a1, a2, p, lam, R, Dn,Ln, Sn,xj,
H, Wd1, Wd2);
[ Jdr1,Jdr2,Jdr1_n,Jdr2_n,Jdr1_tot,Jdr2_tot,Jdr_tot,Jdr,Jdr_n, eV, px ,n] =
dep_Jdr_calc( a1,a2,p,lam,R,xj,Wd1,Wd2);
[ JD,Jphoto,Jph,Jph_n,n] = currents_calc(
J_rr,J_ir,J_diff,J_te,J_tatr,Jn,Jp,Jdr,lam);
```

Jph_JD_temp

Calculating dark current and its components, photocurrent for varying temperature

```
mob_p=50:2:80; %minority hole mobility n-CdS cm^2 V^-1 s^-1
mob_n=620:20:920; %minority electron mobility n-CZTS cm^2 V^-1 s^-1
Tn=1.7*10^-9; %minority electron lifetime s
Es_n=7.969*10^-13; % dielectric permittivity of n-CdS F/cm     ??? -
Es_p=8.854*10^-13; % dielectric permittivity of p-CZTS F/cm    ??? -
me_czts=1.6398*10^-31; % electron effective mass p-CZTS kg
mh_czts=6.4681*10^-31; % hole effective mass p-CZTS kg
me_cds=2.2775*10^-31; % electron effective mass n-CdS kg
mh_cds=6.377*10^-31; % hole effective mass n-CdS kg
Nc_cds=1.8*10^19; % effective density of states of conduction band n-Cds cm^-
3
Nv_cds=2.4*10^18; % effective density of states of valence band n-Cds cm^-3
Nd=1e18; %Donor concentration cm^-3
Na=5e14;  %Acceptor concentration cm^-3
Eg_cds=2.4;%Energy band gap cds eV
Eg_czts=1.5;%Energy band gap czts  eV
del_Ec=-0.3;%Conduction band offset eV
del_Ev=1.2;%Valence band offset  eV
Sp=5*10^4; %Surface recombination speed n-CdS cm s^-1     ??? -
Sn=6*10^5; %Surface recombination speed p-CZTS cm s^-1
S=10^4;%Interface recombination speed cm s^-1     ??? -
cap_cross=10^-13;%Capture cross section of holes cm^2
NT=10^13;       %impurity density cm^-3
Nit=5*10^13;      %interface trap density cm^-2    ???
vth=10^7;       %Hole thermal velocity  cm s^-1     ???
```

```
l_cds=5e-6; %length of cds cm                ??? -
l_czts=5e-4;%length of czts cm                 ??? -
R=0.2; %reflectance
lam=[0.305,0.325,0.350,0.370,0.390,0.400,0.430,0.450,0.470,0.480,0.490,0.500,
0.510,0.530,0.550,0.570,0.610,0.630,0.650,0.670,0.710,0.724,0.753,0.780,0.800
,0.816,0.824,0.840,0.860,0.880,0.905]; %wavelength in micro-meter       ??? -
a1=[1.7*10^5,1.5*10^5,1.2*10^5,9*10^4,8.5*10^4,7.5*10^4,5*10^4,3.5*10^4,1.2*1
0^4,9.0*10^2,6.0*10^2,1.2*10^2,50,0,0,0,0,0,0,0,0,0,0,0,0,0,0,0,0,0,0,0,0,0]; %
cds absorption coeffcient cm^-1
a2=[1.2*10^5,1.1*10^5,1*10^5,9.5*10^4,8.5*10^4,8.1*10^4,7.7*10^4,7.4*10^4,6.9
*10^4,6.5*10^4,5.7*10^4,5.0*10^4,4.6*10^4,4.0*10^4,3.5*10^4,2.7*10^4,1.5*10^4
,1.2*10^4,9*10^3,7.8*10^3,6.5*10^3,5.5*10^3,4.5*10^3,3.5*10^3,2.1*10^3,8.0*10
^2,4.0*10^2,0,0,0,0]; % czts absorption coeffcient cm^-1
p=[9.5*10^-
4,0.0247,0.0484,0.0667,0.0721,0.1013,0.1072,0.1526,0.1581,0.1628,0.1539,0.154
9,0.1587,0.1572,0.1561,0.1502,0.1485,0.1434,0.1420,0.1392,0.1317,0.1043,0.119
4,0.1131,0.1082,0.0849,0.0785,0.0959,0.0979,0.0933,0.0749]; % solar spectral
irradiance at AM 1.5 W/cm^2/micro-m

T=278:5:348; %temperature K
[ JD,JD50,Jph,Jph2,Jn_tot,Jp_tot,Jdr_tot,J_diff,J_te,J_ir,J_rr,J_tatr ] =
Jph_JD_temp_func(
Nd,Na,Es_n,Es_p,Nc_cds,Nv_cds,me_cds,me_czts,mh_czts,Eg_cds,Eg_czts,del_Ec,de
l_Ev,cap_cross,NT,Nit,vth,Tn,mob_p,mob_n,l_cds,l_czts,S,Sp,Sn,a1,a2,p,lam,R,T
);
Pin=trapz(lam,p);
```

opt_Nd_Na

Calculating and displaying performance parameters (photocurrent, dark current, J-V relation, open circuit voltage, short circuit current, fill factor, efficiency) for changing doping density

```
%lcds= 100 nm
%Nd= 10^17 , 10^18 cm^-3
%lczts=2 micro-m
Jph1=[0.0188,0.0187,0.0182,0.0168,0.0163];
JD1=[5.74e-8,1.55e-8,9.72e-9,4.40e-9,3.53e-9];
Jph2=[0.0188,0.0187,0.0182,0.0168,0.0163];
JD2=[1.62e-8,7.35e-9,5.65e-9,3.63e-9,3.18e-9];
%lczts=5 micro-m
Jph5=[0.0214,0.0201,0.0194,0.0180,0.0175];
JD5=[5.74e-8,1.55e-8,9.72e-9,4.40e-9,3.53e-9];
Jph6=[0.0214,0.0201,0.0194,0.0180,0.0175];
JD6=[1.62e-8,7.35e-9,5.65e-9,3.63e-9,3.18e-9];
%lczts=3 micro-m
Jph3=[0.0203,0.0195,0.0189,0.0175,0.0170];
JD3=[5.74e-8,1.55e-8,9.72e-9,4.40e-9,3.53e-9];
Jph4=[0.0203,0.0195,0.0189,0.0175,0.0170];
JD4=[1.62e-8,7.35e-9,5.65e-9,3.63e-9,3.18e-9];

Na=[1e14,5e14,1e15,5e15,1e16];
Na2=[5e14,1e15,5e15,1e16,5e16];
Rs=5.8;
T=300;
%J-V relation
[ V1,V2,V3,V4,V5,J1,J2,J3,J4,J5 ] = JvV_eq2( Jph5,JD5,Rs,T );
[ V6,V7,V8,V9,V10,J6,J7,J8,J9,J10 ] = JvV_eq2( Jph6,JD6,Rs,T );
```

```
%J-V graph
plot(Na,Jph5*1000,'r',Na,Jph6*1000,'b');
title('Photocurrent Density Vs Acceptor Concentration for CdS thickness of
100 nm and CZTS thickness of 5 {\mu}m','Fontsize',16)
xlabel('Acceptor Concentration (cm^{-3})','Fontsize',16)
ylabel('Photocurrent Density (mAcm^{-2})','Fontsize',16)
legend('Donor Concentration=10^{17} cm^{-3}','Donor Concentration=10^{18}
cm^{-3}')
figure
plot(Na,JD5*1e9,'r',Na,JD6*129,'b');
title('Dark Current Density Vs Acceptor Concentration for CdS thickness of
100 nm and CZTS thickness of 5 {\mu}m','Fontsize',16)
xlabel('Acceptor Concentration (cm^{-3})','Fontsize',16)
ylabel('Dark Current Density (nAcm^{-2})','Fontsize',16)
legend('Donor Concentration=10^{17} cm^{-3}','Donor Concentration=10^{18}
cm^{-3}','Fontsize',16,4)

figure
plot(V1,J1*1000,'r',V2,J2*1000,'b',V3,J3*1000,'g',V4,J4*1000,'y',V5,J5*1000,'
k','linewidth',2);
title('Current Density Vs Voltage for CdS thickness of 100 nm and CZTS
thickness of 5 {\mu}m','Fontsize',16)
xlabel('Output Voltage (V)','Fontsize',16)
ylabel('Current Density (mAcm^{-2})','Fontsize',16)
legend('Acceptor Concentration=10^{14} cm^{-3}','Acceptor
Concentration=5*10^{14} cm^{-3}','Acceptor Concentration=10^{15} cm^{-
3}','Acceptor Concentration=5*10^{15} cm^{-3}','Acceptor
Concentration=10^{16} cm^{-3}','Fontsize',16,3)
text(0.5,22,'Donor Concentration=10^{17} cm^{-3}','Fontsize',14)
xlim([0 0.85])
figure
plot(V6,J6*1000,'r',V7,J7*1000,'b',V8,J8*1000,'g',V9,J9*1000,'y',V10,J10*1000
,'k','linewidth',2);
title('Current Density Vs Voltage for  CdS thickness of 100 nm and CZTS
thickness of 5 {\mu}m','Fontsize',16)
xlabel('Output Voltage (V)','Fontsize',16)
ylabel('Current Density (mAcm^{-2})','Fontsize',16)
legend('Acceptor Concentration=10^{14} cm^{-3}','Acceptor
Concentration=5*10^{14} cm^{-3}','Acceptor Concentration=10^{15} cm^{-
3}','Acceptor Concentration=5*10^{15} cm^{-3}','Acceptor
Concentration=10^{16} cm^{-3}','Fontsize',16,3)
text(0.5,22,'Donor Concentration=10^{18} cm^{-3}','Fontsize',14)
xlim([0 0.85])
figure

%find input power
lam=[0.305,0.325,0.350,0.370,0.390,0.400,0.430,0.450,0.470,0.480,0.490,0.500,
0.510,0.530,0.550,0.570,0.610,0.630,0.650,0.670,0.710,0.724,0.753,0.780,0.800
,0.816,0.824,0.840,0.860,0.880,0.905]; %wavelength in micro-meter       ??? -
a1=[1.7*10^5,1.5*10^5,1.2*10^5,9*10^4,8.5*10^4,7.5*10^4,5*10^4,3.5*10^4,1.2*1
0^4,9.0*10^2,6.0*10^2,1.2*10^2,50,0,0,0,0,0,0,0,0,0,0,0,0,0,0,0,0,0,0,0,0]; % cds
absorption coeffcient cm^-1
a2=[1.2*10^5,1.1*10^5,1*10^5,9.5*10^4,8.5*10^4,8.1*10^4,7.7*10^4,7.4*10^4,6.9
*10^4,6.5*10^4,5.7*10^4,5.0*10^4,4.6*10^4,4.0*10^4,3.5*10^4,2.7*10^4,1.5*10^4
,1.2*10^4,9*10^3,7.8*10^3,6.5*10^3,5.5*10^3,4.5*10^3,3.5*10^3,2.1*10^3,8.0*10
^2,4.0*10^2,0,0,0,0]; % czts absorption coeffcient cm^-1
```

```
p=[9.5*10^-
4,0.0247,0.0484,0.0667,0.0721,0.1013,0.1072,0.1526,0.1581,0.1628,0.1539,0.154
9,0.1587,0.1572,0.1561,0.1502,0.1485,0.1434,0.1420,0.1392,0.1317,0.1043,0.119
4,0.1131,0.1082,0.0849,0.0785,0.0959,0.0979,0.0933,0.0749]; % solar spectral
irradiance at AM 1.5 W/cm^2/micro-m

Pin=trapz(lam,p);

%find max output power
[ P1,Pmax1,Vmax1,Jmax1 ] = maxpower( V1,J1 );
[ P2,Pmax2,Vmax2,Jmax2 ] = maxpower( V2,J2 );
[ P3,Pmax3,Vmax3,Jmax3 ] = maxpower( V3,J3 );
[ P4,Pmax4,Vmax4,Jmax4 ] = maxpower( V4,J4 );
[ P5,Pmax5,Vmax5,Jmax5 ] = maxpower( V5,J5 );
[ P6,Pmax6,Vmax6,Jmax6 ] = maxpower( V6,J6 );
[ P7,Pmax7,Vmax7,Jmax7 ] = maxpower( V7,J7 );
[ P8,Pmax8,Vmax8,Jmax8 ] = maxpower( V8,J8 );
[ P9,Pmax9,Vmax9,Jmax9 ] = maxpower( V9,J9 );
[ P10,Pmax10,Vmax10,Jmax10 ] = maxpower( V10,J10 );

%find Voc, Jsc
[ Voc1,Jsc1 ] = find_Voc_Jsc( V1,J1 );
[ Voc2,Jsc2 ] = find_Voc_Jsc( V2,J2 );
[ Voc3,Jsc3 ] = find_Voc_Jsc( V3,J3 );
[ Voc4,Jsc4 ] = find_Voc_Jsc( V4,J4 );
[ Voc5,Jsc5 ] = find_Voc_Jsc( V5,J5 );
[ Voc6,Jsc6 ] = find_Voc_Jsc( V6,J6 );
[ Voc7,Jsc7 ] = find_Voc_Jsc( V7,J7 );
[ Voc8,Jsc8 ] = find_Voc_Jsc( V8,J8 );
[ Voc9,Jsc9 ] = find_Voc_Jsc( V9,J9 );
[ Voc10,Jsc10 ] = find_Voc_Jsc( V10,J10 );

%find Eff, FF
[ Eff1,FF1 ] = Find_Eff_FF(Pmax1,Voc1,Jsc1,Pin );
[ Eff2,FF2 ] = Find_Eff_FF(Pmax2,Voc2,Jsc2,Pin );
[ Eff3,FF3 ] = Find_Eff_FF(Pmax3,Voc3,Jsc3,Pin );
[ Eff4,FF4 ] = Find_Eff_FF(Pmax4,Voc4,Jsc4,Pin );
[ Eff5,FF5 ] = Find_Eff_FF(Pmax5,Voc5,Jsc5,Pin );
[ Eff6,FF6 ] = Find_Eff_FF(Pmax6,Voc6,Jsc6,Pin );
[ Eff7,FF7 ] = Find_Eff_FF(Pmax7,Voc7,Jsc7,Pin );
[ Eff8,FF8 ] = Find_Eff_FF(Pmax8,Voc8,Jsc8,Pin );
[ Eff9,FF9 ] = Find_Eff_FF(Pmax9,Voc9,Jsc9,Pin );
[ Eff10,FF10 ] = Find_Eff_FF(Pmax10,Voc10,Jsc10,Pin );

%graph values
Voc_1=[Voc1,Voc2,Voc3,Voc4,Voc5];
Voc_2=[Voc6,Voc7,Voc8,Voc9,Voc10];

Jsc_1=[Jsc1,Jsc2,Jsc3,Jsc4,Jsc5];
Jsc_2=[Jsc6,Jsc7,Jsc8,Jsc9,Jsc10];

Eff_1=[Eff1,Eff2,Eff3,Eff4,Eff5];
Eff_2=[Eff6,Eff7,Eff8,Eff9,Eff10];

FF_1=[FF1,FF2,FF3,FF4,FF5];
FF_2=[FF6,FF7,FF8,FF9,FF10];
```

```
%plot
plot(Na,Voc_1,'r',Na,Voc_2,'b');
title('Open Circuit Voltage Vs Acceptor Concentration for CdS thickness of
100 nm and CZTS thickness of 5 {\mu}m','Fontsize',16)
xlabel('Acceptor Concentration (cm^{-3})','Fontsize',16)
ylabel('Open Circuit Voltage (V)','Fontsize',16)
legend('Donor Concentration=10^{17} cm^{-3}','Donor Concentration=10^{18}
cm^{-3}','Fontsize',16)
figure
plot(Na,Jsc_1*1000,'r',Na,Jsc_2*1000,'b');
title('Short Curcuit Current Vs Acceptor Concentration for CdS thickness of
100 nm and CZTS thickness of 5 {\mu}m','Fontsize',16)
xlabel('Acceptor Concentration (cm^{-3})','Fontsize',16)
ylabel('Short Curcuit Current Density (mAcm^{-2})','Fontsize',16)
legend('Donor Concentration=10^{17} cm^{-3}','Donor Concentration=10^{18}
cm^{-3}','Fontsize',16)
figure
plot(Na,Eff_1*100,'r',Na,Eff_2*100,'b');
title('Efficiency Vs Acceptor Concentration for CdS thickness of 100 nm and
CZTS thickness of 5 {\mu}m','Fontsize',16)
xlabel('Acceptor Concentration (cm^{-3})','Fontsize',16)
ylabel('Efficiency (%)','Fontsize',16)
legend('Donor Concentration=10^{17} cm^{-3}','Donor Concentration=10^{18}
cm^{-3}','Fontsize',16)
figure
plot(Na,FF_1,'r',Na,FF_2,'b');
title('Fill Factor Vs Acceptor Concentration for CdS thickness of 100 nm and
CZTS thickness of 5 {\mu}m','Fontsize',16)
xlabel('Acceptor Concentration (cm^{-3})','Fontsize',16)
ylabel('Fill Factor','Fontsize',16)
legend('Donor Concentration=10^{17} cm^{-3}','Donor Concentration=10^{18}
cm^{-3}','Fontsize',16,4)
```

opt_len_cds

Calculating and displaying performance parameters (photocurrent, dark current, J-V relation, open circuit voltage, short circuit current, fill factor, efficiency) for changing CdS thickness

```
%lcds= 50,100,200 nm
%lczts= 5 micro-m
Jph1=[0.0203,0.0201,0.0197];
JD1=[7.35e-9,7.35e-9,7.35e-9];

Jph2=[0.0197,0.0195,0.0192];
JD2=[7.35e-9,7.35e-9,7.35e-9];
Rs=5.8;
T=300;
[ V1,V2,V3,J1,J2,J3  ] = JvV_eq4( Jph1,JD1,Rs,T );
lcds=[50,100,200];

plot(lcds,Jph1*1000,'r');
title('Photocurrent Density Vs CdS thickness for Donor Concentration=10^{18}
cm^{-3} and Acceptor Concentration 5*10^{14} cm^{-3}','Fontsize',16)
xlabel('CdS thickness (nm)','Fontsize',16)
ylabel('Photocurrent Density (mA)','Fontsize',16)
```

```
text(0.5,22,'CZTS Thickness = 5 {\mu}m','Fontsize',14)
figure
plot(lcds,JD1*1e9,'r');
title('Short Curcuit Current Vs CZTS Thickness for Donor
Concentration=10^{18} cm^{-3} and Acceptor Concentration 5*10^{14} cm^{-
3}','Fontsize',16)
xlabel('CZTS Thickness ({\mu}m)','Fontsize',16)
ylabel('Dark Current Density (nAcm^{-2})','Fontsize',16)
text(0.5,22,'CdS Thickness = 50nm','Fontsize',14)
figure

plot(V1,J1*1000,'r',V2,J2*1000,'b',V3,J3*1000,'g','linewidth',2);
title('Current Density Vs Voltage for Donor Concentration=10^{18} cm^{-3} and
Acceptor Concentration 5*10^{14} cm^{-3}','Fontsize',16)
xlabel('Output Voltage (V)','Fontsize',16)
ylabel('Current Density (mAcm^{-2})','Fontsize',16)
legend('CdS Thickness=50 nm','CdS Thickness=100 nm','CdS Thickness=200 nm',3)
text(0.5,22,'CZTS Thickness = 5 {\mu}m','Fontsize',14)
xlim([0 0.85])
figure


%find input power
lam=[0.305,0.325,0.350,0.370,0.390,0.400,0.430,0.450,0.470,0.480,0.490,0.500,
0.510,0.530,0.550,0.570,0.610,0.630,0.650,0.670,0.710,0.724,0.753,0.780,0.800
,0.816,0.824,0.840,0.860,0.880,0.905]; %wavelength in micro-meter       ??? -
a1=[1.7*10^5,1.5*10^5,1.2*10^5,9*10^4,8.5*10^4,7.5*10^4,5*10^4,3.5*10^4,1.2*1
0^4,9.0*10^2,6.0*10^2,1.2*10^2,50,0,0,0,0,0,0,0,0,0,0,0,0,0,0,0,0,0,0,0,0]; % cds
absorption coeffcient cm^-1
a2=[1.2*10^5,1.1*10^5,1*10^5,9.5*10^4,8.5*10^4,8.1*10^4,7.7*10^4,7.4*10^4,6.9
*10^4,6.5*10^4,5.7*10^4,5.0*10^4,4.6*10^4,4.0*10^4,3.5*10^4,2.7*10^4,1.5*10^4
,1.2*10^4,9*10^3,7.8*10^3,6.5*10^3,5.5*10^3,4.5*10^3,3.5*10^3,2.1*10^3,8.0*10
^2,4.0*10^2,0,0,0,0]; % czts absorption coeffcient cm^-1
p=[9.5*10^-
4,0.0247,0.0484,0.0667,0.0721,0.1013,0.1072,0.1526,0.1581,0.1628,0.1539,0.154
9,0.1587,0.1572,0.1561,0.1502,0.1485,0.1434,0.1420,0.1392,0.1317,0.1043,0.119
4,0.1131,0.1082,0.0849,0.0785,0.0959,0.0979,0.0933,0.0749]; % solar spectral
irradiance at AM 1.5 W/cm^2/micro-m

Pin=trapz(lam,p);

%find max output power
[ P1,Pmax1,Vmax1,Jmax1 ] = maxpower( V1,J1 );
[ P2,Pmax2,Vmax2,Jmax2 ] = maxpower( V2,J2 );
[ P3,Pmax3,Vmax3,Jmax3 ] = maxpower( V3,J3 );

%find Voc, Jsc
[ Voc1,Jsc1 ] = find_Voc_Jsc( V1,J1 );
[ Voc2,Jsc2 ] = find_Voc_Jsc( V2,J2 );
[ Voc3,Jsc3 ] = find_Voc_Jsc( V3,J3 );

%find Eff, FF
[ Eff1,FF1 ] = Find_Eff_FF(Pmax1,Voc1,Jsc1,Pin );
[ Eff2,FF2 ] = Find_Eff_FF(Pmax2,Voc2,Jsc2,Pin );
[ Eff3,FF3 ] = Find_Eff_FF(Pmax3,Voc3,Jsc3,Pin );
```

```
Voc_1=[Voc1,Voc2,Voc3];

Jsc_1=[Jsc1,Jsc2,Jsc3];

Eff_1=[Eff1,Eff2,Eff3];

FF_1=[FF1,FF2,FF3];

plot(lcds,Voc_1,'r');
title('Open Circuit Voltage Vs CdS thickness for Donor Concentration=10^{18}
cm^{-3} and Acceptor Concentration 5*10^{14} cm^{-3}','Fontsize',16)
xlabel('CdS thickness (nm)','Fontsize',16)
ylabel('Open Circuit Voltage (V)','Fontsize',16)
text(0.5,22,'CZTS Thickness = 5 {\mu}m','Fontsize',14)

figure
plot(lcds,Jsc_1*1000,'r');
title('Short Curcuit Current Vs CdS thickness for Donor Concentration=10^{18}
cm^{-3} and Acceptor Concentration 5*10^{14} cm^{-3}','Fontsize',16)
xlabel('CdS thickness (nm)','Fontsize',16)
ylabel('Short Curcuit Current Density (mAcm^{-2})','Fontsize',16)
text(0.5,22,'CZTS Thickness = 5 {\mu}m','Fontsize',14)
figure
plot(lcds,Eff_1*100,'r');
title('Efficiency Vs CdS thickness for Donor Concentration=10^{18} cm^{-3}
and Acceptor Concentration 5*10^{14} cm^{-3}','Fontsize',16)
xlabel('CdS thickness (nm)','Fontsize',16)
ylabel('Efficiency (%)','Fontsize',16)
text(0.5,22,'CZTS Thickness = 1 {\mu}m','Fontsize',14)

figure
plot(lcds,FF_1,'r');
title('Fill Factor Vs CdS thickness for Donor Concentration=10^{18} cm^{-3}
and Acceptor Concentration 5*10^{14} cm^{-3}','Fontsize',16)
xlabel('CdS thickness (nm)','Fontsize',16)
ylabel('Fill Factor','Fontsize',16)
text(0.5,22,'CZTS Thickness = 1 {\mu}m','Fontsize',14)
```

opt_len_czts

Calculating and displaying performance parameters (photocurrent, dark current, J-V relation, open circuit voltage, short circuit current, fill factor, efficiency) for changing CZTS thickness

```
Jph1=[0.0160,0.0189,0.0197,0.0201,0.0203];
JD1=[7.35e-9,7.35e-9,7.35e-9,7.35e-9,7.35e-9];
Jph2=[0.0202,0.0202,0.0202,0.0201,0.0201];
JD2=[7.35e-9,7.35e-9,7.35e-9,7.35e-9,7.35e-9];
lczts=1:1:10;
Rs=5.8;
T=300;

[ V1,V2,V3,V4,V5,J1,J2,J3,J4,J5 ] = JvV_eq2( Jph1,JD1,Rs,T );
[ V6,V7,V8,V9,V10,J6,J7,J8,J9,J10 ] = JvV_eq2( Jph2,JD2,Rs,T );
Jph_1=[0.0160,0.0189,0.0197,0.0201,0.0203,0.0202,0.0202,0.0202,0.0201,0.0201]
;
```

```
JD_1=[7.35e-9,7.35e-9,7.35e-9,7.35e-9,7.35e-9,7.35e-9,7.35e-9,7.35e-9,7.35e-
9,7.35e-9];

plot(V1,J1*1000,'r',V2,J2*1000,'b',V3,J3*1000,'g',V4,J4*1000,'y',V5,J5*1000,'
k','linewidth',2);
title('Current Density Vs Voltage for Donor Concentration=10^{18} cm^{-3} and
Acceptor Concentration 5*10^{14} cm^{-3}','Fontsize',16)
xlabel('Output Voltage (V)','Fontsize',16)
ylabel('Current Density (mAcm^{-2})','Fontsize',16)
legend('CZTS Thickness=1 {\mu}m','CZTS Thickness=2 {\mu}m','CZTS Thickness=3
{\mu}m','CZTS Thickness=4 {\mu}m','CZTS Thickness=5 {\mu}m',3)
text(0.5,22,'CdS Thickness = 50 nm','Fontsize',14)
xlim([0 0.85])
figure
plot(V6,J6*1000,'r',V7,J7*1000,'b',V8,J8*1000,'g',V9,J9*1000,'y',V10,J10*1000
,'k','linewidth',2);
title('Current Density Vs Voltage for Donor Concentration=10^{18} cm^{-3} and
Acceptor Concentration 5*10^{14} cm^{-3}','Fontsize',16)
xlabel('Output Voltage (V)','Fontsize',16)
ylabel('Current Density (mAcm^{-2})','Fontsize',16)
legend('CZTS Thickness=6 {\mu}m','CZTS Thickness=7 {\mu}m','CZTS Thickness=8
{\mu}m','CZTS Thickness=9 {\mu}m','CZTS Thickness=10 {\mu}m',3)
text(0.5,22,'CdS Thickness = 50 nm','Fontsize',14)
xlim([0 0.85])
figure
%find input power
lam=[0.305,0.325,0.350,0.370,0.390,0.400,0.430,0.450,0.470,0.480,0.490,0.500,
0.510,0.530,0.550,0.570,0.610,0.630,0.650,0.670,0.710,0.724,0.753,0.780,0.800
,0.816,0.824,0.840,0.860,0.880,0.905]; %wavelength in micro-meter      ??? -
p=[9.5*10^-
4,0.0247,0.0484,0.0667,0.0721,0.1013,0.1072,0.1526,0.1581,0.1628,0.1539,0.154
9,0.1587,0.1572,0.1561,0.1502,0.1485,0.1434,0.1420,0.1392,0.1317,0.1043,0.119
4,0.1131,0.1082,0.0849,0.0785,0.0959,0.0979,0.0933,0.0749]; % solar spectral
irradiance at AM 1.5 W/cm^2/micro-m

Pin=trapz(lam,p);

%find max power
[ P1,Pmax1,Vmax1,Jmax1 ] = maxpower( V1,J1 );
[ P2,Pmax2,Vmax2,Jmax2 ] = maxpower( V2,J2 );
[ P3,Pmax3,Vmax3,Jmax3 ] = maxpower( V3,J3 );
[ P4,Pmax4,Vmax4,Jmax4 ] = maxpower( V4,J4 );
[ P5,Pmax5,Vmax5,Jmax5 ] = maxpower( V5,J5 );
[ P6,Pmax6,Vmax6,Jmax6 ] = maxpower( V6,J6 );
[ P7,Pmax7,Vmax7,Jmax7 ] = maxpower( V7,J7 );
[ P8,Pmax8,Vmax8,Jmax8 ] = maxpower( V8,J8 );
[ P9,Pmax9,Vmax9,Jmax9 ] = maxpower( V9,J9 );
[ P10,Pmax10,Vmax10,Jmax10 ] = maxpower( V10,J10 );
%find Voc, Jsc
[ Voc1,Jsc1 ] = find_Voc_Jsc( V1,J1 );
[ Voc2,Jsc2 ] = find_Voc_Jsc( V2,J2 );
[ Voc3,Jsc3 ] = find_Voc_Jsc( V3,J3 );
[ Voc4,Jsc4 ] = find_Voc_Jsc( V4,J4 );
[ Voc5,Jsc5 ] = find_Voc_Jsc( V5,J5 );
[ Voc6,Jsc6 ] = find_Voc_Jsc( V6,J6 );
[ Voc7,Jsc7 ] = find_Voc_Jsc( V7,J7 );
[ Voc8,Jsc8 ] = find_Voc_Jsc( V8,J8 );
```

```
[ Voc9,Jsc9 ] = find_Voc_Jsc( V9,J9 );
[ Voc10,Jsc10 ] = find_Voc_Jsc( V10,J10 );
%find Eff, FF
[ Eff1,FF1 ] = Find_Eff_FF(Pmax1,Voc1,Jsc1,Pin );
[ Eff2,FF2 ] = Find_Eff_FF(Pmax2,Voc2,Jsc2,Pin );
[ Eff3,FF3 ] = Find_Eff_FF(Pmax3,Voc3,Jsc3,Pin );
[ Eff4,FF4 ] = Find_Eff_FF(Pmax4,Voc4,Jsc4,Pin );
[ Eff5,FF5 ] = Find_Eff_FF(Pmax5,Voc5,Jsc5,Pin );
[ Eff6,FF6 ] = Find_Eff_FF(Pmax6,Voc6,Jsc6,Pin );
[ Eff7,FF7 ] = Find_Eff_FF(Pmax7,Voc7,Jsc7,Pin );
[ Eff8,FF8 ] = Find_Eff_FF(Pmax8,Voc8,Jsc8,Pin );
[ Eff9,FF9 ] = Find_Eff_FF(Pmax9,Voc9,Jsc9,Pin );
[ Eff10,FF10 ] = Find_Eff_FF(Pmax10,Voc10,Jsc10,Pin );


Pmax_1=[Pmax1,Pmax2,Pmax3,Pmax4,Pmax5,Pmax6,Pmax7,Pmax8,Pmax9,Pmax10];
Vmax_1=[Vmax1,Vmax2,Vmax3,Vmax4,Vmax5,Vmax6,Vmax7,Vmax8,Vmax9,Vmax10];
Jmax_1=[Jmax1,Jmax2,Jmax3,Jmax4,Vmax5,Vmax6,Vmax7,Vmax8,Vmax9,Vmax10];
Voc_1=[Voc1,Voc2,Voc3,Voc4,Voc5,Voc6,Voc7,Voc8,Voc9,Voc10];
Jsc_1=[Jsc1,Jsc2,Jsc3,Jsc4,Jsc5,Jsc6,Jsc7,Jsc8,Jsc9,Jsc10];
Eff_1=[Eff1,Eff2,Eff3,Eff4,Eff5,Eff6,Eff7,Eff8,Eff9,Eff10];
FF_1=[FF1,FF2,FF3,FF4,FF5,FF6,FF7,FF8,FF9,FF10];

plot(lczts,Jph_1*1000,'r');
title('Short Curcuit Current Vs CZTS Thickness for Donor
Concentration=10^{18} cm^{-3} and Acceptor Concentration 5*10^{14} cm^{-
3}','Fontsize',16)
xlabel('CZTS Thickness ({\mu}m)','Fontsize',16)
ylabel('Photocurrent Density (mAcm^{-2})','Fontsize',16)
text(0.5,22,'CdS Thickness = 50nm','Fontsize',14)
figure
plot(lczts,JD_1*1e9,'r');
title('Short Curcuit Current Vs CZTS Thickness for Donor
Concentration=10^{18} cm^{-3} and Acceptor Concentration 5*10^{14} cm^{-
3}','Fontsize',16)
xlabel('CZTS Thickness ({\mu}m)','Fontsize',16)
ylabel('Dark Current Density (nAcm^{-2})','Fontsize',16)
text(0.5,22,'CdS Thickness = 50nm','Fontsize',14)
figure

plot(lczts,Voc_1,'r');
title('Open Circuit Voltage Vs CZTS Thickness for Donor Concentration=10^{18}
cm^{-3} and Acceptor Concentration 5*10^{14} cm^{-3}','Fontsize',16)
xlabel('CZTS Thickness ({\mu}m)','Fontsize',16)
ylabel('Open Circuit Voltage (V)','Fontsize',16)
text(0.5,22,'CdS Thickness = 50nm','Fontsize',14)
figure
plot(lczts,Jsc_1*1000,'r');
title('Short Curcuit Current Vs CZTS Thickness for Donor
Concentration=10^{18} cm^{-3} and Acceptor Concentration 5*10^{14} cm^{-
3}','Fontsize',16)
xlabel('CZTS Thickness ({\mu}m)','Fontsize',16)
ylabel('Short Curcuit Current Density (mAcm^{-2})','Fontsize',16)
text(0.5,22,'CdS Thickness = 50nm','Fontsize',14)
figure
plot(lczts,Eff_1*100,'r');
```

```
title('Efficiency Vs CZTS Thickness for Donor Concentration=10^{18} cm^{-3}
and Acceptor Concentration 5*10^{14} cm^{-3}','Fontsize',16)
xlabel('CZTS Thickness ({\mu}m)','Fontsize',16)
ylabel('Efficiency (%)','Fontsize',16)
text(0.5,22,'CdS Thickness = 50nm','Fontsize',14)
figure
plot(lczts,FF_1,'r');
title('Fill Factor Vs CZTS Thickness for Donor Concentration=10^{18} cm^{-3}
and Acceptor Concentration 5*10^{14} cm^{-3}','Fontsize',16)
xlabel('CZTS Thickness ({\mu}m)','Fontsize',16)
ylabel('Fill Factor','Fontsize',16)
text(0.5,22,'CdS Thickness = 50nm','Fontsize',14)
```

Eff_FF_temp

Calculating performance parameters (photocurrent, dark current, J-V relation, open circuit voltage, short circuit current, fill factor, efficiency) for changing temperature

```
Jph1=[0.02026,0.02027,0.02029];
Jph2=[0.02030,0.02032,0.02033];
Jph3=[0.02034,0.02036,0.02037];
Jph4=[0.02038,0.02039,0.02040];
Jph5=[0.02041,0.02042,0.02044];


JD1=[JD(1),JD(2),JD(3)];
JD2=[JD(4),JD(5),JD(6)];
JD3=[JD(7),JD(8),JD(9)];
JD4=[JD(10),JD(11),JD(12)];
JD5=[JD(13),JD(14),JD(15)];
T=278:5:348;
T1=5:5:75;
Rs=5.8;
Jph_1=[0.02026,0.02027,0.02029,0.02030,0.02032,0.02033,0.02034,0.02036,0.0203
7,0.02038,0.02039,0.02040,0.02041,0.02042,0.02044];
[ V1,V2,V3,J1,J2,J3 ] = JvV_eq3( Jph1,JD1,Rs,T(1:3) );
[ V4,V5,V6,J4,J5,J6 ] = JvV_eq3( Jph2,JD2,Rs,T(4:6) );
[ V7,V8,V9,J7,J8,J9 ] = JvV_eq3( Jph3,JD3,Rs,T(7:9) );
[ V10,V11,V12,J10,J11,J12 ] = JvV_eq3( Jph4,JD4,Rs,T(10:12) );
[ V13,V14,V15,J13,J14,J15 ] = JvV_eq3( Jph5,JD5,Rs,T(13:15) );
plot(T1,Jph_1,'r');
title('Photocurrent Density Vs Temperature','Fontsize',16)
xlabel('Temperature (C)','Fontsize',16)
ylabel('Photocurrent Density (mAcm^{-2})','Fontsize',16)
figure

plot(V1,J1,'r',V2,J2,'b',V3,J3,'g',V4,J4,'y',V5,J5,'c');
title('Current Density Vs Output Voltage for lcds=5*10^-6 cm and lczts=5*10^-
4 cm','Fontsize',16)
xlabel('Output Voltage (V)','Fontsize',16)
ylabel('Current Density (mAcm^{-2})','Fontsize',16)
legend('Temperature=5 C','Temperature=10 C','Temperature=15
C','Temperature=20 C','Temperature=25 C',3)
xlim([0 0.85])
figure
plot(V6,J6,'r',V7,J7,'b',V8,J8,'g',V9,J9,'y',V10,J10,'c');
```

```
title('Current Density Vs Output Voltage for lcds=5*10^-6 cm and lczts=5*10^-
4 cm','Fontsize',16)
xlabel('Output Voltage (V)','Fontsize',16)
ylabel('Current Density (mAcm^{-2})','Fontsize',16)
legend('Temperature=30 C','Temperature=35 C','Temperature=40
C','Temperature=45 C','Temperature=50 C',3)
xlim([0 0.85])
figure
plot(V11,J11,'r',V12,J12,'b',V13,J13,'g',V14,J14,'y',V15,J15,'c');
title('Current Density Vs Output Voltage for lcds=5*10^-6 cm and lczts=5*10^-
4 cm','Fontsize',16)
xlabel('Output Voltage (V)','Fontsize',16)
ylabel('Current Density (mAcm^{-2})','Fontsize',16)
legend('Temperature=55 C','Temperature=60 C','Temperature=65
C','Temperature=70 C','Temperature=75 C',3)
xlim([0 0.85])

[ P1,Pmax1,Vmax1,Imax1 ] = maxpower( V1,J1 );
[ P2,Pmax2,Vmax2,Imax2 ] = maxpower( V2,J2 );
[ P3,Pmax3,Vmax3,Imax3 ] = maxpower( V3,J3 );
[ P4,Pmax4,Vmax4,Imax4 ] = maxpower( V4,J4 );
[ P5,Pmax5,Vmax5,Imax5 ] = maxpower( V5,J5 );
[ P6,Pmax6,Vmax6,Imax6 ] = maxpower( V6,J6 );
[ P7,Pmax7,Vmax7,Imax7 ] = maxpower( V7,J7 );
[ P8,Pmax8,Vmax8,Imax8 ] = maxpower( V8,J8 );
[ P9,Pmax9,Vmax9,Imax9 ] = maxpower( V9,J9 );
[ P10,Pmax10,Vmax10,Imax10 ] = maxpower( V10,J10 );
[ P11,Pmax11,Vmax11,Imax11 ] = maxpower( V11,J11 );
[ P12,Pmax12,Vmax12,Imax12 ] = maxpower( V12,J12 );
[ P13,Pmax13,Vmax13,Imax13 ] = maxpower( V13,J13 );
[ P14,Pmax14,Vmax14,Imax14 ] = maxpower( V14,J14 );
[ P15,Pmax15,Vmax15,Imax15 ] = maxpower( V15,J15 );
[ Voc1,Jsc1 ] = find_Voc_Jsc( V1,J1 );
[ Voc2,Jsc2 ] = find_Voc_Jsc( V2,J2 );
[ Voc3,Jsc3 ] = find_Voc_Jsc( V3,J3 );
[ Voc4,Jsc4 ] = find_Voc_Jsc( V4,J4 );
[ Voc5,Jsc5 ] = find_Voc_Jsc( V5,J5 );
[ Voc6,Jsc6 ] = find_Voc_Jsc( V6,J6 );
[ Voc7,Jsc7 ] = find_Voc_Jsc( V7,J7 );
[ Voc8,Jsc8 ] = find_Voc_Jsc( V8,J8 );
[ Voc9,Jsc9 ] = find_Voc_Jsc( V9,J9 );
[ Voc10,Jsc10 ] = find_Voc_Jsc( V10,J10 );
[ Voc11,Jsc11 ] = find_Voc_Jsc( V11,J11 );
[ Voc12,Jsc12 ] = find_Voc_Jsc( V12,J12 );
[ Voc13,Jsc13 ] = find_Voc_Jsc( V13,J13 );
[ Voc14,Jsc14 ] = find_Voc_Jsc( V14,J14 );
[ Voc15,Jsc15 ] = find_Voc_Jsc( V15,J15 );
[ Eff1,FF1 ] = Find_Eff_FF(Pmax1,Voc1,Jsc1,Pin );
[ Eff2,FF2 ] = Find_Eff_FF(Pmax2,Voc2,Jsc2,Pin );
[ Eff3,FF3 ] = Find_Eff_FF(Pmax3,Voc3,Jsc3,Pin );
[ Eff4,FF4 ] = Find_Eff_FF(Pmax4,Voc4,Jsc4,Pin );
[ Eff5,FF5 ] = Find_Eff_FF(Pmax5,Voc5,Jsc5,Pin );
[ Eff6,FF6 ] = Find_Eff_FF(Pmax6,Voc6,Jsc6,Pin );
[ Eff7,FF7 ] = Find_Eff_FF(Pmax7,Voc7,Jsc7,Pin );
[ Eff8,FF8 ] = Find_Eff_FF(Pmax8,Voc8,Jsc8,Pin );
[ Eff9,FF9 ] = Find_Eff_FF(Pmax9,Voc9,Jsc9,Pin );
[ Eff10,FF10 ] = Find_Eff_FF(Pmax10,Voc10,Jsc10,Pin );
```

```
[ Eff11,FF11 ] = Find_Eff_FF(Pmax11,Voc11,Jsc11,Pin );
[ Eff12,FF12 ] = Find_Eff_FF(Pmax12,Voc12,Jsc12,Pin );
[ Eff13,FF13 ] = Find_Eff_FF(Pmax13,Voc13,Jsc13,Pin );
[ Eff14,FF14 ] = Find_Eff_FF(Pmax14,Voc14,Jsc14,Pin );
[ Eff15,FF15 ] = Find_Eff_FF(Pmax15,Voc15,Jsc15,Pin );
```

Eff_FF_temp_graph

Displaying performance parameters (photocurrent, dark current, J-V relation, open circuit voltage, short circuit current, fill factor, efficiency) for changing temperature

```
Voc=[Voc1,Voc2,Voc3,Voc4,Voc5,Voc6,Voc7,Voc8,Voc9,Voc10,Voc11,Voc12,Voc13,Voc
14,Voc15];
Jsc=[Jsc1,Jsc2,Jsc3,Jsc4,Jsc5,Jsc6,Jsc7,Jsc8,Jsc9,Jsc10,Jsc11,Jsc12,Jsc13,Jsc
14,Jsc15];
Eff=[Eff1,Eff2,Eff3,Eff4,Eff5,Eff6,Eff7,Eff8,Eff9,Eff10,Eff11,Eff12,Eff13,Eff
14,Eff15];
FF=[FF1,FF2,FF3,FF4,FF5,FF6,FF7,FF8,FF9,FF10,FF11,FF12,FF13,FF14,FF15];
T=5:5:75;
plot(T,Voc,'r');
title('Open Circuit Voltage Vs Temperature for CdS Thickness = 50nm, CZTS
Thickness 5 {\mu}m, Nd= 10^{18} cm^{-3}, Na= 5*10^{14} cm^{-3}
','Fontsize',16)
xlabel('Temperature (C)','Fontsize',16)
ylabel('Open Circuit Voltage (V)','Fontsize',16)
figure
plot(T,Jsc*1000,'b');
title('Short Circuit Current Vs Temperature for CdS Thickness = 50nm, CZTS
Thickness 5 {\mu}m, Nd= 10^{18} cm^{-3}, Na= 5*10^{14} cm^{-3}
','Fontsize',16)
xlabel('Temperature (C)','Fontsize',16)
ylabel('Short Curcuit Current (mA)','Fontsize',16)

figure
plot(T,Eff*100,'r');
title('Efficiency Vs Temperature for CdS Thickness = 50nm, CZTS Thickness 5
{\mu}m, Nd= 10^{18} cm^{-3}, Na= 5*10^{14} cm^{-3} ','Fontsize',16)
xlabel('Temperature (C)','Fontsize',16)
ylabel('Efficiency (%)','Fontsize',16)
figure
plot(T,FF,'b');
title('Fill Factor Vs Temperature for CdS Thickness = 50nm, CZTS Thickness 5
{\mu}m, Nd= 10^{18} cm^{-3}, Na= 5*10^{14} cm^{-3} ','Fontsize',16)
xlabel('Temperature (C)','Fontsize',16)
ylabel('Fill Factor','Fontsize',16)
figure
plot(T,J_diff*1e9,'b',T,J_te*1e9,'r',T,J_ir*1e9,'g',T,J_rr*1e9,'m',T,J_tatr*1
e9,'c',T,JD*1e9,'k');
title('Dark Current Densities Vs Temperature for CdS Thickness = 50nm, CZTS
Thickness 5 {\mu}m, Nd= 10^{18} cm^{-3}, Na= 5*10^{14} cm^{-3}
','Fontsize',16)
xlabel('Temperature (C)','Fontsize',16)
ylabel('Dark Current Densities (nAcm^{-2})','Fontsize',16)
legend('Diffusion Current Density','TE Current Density','IR Current Density
','RR Current Density','TATR Current Density','Dark Current Density',4)
```